FLOATING LNG TERMINAL AND LNG CARRIER INTERACTION ANALYSIS FOR SIDE-BY-SIDE OFFLOADING OPERATION

A Thesis

by

VINU P. KURIAKOSE

Submitted to the Office of Graduate Studies of
Texas A&M University
in partial fulfillment of the requirements for the degree of

MASTER OF SCIENCE

August 2005

Major Subject: Ocean Engineering

FLOATING LNG TERMINAL AND LNG CARRIER INTERACTION ANALYSIS FOR SIDE-BY-SIDE OFFLOADING OPERATION

A Thesis

by

VINU P. KURIAKOSE

Submitted to the Office of Graduate Studies of
Texas A&M University
in partial fulfillment of the requirements for the degree of

MASTER OF SCIENCE

Approved by:

Chair of Committee,	M. H. Kim
Committee Members,	Robert Randall
	Achim Stössel
Head of Department,	David V. Rosowsky

August 2005

Major Subject: Ocean Engineering

ABSTRACT

Floating LNG Terminal and LNG Carrier Interactions for
Side-by-Side Offloading Operation. (August 2005)
Vinu P. Kuriakose, B.Tech., Cochin University of Science and Technology
Chair of Advisory Committee: Dr. M. H. Kim

Floating LNG terminals are a relatively new concept with the first such terminal in the world installed this year. The hydrodynamic interaction effects between the terminal and a LNG carrier in a side-by-side offloading arrangement is investigated. The side-by-side arrangement is compared with each body floating alone to identify the interaction effects. The hydrodynamic coefficients are obtained using the Constant Panel Method and the analysis of body motions, mooring line tensions are done in time domain. The relative motion between the two bodies is analyzed using WAMIT in frequency domain and WINPOST in time domain to ascertain the offloading operability of the terminal under 1 year storm condition.

DEDICATION

To my father P. T. Kuriakose and mother C. K. Aleyamma

ACKNOWLEDGMENTS

I would like to thank my committee chair Dr. M. H. Kim, for his guidance and untiring support during this work. I thank my committee members Dr. Robert Randall for providing me with the LNG terminal reference materials and Dr. Stössel for his guidance and support throughout the course of this research. I also thank my friends Mr. Chankyu Yang, Dr. D. H. Lee, Mr. Seung Jae Lee and Mr. Harish Pillai for their support. I also want to express my gratitude to Dr. S. Y. Hong, KRISO, for his valuable advice and inputs.

Finally, special thanks to my family for their constant motivation and support.

NOMENCLATURE

LNG	Liquefied Natural Gas
LNGT	LNG Terminal
LNGC	LNG Carrier
SBS	Side by side
deg	Degrees
rad	Radians
g	Acceleration due to gravity
ω	Cyclic frequency
API	American Petroleum Institute

TABLE OF CONTENTS

Page

LIST OF FIGURES

Page

Page

Page

LIST OF TABLES

Page

1. INTRODUCTION

1.1 General

With the rise in energy demand in the world market and the comparative advantages of natural gas over oil, lot of new LNG terminals are under consideration. Many of these are floating offshore LNG terminals. The advantages of these are many. Land based LNG terminals are very close to civilization and pose a grave threat in the scenario of an accident or a terrorist attack. Offshore LNG terminals are typically 3 or 4 miles away from the coast and offer relatively little threat to the people and environment nearby. But the offshore LNG terminals are exposed to the waves which is not the case for a land based terminal. For the proper design and cost analysis of an offshore LNG terminal, a detailed study of the loads acting on the terminal in the case of extreme weather condition is needed.

Another important design aspect is the offloading operation during extreme weather conditions. For maximum utilization of the facility it should be operable even in adverse environmental conditions. Two bodies moored side by side pose very interesting hydrodynamic behavior. The motion of one body affects the motion characteristics of the other body. There can also be resonance of the water trapped between the two vessels. It is this interesting problem that is being analyzed in this research. The drift forces and moments can be much higher than the single body case due to interaction and their prediction is important for the design of mooring systems. The slowly varying forces are a very important consideration since the frequency of these forces can fall near the natural frequencies of horizontal response. The accurate calculation of the forces can lead to a better design of the multi-body system. The relative motions due to interaction effects are very significant for LNG Terminal – LNG Carrier system since it decides the downtime and hence the economic viability of the system being there and needs to be considered carefully.

The thesis follows the style and format of Ocean Engineering.

1.2 Design Parameters

This analysis is based on the terminal design came up with by the Texas A&M University Team 3 (Miller, Regan et al., 2004) in the International Student Offshore Design Competition (ISODC) 2004. The terminal design location was off the coast of West Africa at 40.0m water depth, where the wave characteristics are as given in Table 1-1.

Table 1-1. Wave Characteristics

Significant Wave Height	2.29 m
Peak Period	15.0 s
Wave Length	375.3 m

They defined a few constraints as the main parameters of their design which are given below:

- Will be permanently moored in 40 m of water
- Must be able to process 1 billion cubic feet (bcf) of gas per day
- Must have a storage capacity of 330,000 m3 of LNG
- Must sustain offloading operations in a 1-year storm event
- Must sustain shoreline delivery of LNG in a 10-year storm event
- Must survive a 100-year storm event

The environmental conditions for the 40.0 m water depth for the 1-year, 10-year, 100-year return periods were given as shown in Table 1-2 and the current profile is given in Table 1-3. For the analysis the current is assumed to act in the same direction as that of the waves.

Table 1-2. Environmental Conditions

Return Period	Significant Wave Height [m]	Peak Period [s]	Period of Maximum Wave [s]
1-year	2.29	15.0	13.4
10-year	2.66	15.3	13.6
100-year	3.04	15.5	13.8

Table 1-3. Current Profile

Current velocity at surface (m/s)	1.0
Current velocity at 25 % of site depth (m/s)	0.8
Current velocity at 75 % of site depth (m/s)	0.6
Current velocity at sea floor (m/s)	0.5

The allowable relative body displacements due to the offloading arm constraints are as given below:

Vertical : ± 2.0m
Horizontal : ± 1.7m

1.3 Literature Review

Kodan(1984) analyzed the hydrodynamic interaction between two parallel slender bodes using the strip method. Sannasiraj et al.(2000) studied the diffraction-radiation of multiple floating structures in directional waves using Finite Element Method. The study showed that interaction tends to become less in the higher frequency zone. The responses were analyzed against the scatter parameter and the resonance of the water column in the gap was noted to occur when $\frac{\omega^2 B_T}{g} = n\pi, (n = 1, 2, ...)$ where B_T (=2B+q),

is the total breadth of the structure and q is the gap between the bodies. Choi and Hong et al. (2002) made use of Higher Order Boundary Element Method (HOBEM) to study the interaction problem. Huijsmans et al. (2001) used the 'lid' technique to suppress the 'pumping mode' in the gap between two bodies lying close to each other The results for multi body analysis using single body hydrodynamics was compared with the lid technique and the Gauss Quadrature approach which is directly related to the accuracy of the integration of the Green's function. It was concluded that multibody hydrodynamics suffers from serious inaccuracies when analysed with linear diffraction codes. Buchner et al. (2001) studied the interaction effects between a LNG Carrier in side-by-side mooring to a LNG FPSO. A new free surface boundary condition was developed in the gap between the two bodies to resolve the problem of occurrence of high velocities in the gap, as a result of the potential theory application which ignores the viscous effects. It is found that hydrodynamic cross coupling should not be ignored when analyzing bodies in close proximity to each other. Buchner et al. (2004) studied the interaction problem of a LNG Carrier alongside a Gravity Based Structure in shallow water. Lee and Kim (2005) compared the two-body resonant interaction using fully coupled method and partially coupled method. Inoue et al. (1999) estimated the wave drift forces using the momentum approach which was extended to multibody systems by Nori (1994) and Liu (1998). Huijsmans et al. (2001) made use of pressure integration technique for the calculation of wave drift forces. Hong et al (2005) studied the hydrodynamic interaction of side-by-side moored multiple vessels experimentally and numerically using 9-node bi-quadratic HOBEM. The model test results showed that Helmholtz resonance is not significant compared to the numerical results in the head sea case. They concluded that wave drift force is not significantly influenced by roll resonance motion for side-by-side moored vessels.

1.4 Problem Description

The problem being analyzed is the hydrodynamic interaction between a side-by-side moored Floating LNG Terminal and a LNG Carrier. The interactions between the

two floating bodies is an interesting area of study mainly due to the resonance of the entrapped water column between the two vessels (known as Helmholtz resonance). This needs to be analyzed to accurately predict the motion characteristics of the system. The interaction effects due to wind was not analyzed for the sake of simplicity. Previous studies have shown that the second order drift forces can be significant for a multi-body system and can be a critical factor in the design of the mooring system. The analysis of mean drift forces (using Newman's approximation) is also employed in the present study.

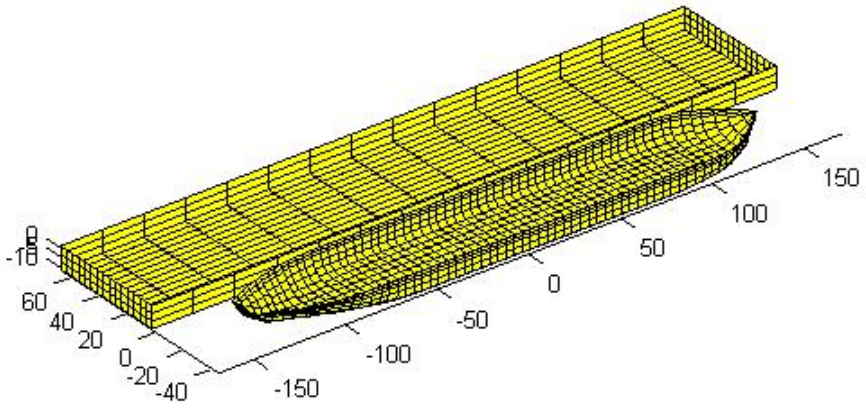

Figure 1-1. WAMIT model of the two-body system

The layout of the two body system is as shown in Figure 1-1. The LNG Terminal and the LNG Carrier models are made up of 2057 and 1042 panels respectively. The panel size is chosen as 4.0 m, which is approximately $1/8^{th}$ of the wave length corresponding to the maximum wave frequency considered. The dimensions of the two bodies are given in Table 1-4. The gap between the two vessels is set as 4.0 m. The

system is placed at 40.0 m water depth. The LNG Terminal will be placed off the coast of West Africa, where swells are predominant. This makes the wave heading during storm conditions more predictable. Thus a spread moored system can be made use of rather than a costlier turret moored system. In a spread moored system the mooring lines which are anchored at the sea bottom hold the vessel in position. Figure 1-2 shows the 12-point spread moored system for the LNG Terminal. In a turret moored system, the vessel is connected to a turret, through a swivel joint, which enables the vessel to rotate around the turret so that the fore end of the vessel is always facing the weather. This is known as ‘weather waning’. Even though turret moored system has got many advantages over spread moored system, the costs of the former is substantially higher and it makes a good engineering sense to opt for a spread moored where the wave headings do not vary much.

The mooring arrangement of the LNG Terminal is shown in Figure 1-2. Table 1-5 shows the position of the bottom end of the mooring lines with respect to the body fixed coordinate system, whose origin is at the center of the interior water plane.

Table 1-4. Main Particulars of the Floating Bodies

	LNG Terminal	LNG Carrier
Length [m]	340	280
Breadth [m]	65	43.2
Depth [m]	33	26.1
Draft [m]	11.6	12.1
KG [m]	17.4	8.528
Transverse radius of gyration [m]	21.61	14.51
Longitudinal radius of gyration [m]	98.73	70.43
Yaw radius of gyration [m]	99.93	71.93

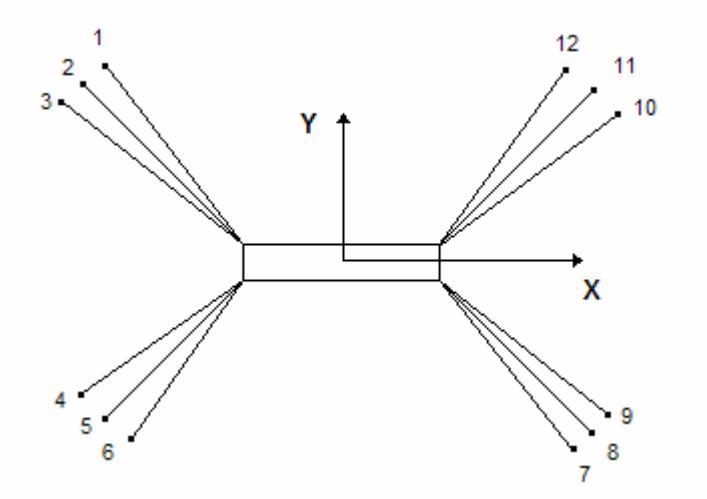

Figure 1-2. Plan View of the LNG terminal mooring system

Table 1-5. Co-ordinates of the Mooring Line Bottom End

Mooring Line #	X	Y
1	-353.3	250.74
2	-371.62	234.12
3	-388.39	215.62
4	-388.39	-215.62
5	-371.62	-234.12
6	-353.3	-250.74
7	353.3	-250.74
8	371.62	-234.12
9	388.39	-215.62
10	388.39	215.62
11	371.62	234.12
12	353.3	250.74

The mooring line selected by the student team after considering relevant API requirements has the characteristics as given in Table 1-6.

Table 1-6. Mooring Line Properties

Type	Chain
Diameter	114.3 mm
Breaking Strength	12,440 kN
Axial Stiffness	1.004E06 kN
Mass per unit length	248.0 kg/m
Inertia coefficient (Inertia force per unit length per unit acceleration)	221
Drag coefficient (Drag force per unit length at unit relative velocity squared)	658
Minimum length	285.0 m

The hawser/ breast lines connecting the LNG Carrier to the LNG Terminal during the offloading operation are arranged as shown in Figure 1-3.

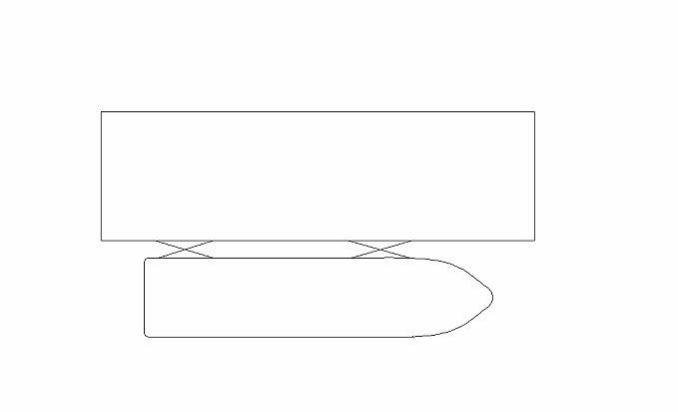

Figure 1-3. Hawser arrangement

The properties of the hawser/ breast line are as given in Table 1-7.

Table 1-7. Hawser Line Properties

Type	Polyester rope
Diameter	230 mm
Breaking Strength	15,515 kN
Axial Stiffness	38.79 kN
Mass per unit length	35.6 kg/m
Inertia coefficient (Inertia force per unit length per unit acceleration)	31.7
Drag coefficient (Drag force per unit length at unit relative velocity squared)	65

1.5 Analysis and Design Tools

Two main commercial software tools are used for the analysis.

WAMIT is a frequency domain hydrodynamic analysis software program developed at MIT (Lee, C.H., 1995). This program is widely used in the offshore industry for hydrodynamic analysis. Inputs to program include a geometric description of the wetted surface area (as shown in Figure 1-1), mass matrix, centre of gravity information, external stiffness matrix, external damping matrix and wave information. The output from WAMIT contains added mass, potential damping, motion RAOs, wave exciting forces and wave drift forces.

WINPOST is program developed at Texas A&M University by Dr. M. H. Kim for the analysis of coupled hull, mooring and riser system (Kim, M. H., 1997). It makes use of the added mass, damping and wave force information from the WAMIT output. The analysis is done in three steps. First, the uncoupled analysis is done to find the equilibrium position of the mooring system. This is followed by a coupled static analysis to estimate the equilibrium position of the coupled system. Subsequently, a time domain or frequency domain analysis is done to obtain the dynamic response of the coupled system.

2. HYDRODYNAMIC ANALYSIS

2.1 Introduction

The analysis is based on potential theory. The fluid is assumed to be incompressible, inviscid and irrotational. The flow, then can be represented by the velocity potential. The Laplace equation is governing equation and the boundary conditions are satisfied. The velocity potential can be written as

$$\Phi(x;t) = \mathrm{Re}[\phi(x)e^{i\omega t}] \tag{2.1}$$

where Re denotes the real part and ω is the angular frequency.
It satisfies the Laplace equation.

$$\nabla^2\Phi(x,y,z,t) = 0 \tag{2.2}$$

For diffraction-radiation boundary value problem, the velocity potential is considered as a sum of incident potential, Φ_I, scattered potential, Φ_s and radiation potential, Φ_R.

The radiation potential can be considered as the potential due to sum of potential due to 6 modes of motion, i.e. $\Phi_R = \sum_{j=1}^{6}\Phi_j$

The total potential can hence be expressed as

$$\Phi(x,y,z,t) = \Phi_I + \Phi_S + \sum_{j=1}^{6}\Phi_j$$

$$= \Phi_I + \Phi_S + \sum_{j=1}^{6}\dot{\delta}_j\phi_j \tag{2.3}$$

where ϕ_j is the velocity potential of the radiated waves due to unit body velocity and $\dot{\delta}_j$ is the complex amplitude of the body generated velocity in j^{th} mode, $\dot{X}_j$

$$\dot{X}_j = \dot{\delta}_j e^{-i\omega t} \qquad \text{(Sannasiraj, 2000)} \qquad (2.4)$$

For a multibody system there will 6 x NB degrees of freedom assuming each body as a rigid body, where NB is the number of bodies (Lee & Choi, 1998). The total potential can then be expressed as

$$\Phi(x, y, z, t) = \Phi_I + \Phi_S + \sum_{j=1}^{6\times NB} \dot{\delta}_j \phi_j \qquad (2.5)$$

Using Green's second identity, the solution to the boundary integral equation can be written in terms of the potential

$$\alpha(\vec{x})\Phi(\vec{x}) = -\sum_{j=1}^{NB} \int_{S_j} \Phi(\vec{\xi}) \frac{\partial G(\vec{x}, \vec{\xi})}{\partial \vec{n}} dS + \sum_{j=1}^{NB} \int_{S_j} \frac{\partial \Phi(\vec{\xi})}{\partial \vec{n}} G(\vec{x}, \vec{\xi}) dS \qquad (2.6)$$

where $\alpha(\vec{x})$ is the solid angle, NB the number of bodies, G the wave Green function (Wehausen and Laitone, 1960) and $\vec{n}$ the unit normal vector on the body surface pointing towards the fluid, S_j the wetted surface area of the j^{th} body.

At certain frequencies known as irregular frequencies the above integral equation may not have a unique solution. This might lead to results which might be incorrectly interpreted as the interaction effects in case of multiple bodies. To avoid such confusion the irregular frequencies need to be removed and this is done by distribution of additional dipoles on the interior water plane (Hong, 1987).

$$\alpha(\vec{x})\Phi(\vec{x}) = -\sum_{j=1}^{NB}\int_{S_j}\Phi(\vec{\xi})\frac{\partial G(\vec{x},\vec{\xi})}{\partial \vec{n}}dS - \sum_{j=1}^{NB}\int_{S_{Ij}}\Phi(\vec{\xi})\frac{\partial G(\vec{x},\vec{\xi})}{\partial \vec{n}}dS + \sum_{j=1}^{NB}\int_{S_j}\frac{\partial \Phi(\vec{\xi})}{\partial \vec{n}}G(\vec{x},\vec{\xi})dS$$

(2.7)

where S_{Ij} denotes the interior water plane of the j^{th} body (Lee & Kim, 2005)

2.1.1 Time Domain Analysis

The equation of motion in time domain for multiple bodies can be obtained by expanding the transient equation of motion for a single body (Buchner, 2001).

$$\sum_{j=1}^{6}\left(M_{i,j} + A_{i,j}\right)\ddot{x}_j + \int_{-\infty}^{t} R_{i,j}(t-\tau)\dot{x}_j(\tau)d\tau + C_{i,j}x_j = F_i(t) \qquad (2.8)$$

where

x_j = motion in j-direction

$F_i(t)$ = external force in i^{th} mode including the first and second order wave exciting forces and nonlinear drag forces from the Morison's formula

$M_{i,j}$ = mass matrix

$A_{i,j}$ = added mass matrix

$R_{i,j}$ = retardation function matrix

$C_{i,j}$ = hydrostatic restoring force matrix

Mass matrix of a body is defined as

$$M = \begin{bmatrix} m & 0 & 0 & 0 & mz_G & -my_G \\ 0 & m & 0 & -mz_G & 0 & mx_G \\ 0 & 0 & m & my_G & -mx_G & 0 \\ 0 & -mz_G & my_G & I_{11} & I_{12} & I_{13} \\ mz_G & 0 & -mx_G & I_{21} & I_{22} & I_{23} \\ -my_G & mx_G & 0 & I_{31} & I_{32} & I_{33} \end{bmatrix} \quad (2.9)$$

where m is the body mass and the centre of gravity is at (x_G, y_G, z_G) and the moment of inertia is defined by

$$I_{ij} = \iiint_{V_B} \rho_B [\vec{x}.\vec{x}\delta_{ij} - x_i x_j] dV \quad (2.10)$$

where V_B is the body volume and δ_{ij} is the Kroenecker-delta function.

2.1.2 Mooring Line Dynamics

The mooring lines can be considered as slender structures with little bending stiffness. The restoring effects of these lines to the platform come from a combination of the gravity force of the line, line geometry and tension (Ran, 2000). The mooring lines are modeled using slender rod theory.

If the axial deformation of the rod is considered linear and small, the inextensibility condition for rods can be expressed as

$$\frac{1}{2}(\vec{r}'.\vec{r}'-1)=\frac{T}{AE}\approx\frac{\lambda}{AE} \tag{2.11}$$

where $\vec{r}'$ is the unit tangent vector to the space curve, T is the tension, AE is the axial stiffness (Ran, 2000). λ is a scalar function defined as

$$\lambda = T - EI\kappa^2 \tag{2.12}$$

where EI is the bending stiffness and κ is the curvature of the line. The equation of rod subjected to self weight, hydrostatic and hydrodynamic forces in water becomes

$$\rho\ddot{\vec{r}} + C_a\rho_w\ddot{\vec{r}}^n + (EI\vec{r}'')'' + (\vec{\lambda}\vec{r}')' = \tilde{\vec{w}} + \tilde{\vec{F}}_d \tag{2.13}$$

where

$\tilde{\vec{w}} = \vec{w} + \vec{B}$, sum of weight and buoyancy forces of the rod per unit length

$\tilde{\vec{F}}_d = C_M\dot{\vec{V}}^n + C_D|\vec{V}^n - \dot{\vec{r}}^n|(\vec{V}^n - \dot{\vec{r}}^n)$ where C_M is the inertial coefficient (inertia force per unit length per unit normal acceleration), C_D is the drag coefficient (drag force per unit length per unit normal velocity), $\vec{V}^n$ is the fluid velocity normal to the rod centerline and $\dot{\vec{V}}^n$ is the fluid acceleration normal to the rod centerline.

The connection between the mooring lines and the floating body is modeled as a combination of linear springs which defines the relation of translational motion between the body, at the connecting point) and the top of the mooring line, and rotational springs which defines the relation between the rotation of the body and the tangential direction of the line (Ran, 2000).

2.2 Uncoupled Analysis in Frequency Domain

Frequency domain analysis refers to the solution of the equations of motion by methods of Laplace or Fourier transforms. As a result of the frequency domain analysis we get the unknowns (body motions, body forces, mooring line tensions, mooring line displacements, etc.) as a function of frequency.

The uncoupled analysis in frequency domain is accomplished using WAMIT which gives the hydrodynamic coefficients. The global co-ordinate system is set up as shown in Figure 2-1. In uncoupled analysis the bodies are considered as freely floating without any external restraints like mooring lines.

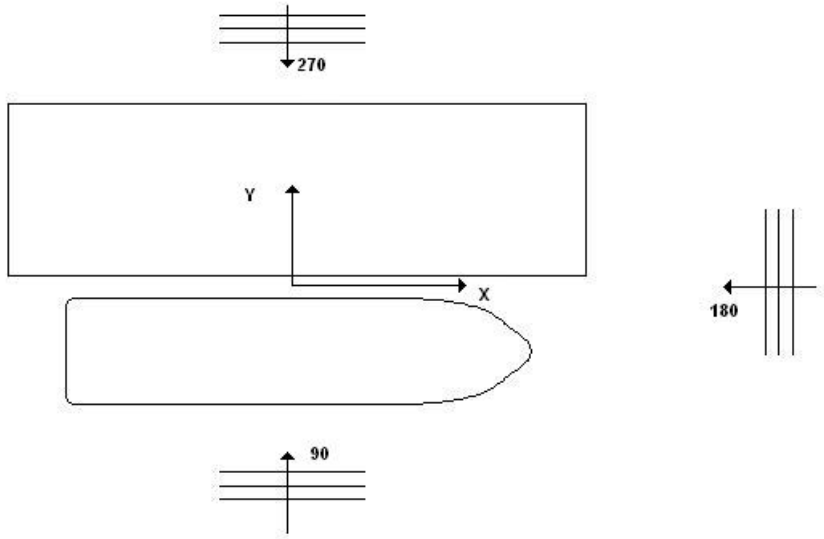

Figure 2-1. Global co-ordinate system

The natural frequencies in heave, roll and pitch estimated using the hydrodynamic coefficients obtained from WAMIT are given in Table 2-1.

Table 2-1. Natural Frequencies

	LNG Terminal	LNG Carrier
Heave [rad/s]	0.5238	0.6321
Roll [rad/s]	0.4717	0.6125
Pitch [rad/s]	0.5368	0.7679

2.2.1 Irregular Frequency Effects

The boundary value problem defined in section 2.1 may not have a unique solution at certain frequencies known as irregular frequencies. The derived responses at such frequencies may show a behaviour similar to that of the interaction effects. Hence to accurately identify the interaction effects we need to remove the irregular frequency effects. WAMIT does provide an option to remove the irregular frequency effects by discretizing the free surface.

Figure 2-2 shows the heave response of the LNG Carrier with and without irregular frequencies at 270 deg wave heading. It can be gathered from the figure that in the range of frequencies analyzed there is no significant effect of irregular frequencies and hence the irregular frequency effects can be neglected for the present study.

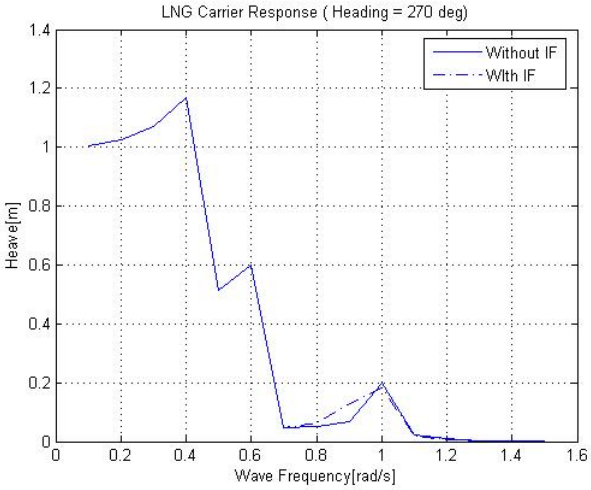

Figure 2-2. LNG Carrier heave response

2.2.2 Added Mass and Damping Coefficients

Added mass for both LNG Terminal and LNG Carrier shows a spiky behavior at around 0.7 rad/s and can even become negative due to interaction effects. Figure 2-3 shows the added mass coefficients for the terminal and the LNG Carrier. The damping coefficients have also got sharp peaks at 0.7 rad/s due to the interaction. Figure 2-4 shows the damping coefficients of the terminal and the carrier.

Situations where the wave heading angles range from 90 degrees to 270 degrees are considered and the multi-body case compared with single-body case to identify the interaction effects by analyzing the motion responses, wave exciting and mean drift forces and moments in the frequency domain.

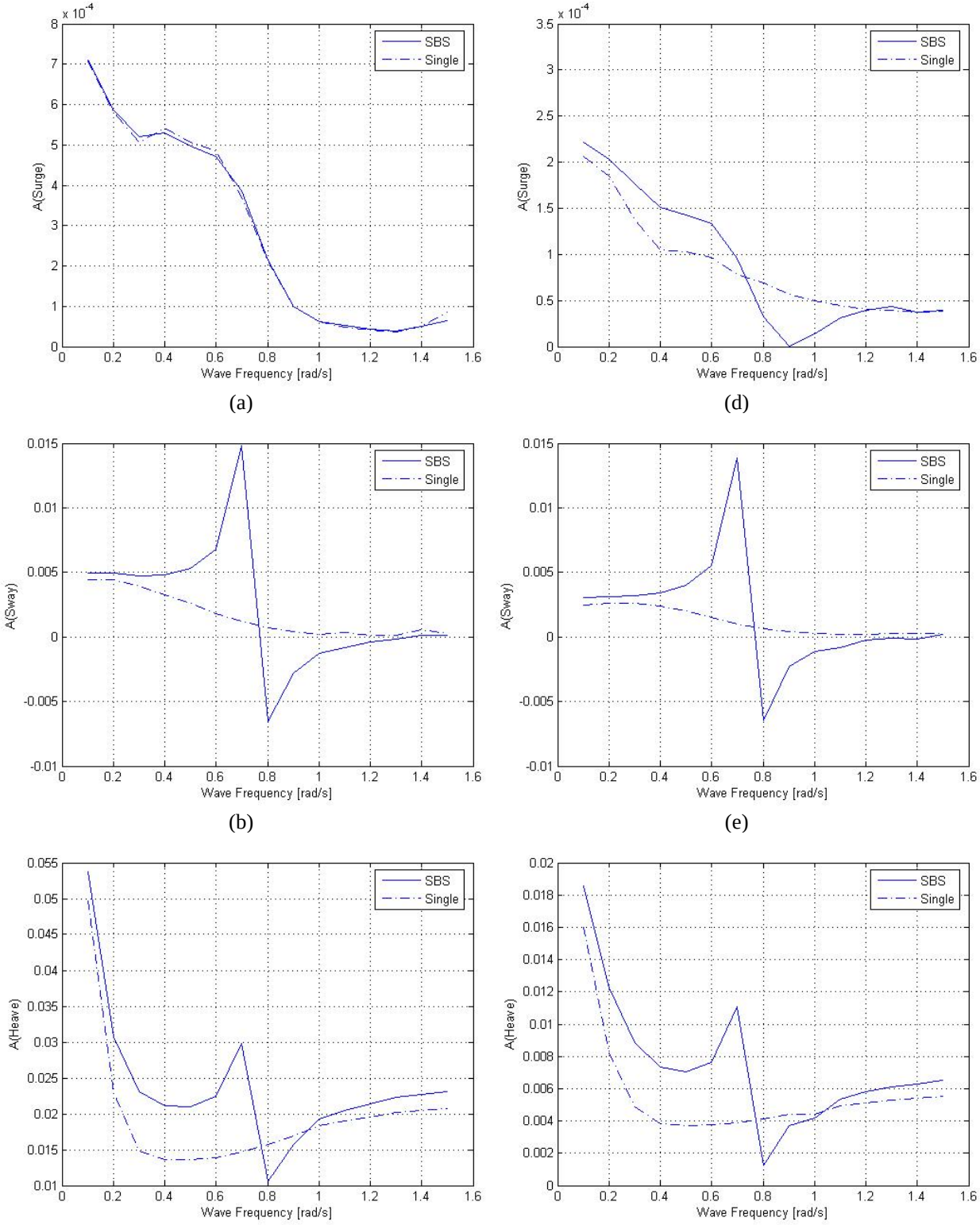

Figure 2-3. Added mass coefficients of terminal (a-c) and carrier(d-f)

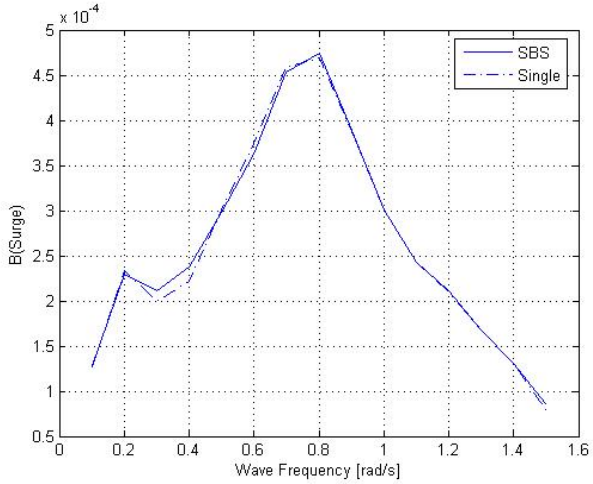

(a)

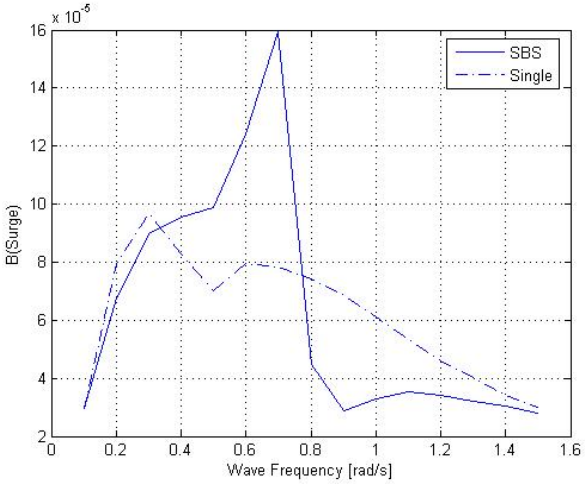

(d)

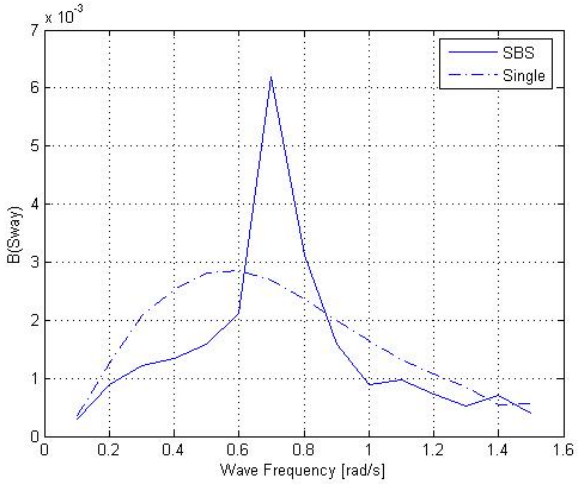

(b)

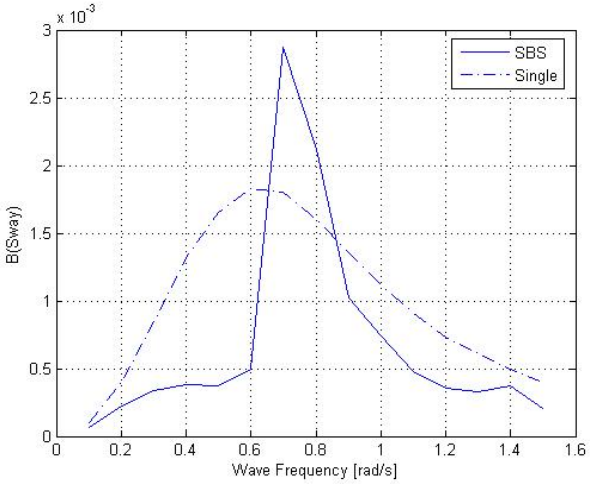

(e)

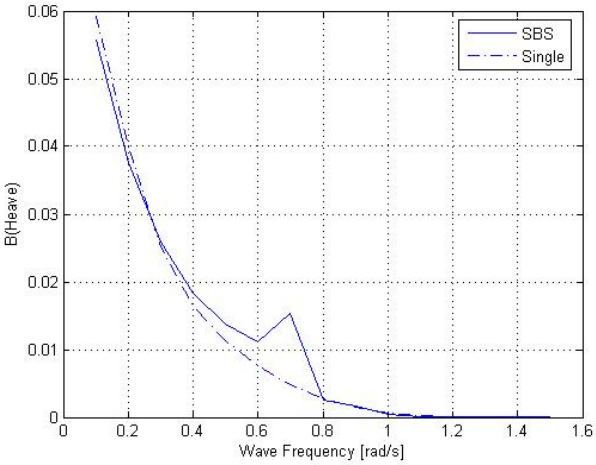

(c)

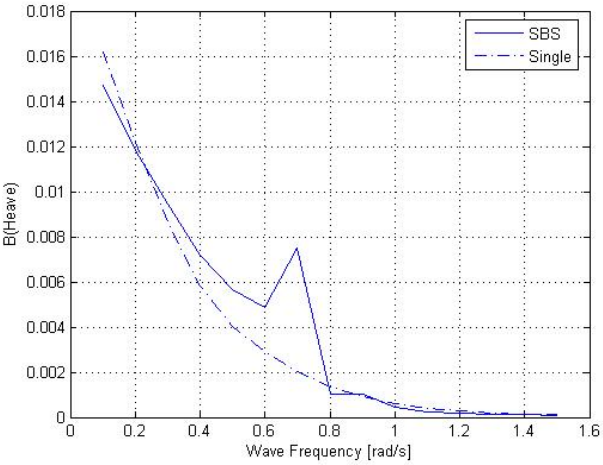

(f)

Figure 2-4. Damping coefficients of terminal (a-c) and carrier (d-f)

2.2.3 Case 1. Wave Heading = 90 Degrees

This is the beam sea condition with the LNG Carrier on the weather side. Figure 2-5 shows the motion responses of the terminal. Figure 2-5(a), (e) and (f) shows that even though there is no response in the single body case for surge, pitch and yaw, there exists some response in the two body case due to interaction. The waves get reflected at the carrier in a non-symmetrical fashion and this causes the surge, pitch and yaw response in the terminal. At higher frequencies more waves get reflected back at the carrier itself and less energy is carried forward towards the terminal. The effect can be seen as a reduced heave response at higher frequencies compared to the single body case.

Figure 2-6 shows the motion response of the LNG Carrier for 90 deg wave heading and Figure 2-7 shows the relative motion response for 90 deg wave heading. Figure 2-6(c) shows that the heave response of the LNG Carrier at 0.6 rad/s can be more than 1.0 m higher than the single-body case. Figure 2-7(b) shows the relative sway response having a high of around 1.2 m for wave frequencies less than 0.4 rad/s. It can be seen from Figure 2-7(c) that the relative heave response can be as high as 3.5 m when the wave frequency is around 0.6 rad/s. The reason can be found in Figure 2-6(c).

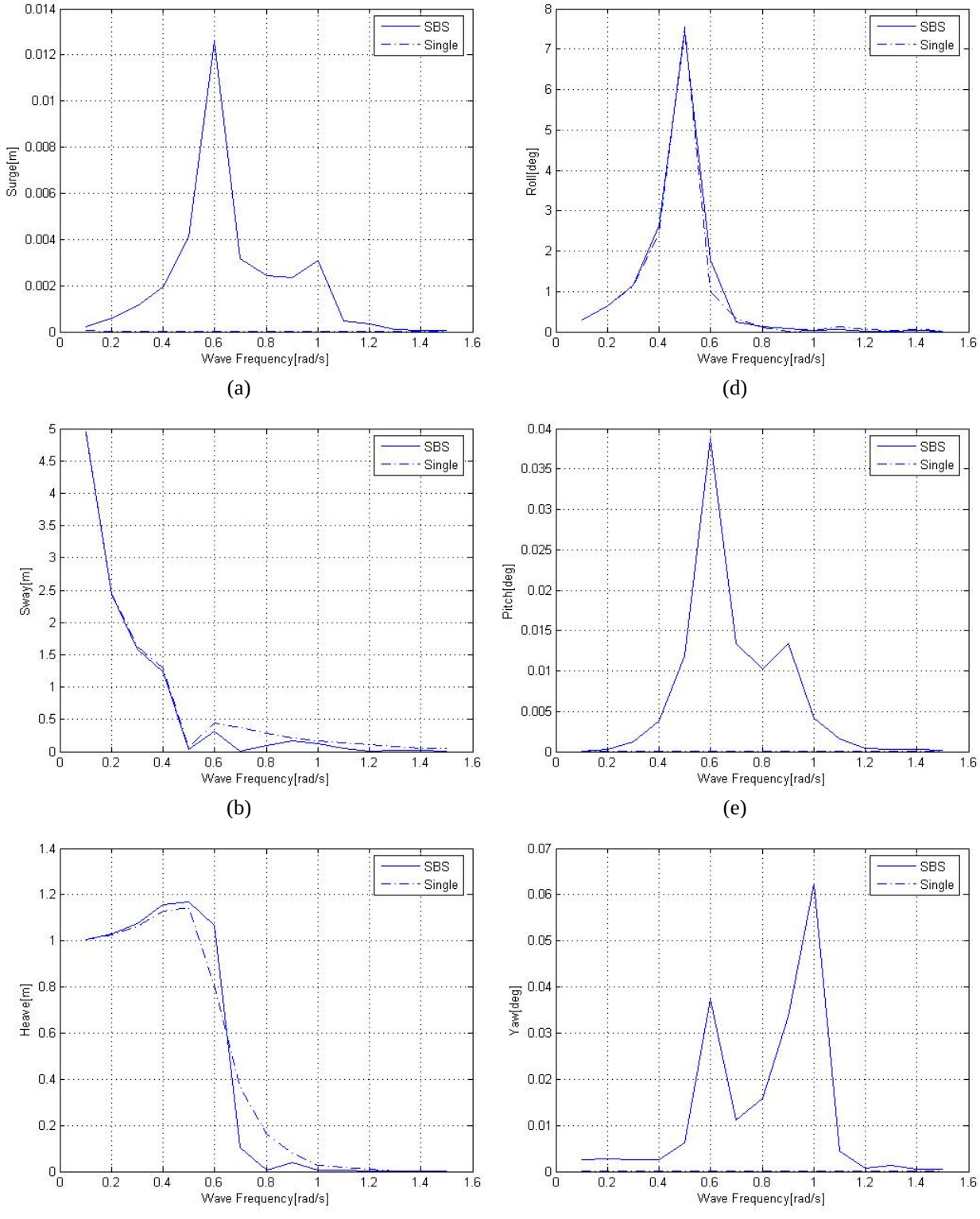

Figure 2-5. Motion response of LNG Terminal for 90 deg wave heading

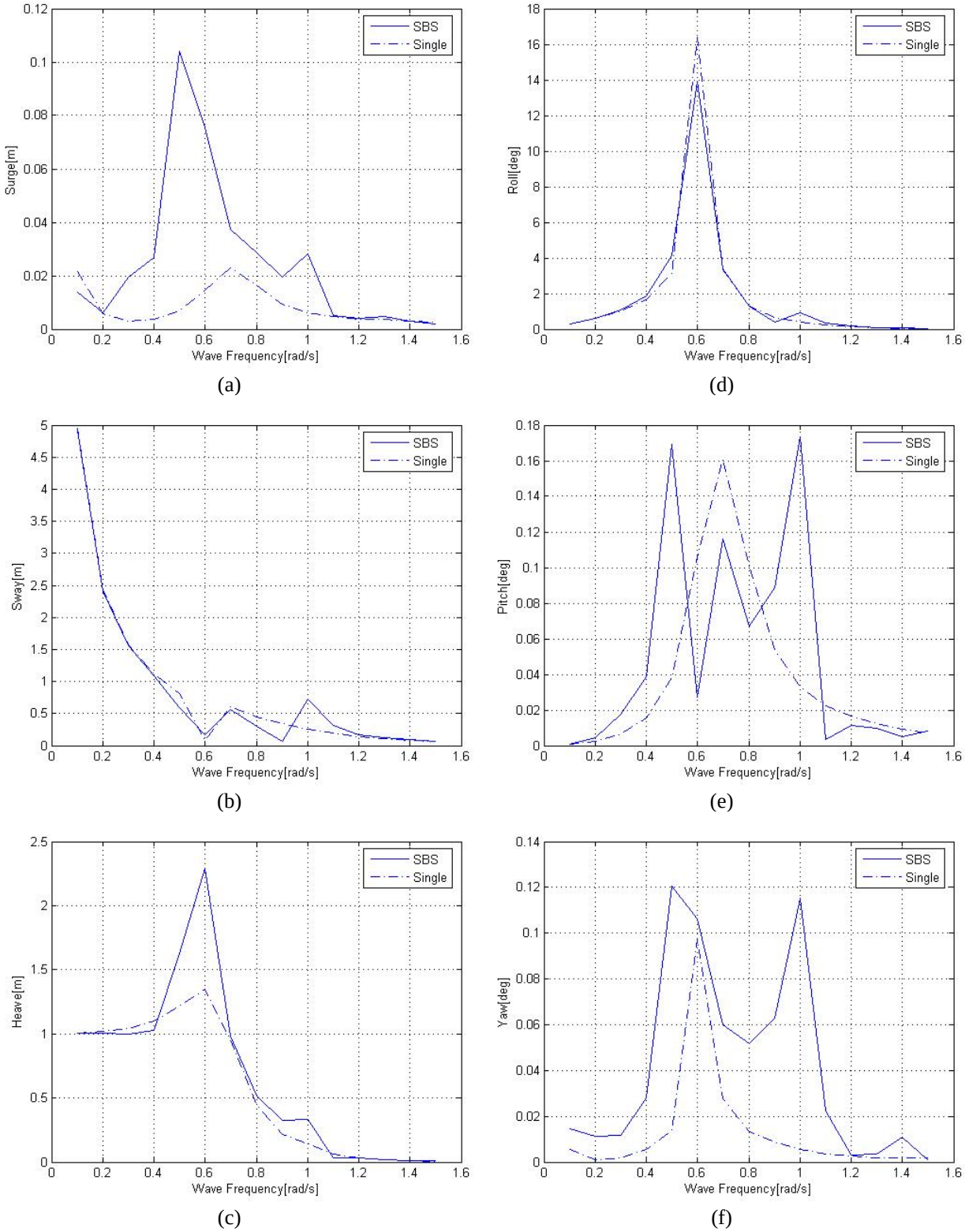

Figure 2-6. Motion response of the LNG Carrier for 90 deg wave heading

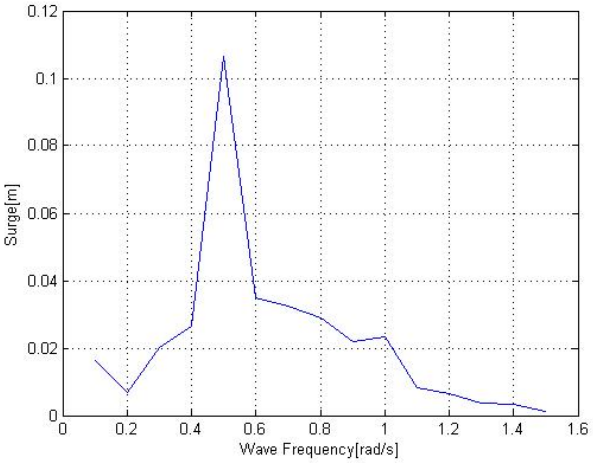

(a)

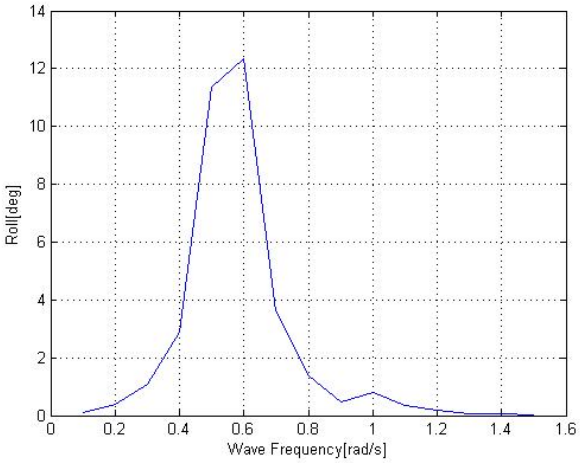

(d)

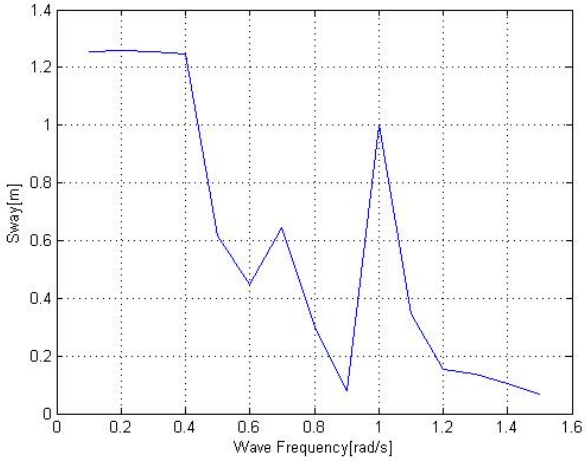

(b)

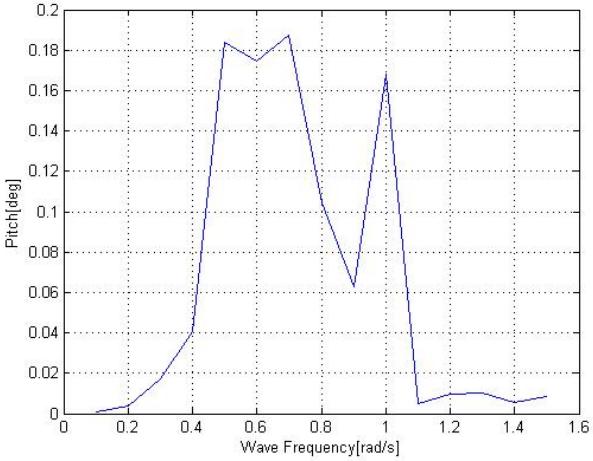

(e)

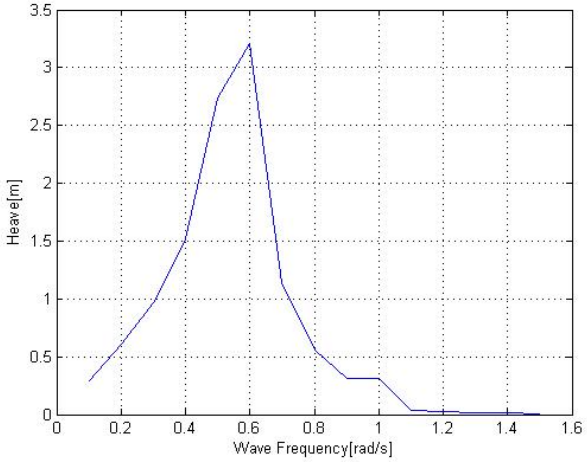

(c)

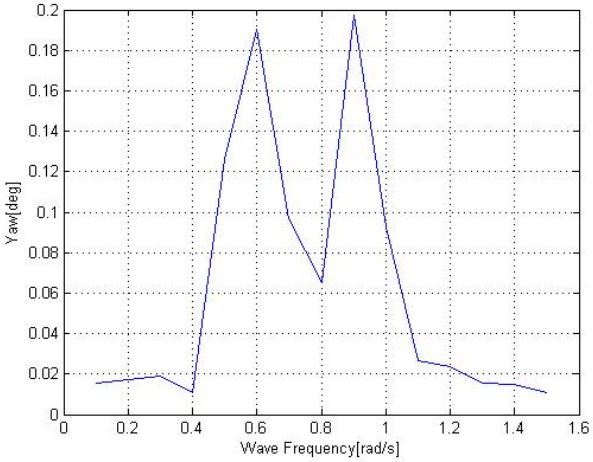

(f)

Figure 2-7. Relative motion response for 90 deg wave heading

The heave response of the carrier in the two body case is almost double that of the one in the single body case. The reason being the occurrence of standing waves in the region between the two the two bodies with the incident waves and the waves reflected from the terminal. The relative heave response is the highest in the 90 deg wave heading case compared to other angles of wave heading and due to this particular reason, it is preferred to always keep the terminal on the seaward side so as to enjoy the least downtime even during rough weather conditions.

Figure 2-8 shows the wave exciting forces on the LNG Terminal for 90 deg wave heading. The interaction effects can be clearly seen in all the figures. In Figure 2-8(b-d), it can be seen that the force is less than that in the single body case because the carrier partially shields the terminal from the incident waves. However, at 0.7 rad/s the force is a little higher than that in the single body case because of the ‘helmholtz’ resonance in the region between the two bodies.

Figure 2-9 shows the wave exciting forces on the LNG Carrier for 90 deg wave heading. The interaction effects can be clearly observed in all the figures. Figure 2-10 shows the mean drift forces on the terminal and Figure 2-11 shows the mean drift forces on the carrier. It can be seen that at 1 rad/s there is a large sway drift force acting on the bodies toward each other. The accurate estimation of this force is important for fender system design.

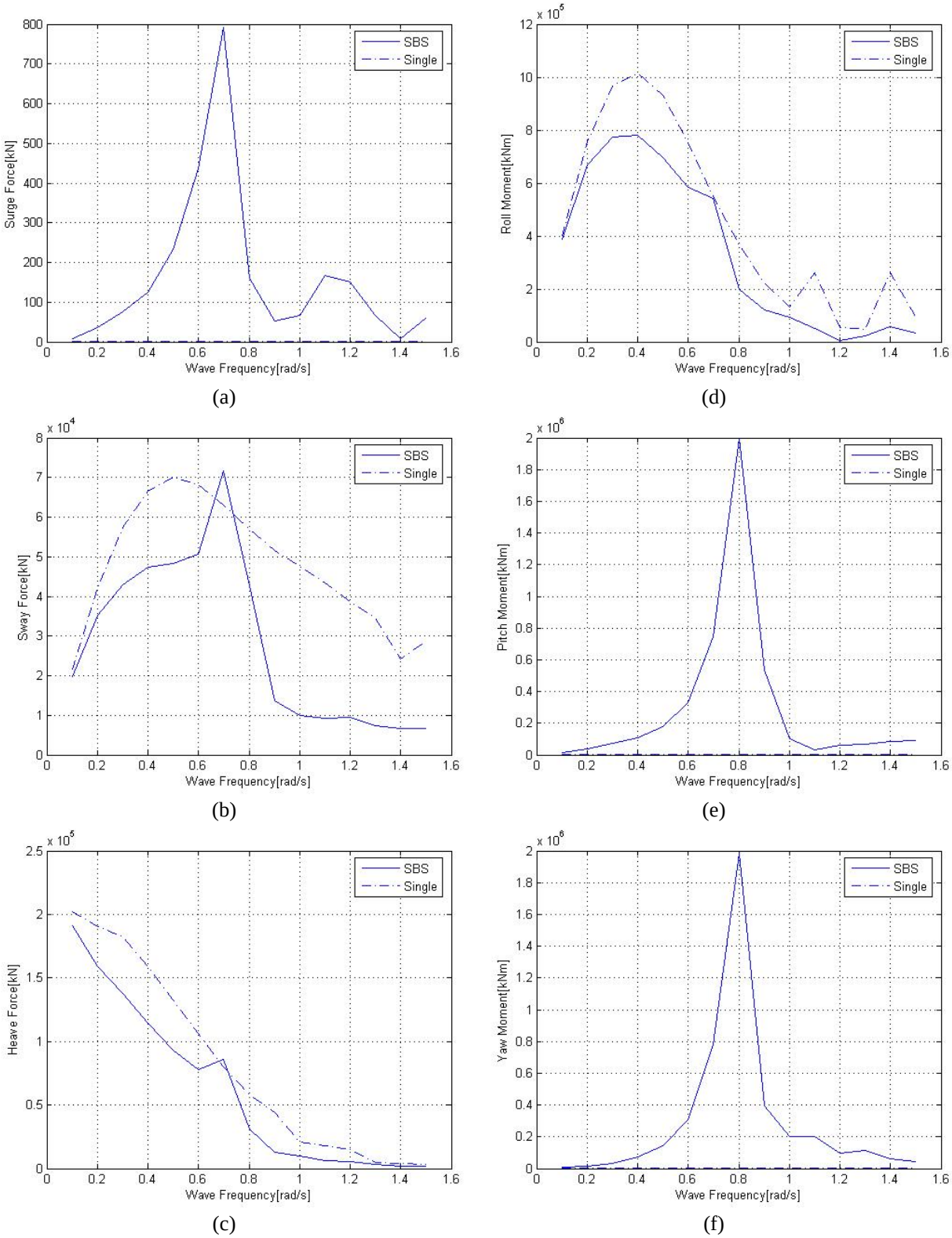

Figure 2-8. Wave exciting force on LNG Terminal for 90 deg wave heading

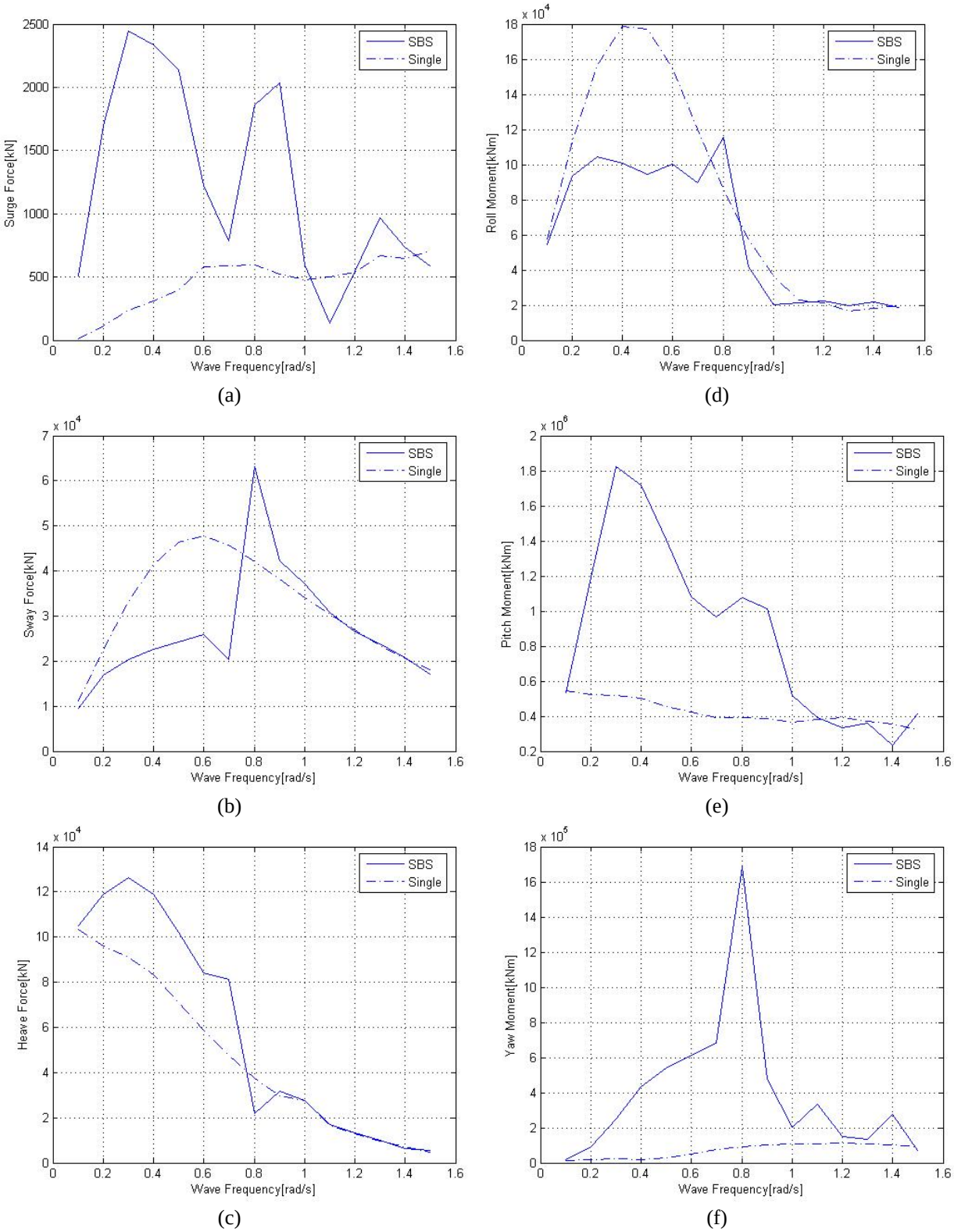

Figure 2-9. Wave exciting force on LNG Carrier for 90 deg wave heading

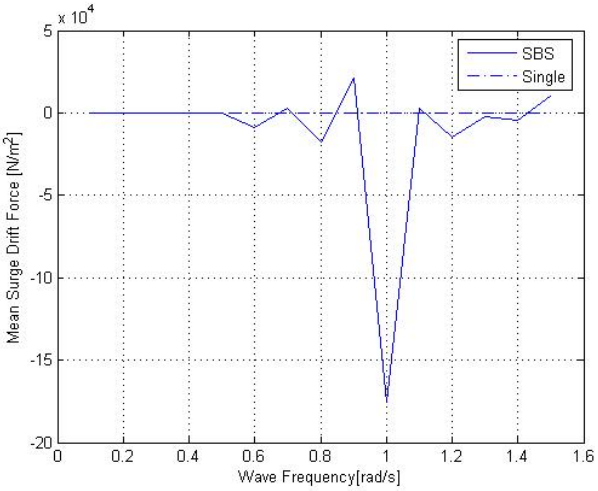

(a)

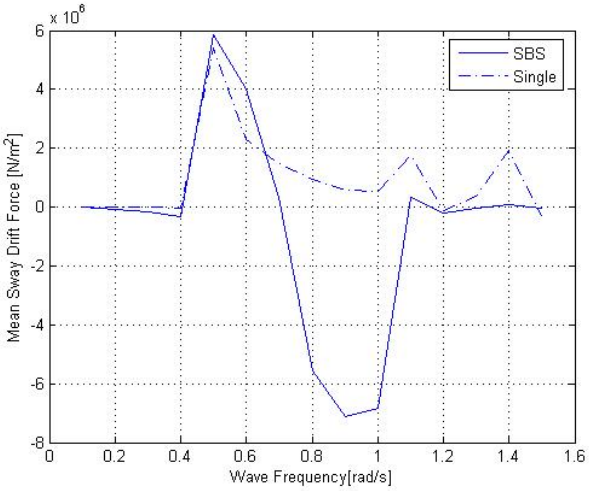

(b)

Figure 2-10. Mean drift force on LNG Terminal for 90 deg wave heading

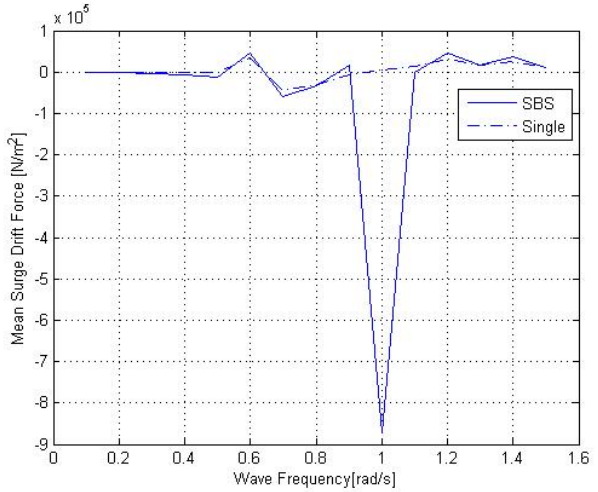

(a)

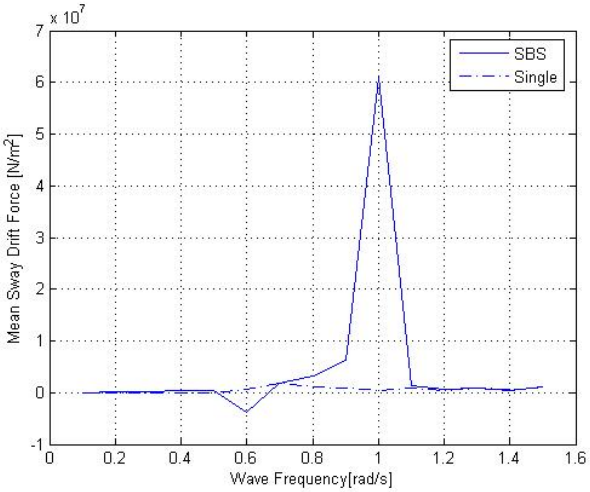

(b)

Figure 2-11. Mean drift force on LNG Carrier for 90 deg wave heading

This excessive force could also be an over prediction due to the inherent assumptions in potential flow theory. Buchner et al(2004) showed that this is a result of the excessive flow velocities in the gap between the two bodies as a result of neglecting the viscosity effects in potential flow.

2.2.4 Case 2. Wave Heading = 135 Degrees

The responses when the wave heading is 135 deg is not significantly different for the single body and multi-body cases. Figure 2-12 shows the motion response of the LNG Terminal for 135 deg wave heading. The response is not significantly different from the single body case. Figure 2-13 shows the motion response of the LNG Carrier. The response in multi-body case is slightly greater than the single body case due to reflection of waves from the LNG Terminal. Figure 2-14 shows the relative motion response for the 135 deg wave heading.

Figure 2-15 shows the wave exciting force and moments on the terminal and Figure 2-16 shows the wave exciting forces and moments on the carrier. As in the 90 deg wave heading case, in the 135 deg case too there exists large sway drift forces at higher frequencies trying to push the two bodies towards each other. Figure 2-17(b) shows the mean sway drift force on the LNG Terminal and Figure 2-18(b) shows the mean sway drift force on the LNG Carrier.

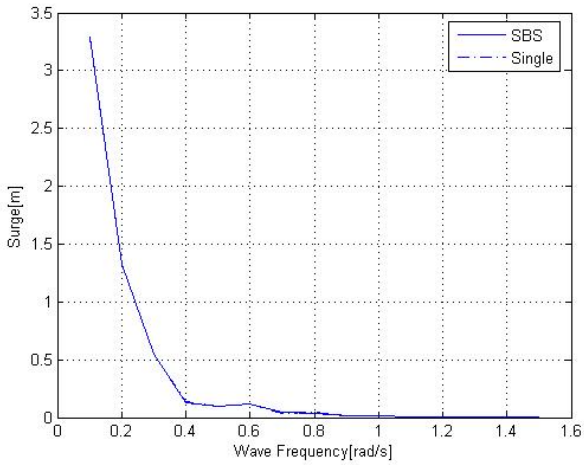

(a)

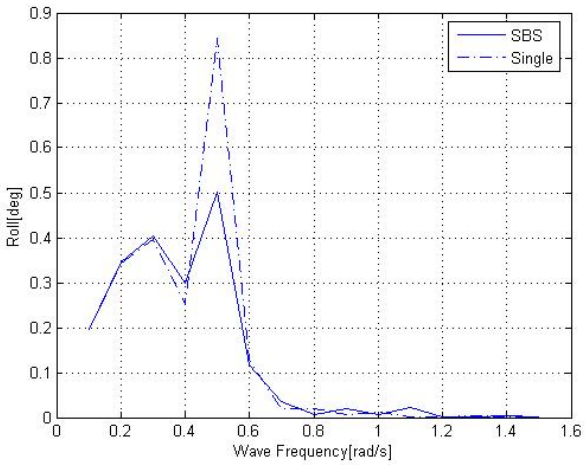

(d)

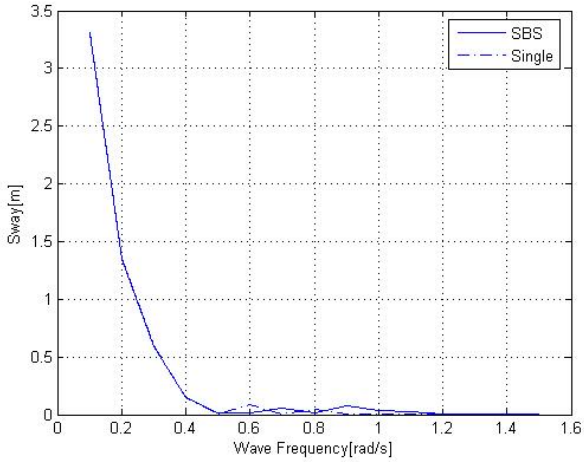

(b)

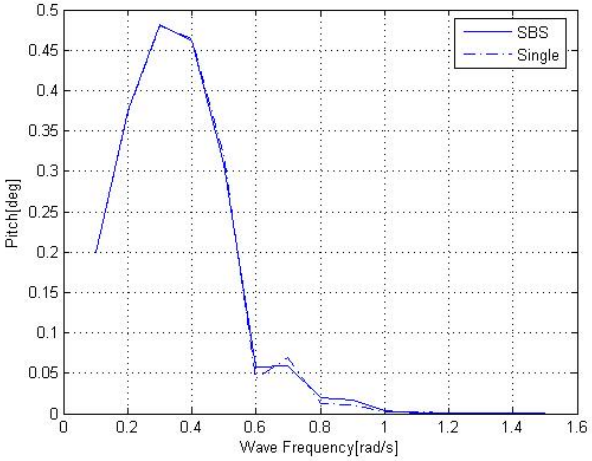

(e)

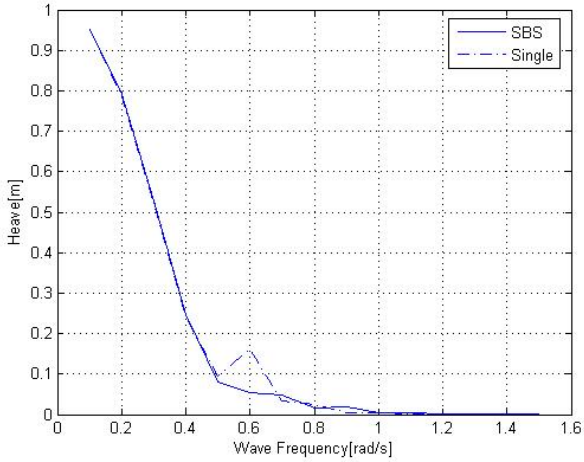

(c)

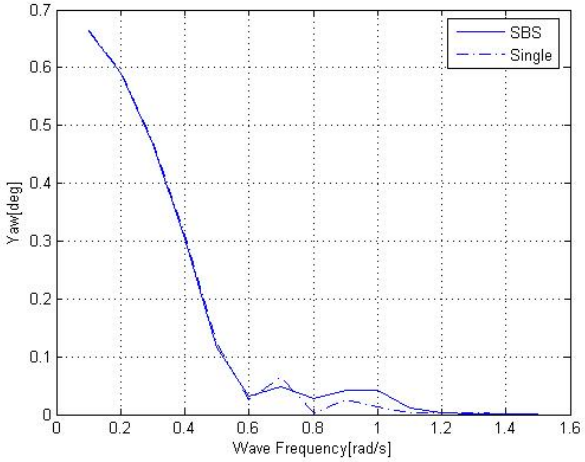

(f)

Figure 2-12. Motion response of LNG Terminal for 135 deg wave heading

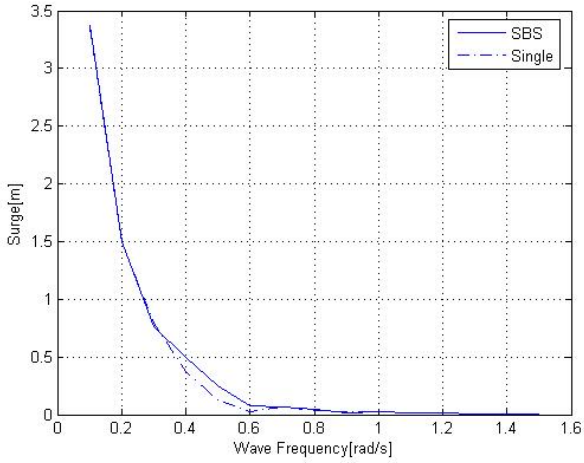

(a)

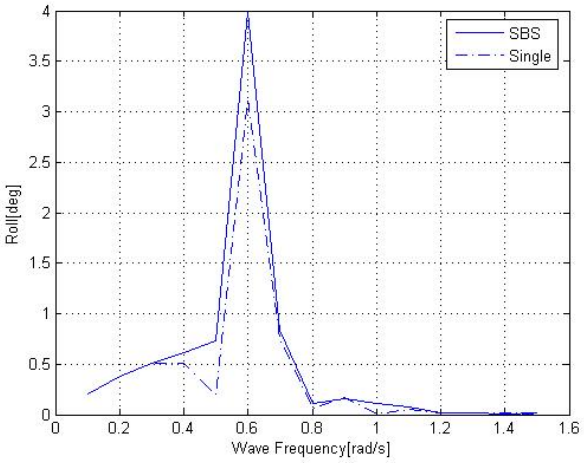

(d)

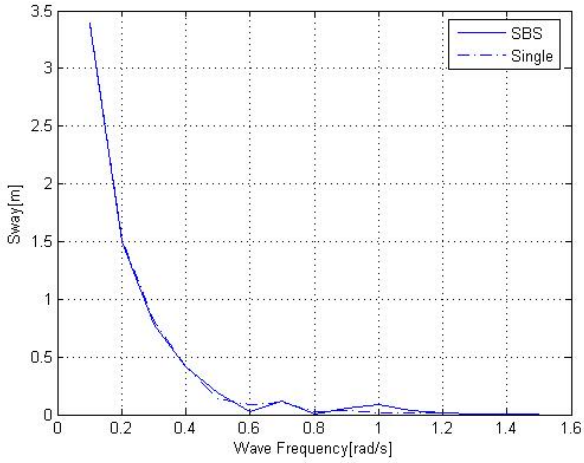

(b)

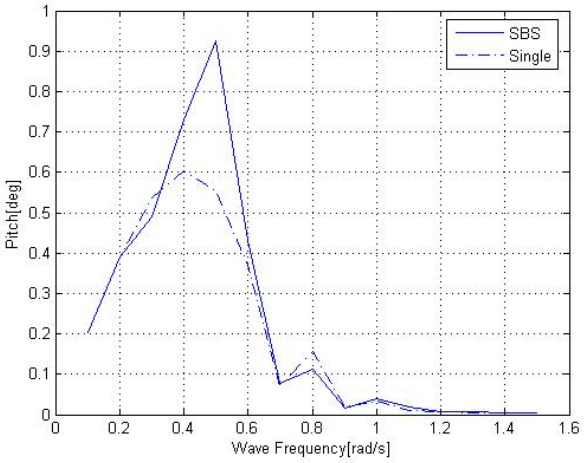

(e)

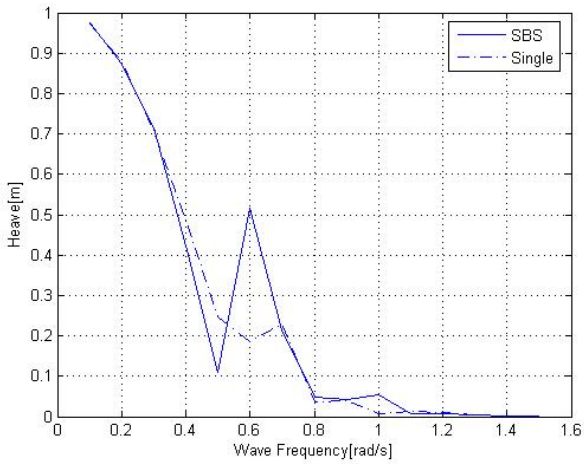

(c)

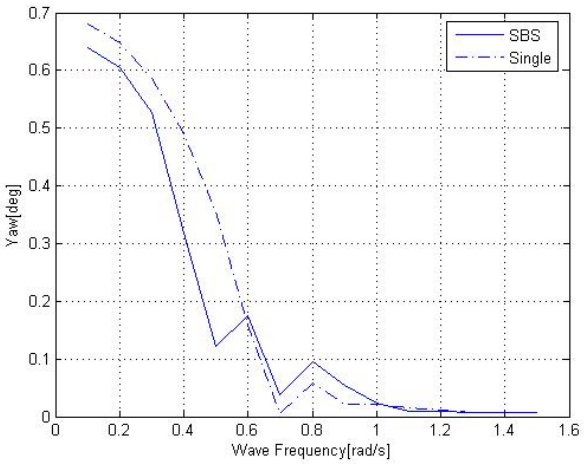

(f)

Figure 2-13. Motion response of LNG Carrier for 135 deg wave heading

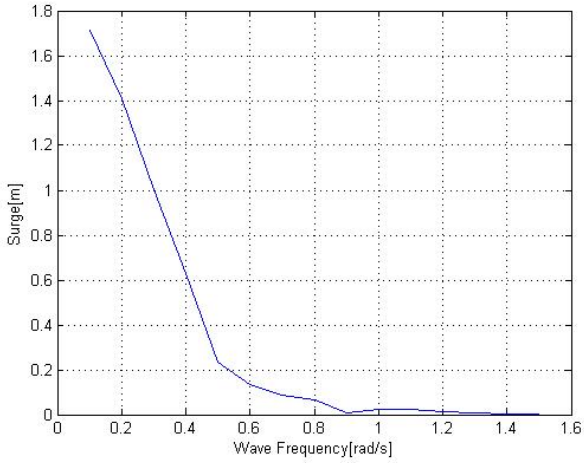

(a)

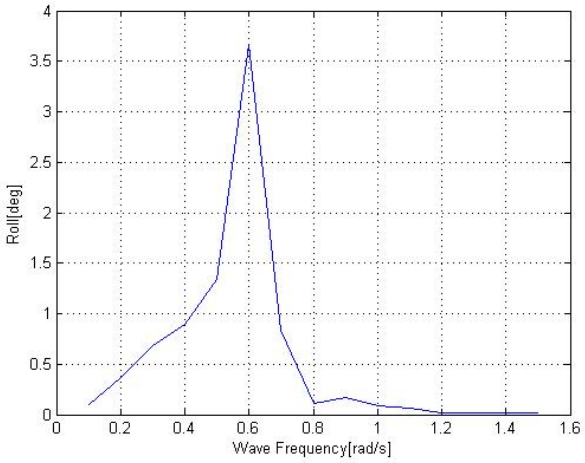

(d)

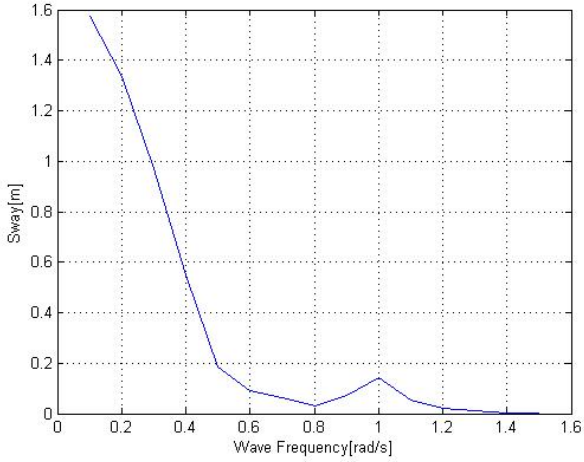

(b)

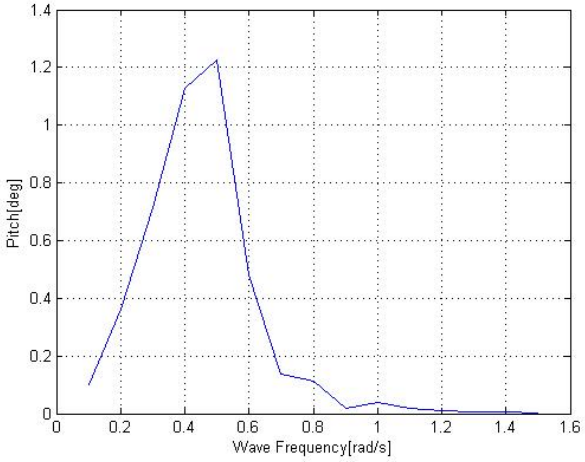

(e)

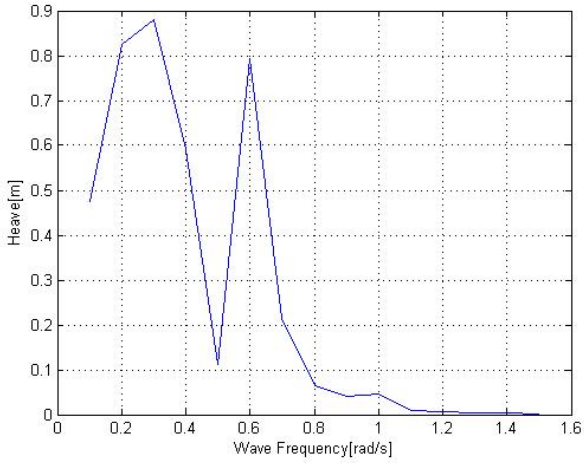

(c)

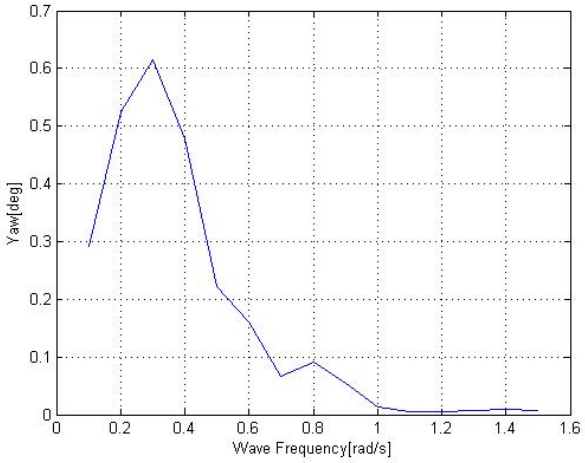

(f)

Figure 2-14. Relative motion response for 135 deg wave heading

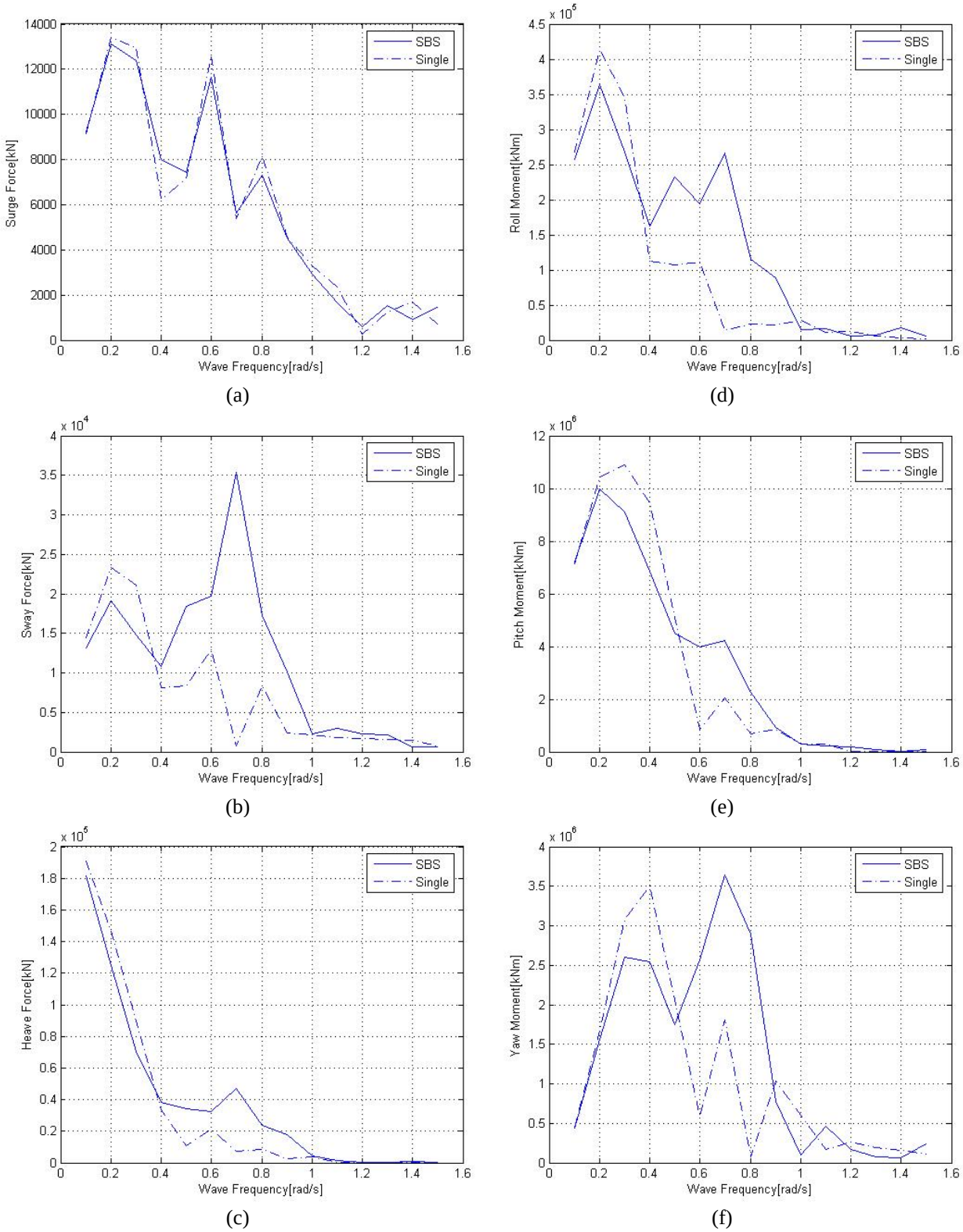

Figure 2-15. Wave exciting force on LNG Terminal for 135 deg wave heading

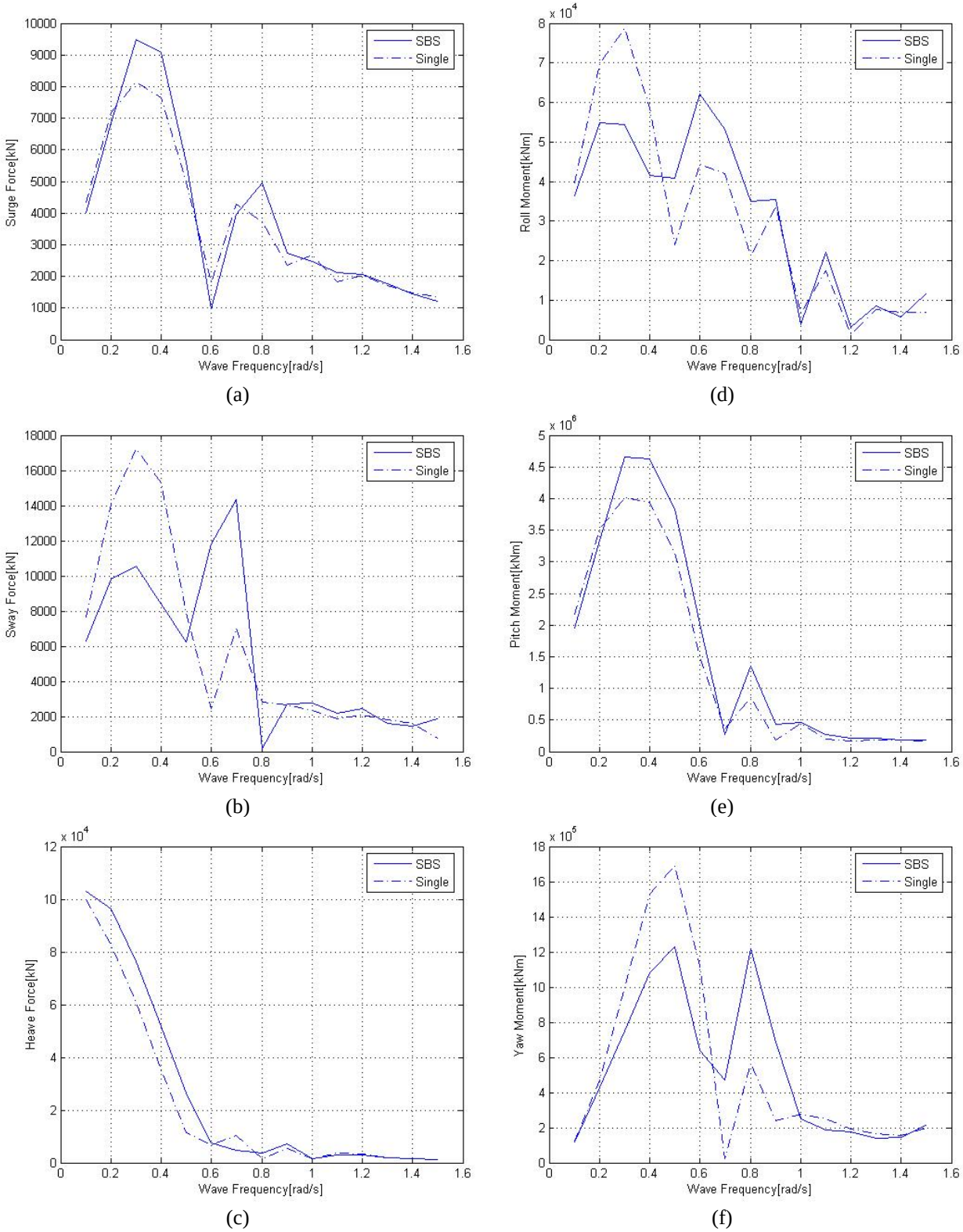

Figure 2-16. Wave exciting force on LNG Carrier for 135 deg wave heading

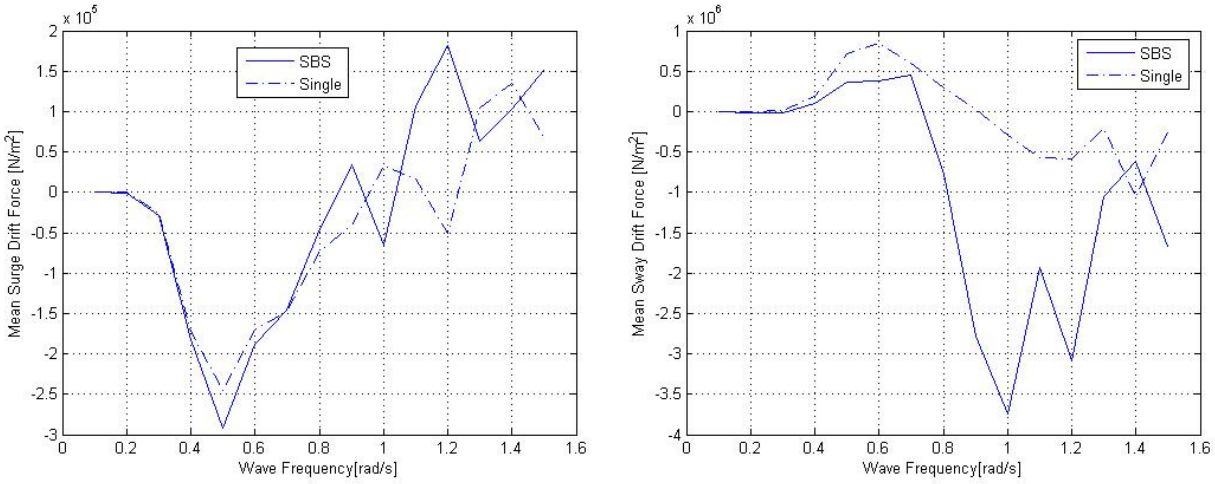

(a) (b)

Figure 2-17. Mean drift force on LNG Terminal for 135 deg wave heading

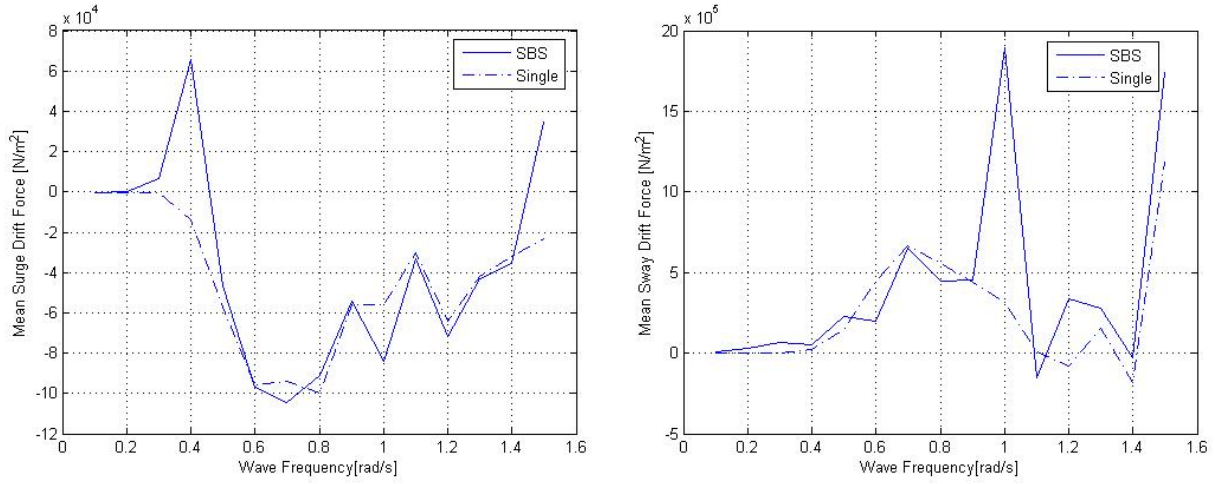

(a) (b)

Figure 2-18. Mean drift force on LNG Carrier for 135 deg wave heading

2.2.5 Case 3. Wave Heading = 180 Degrees

This is the head sea condition. Figure 2-19(b) shows the LNG Terminal sway response and Figure 2-20(b) shows the sway response of the LNG Carrier. Since both the terminal and carrier are symmetric w.r.t. their respective centerline planes, the sway response is zero in the single body case. Figure 2-20(c) shows the heave response of the LNG Carrier. The response is a little higher than in the single body case due to the existence of the reflected waves in the region between the two bodies. Figure 2-19(c) shows the heave response of the LNG Terminal. The response is much less than the LNG carrier since the terminal is a much bigger structure and hence less responsive.

The notable response in this case is that of LNG carrier roll response as shown in Figure 2-20(d). The roll response exhibits a sharp peak at 0.6 rad/s. Figure 2-21 shows the relative response between the terminal and the carrier.

Figure 2-22 shows the wave exciting forces and moments on the terminal and Figure 2-23 shows the wave exciting forces and moments on the carrier. As in the previous cases, the mean sway drift forces are acting on the bodies towards each other at 1 rad/s. Figure 2-24(b) shows the mean sway drift force on the LNG Terminal and Figure 2-25(b) shows the mean sway drift force on the LNG Carrier.

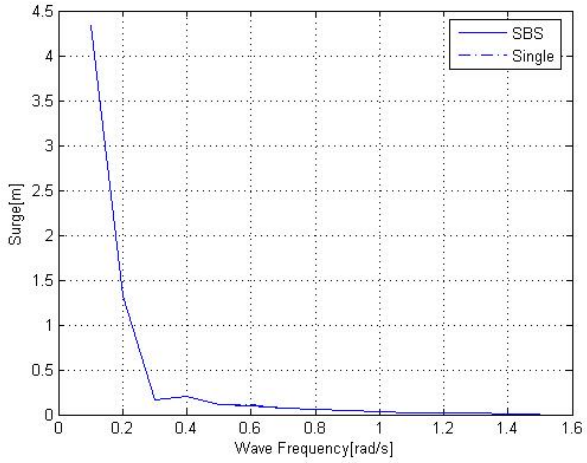

(a)

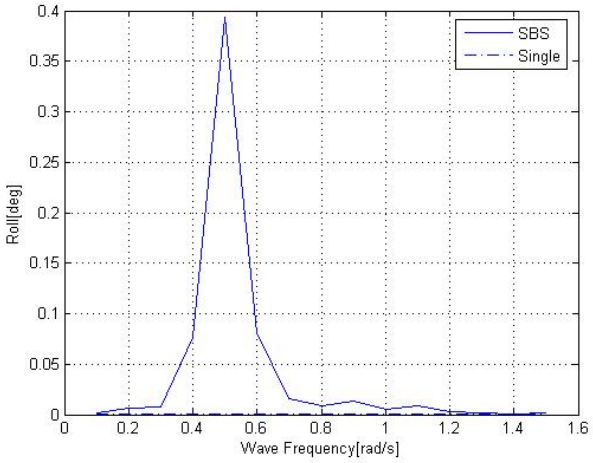

(d)

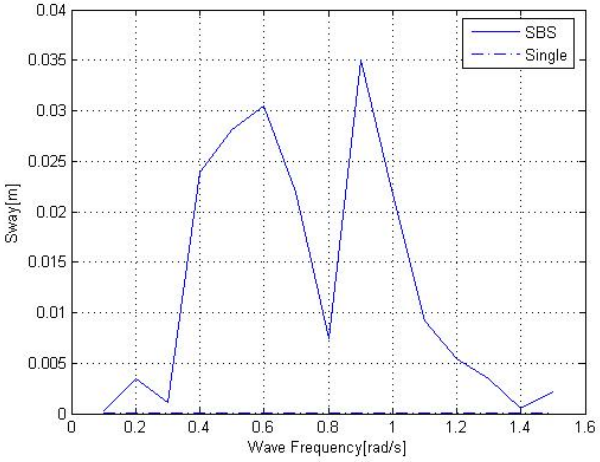

(b)

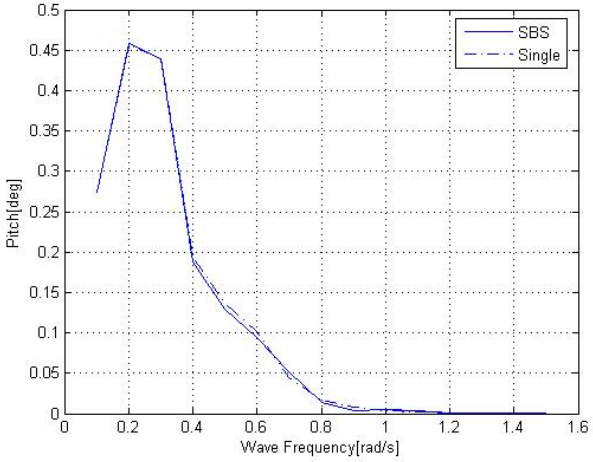

(e)

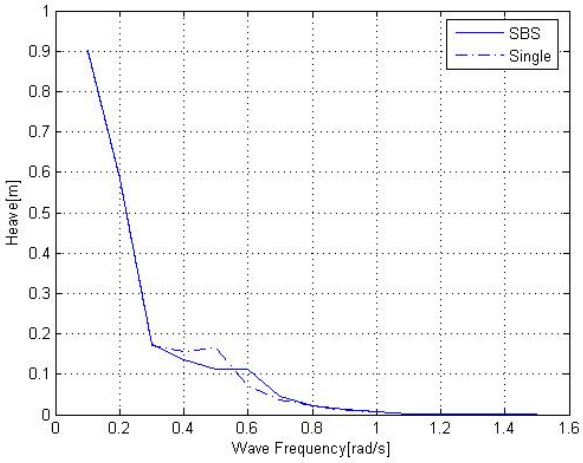

(c)

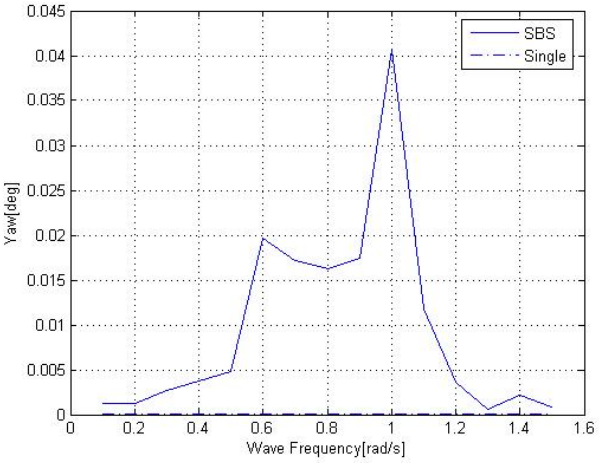

(f)

Figure 2-19. Motion response of LNG Terminal for 180 deg wave heading

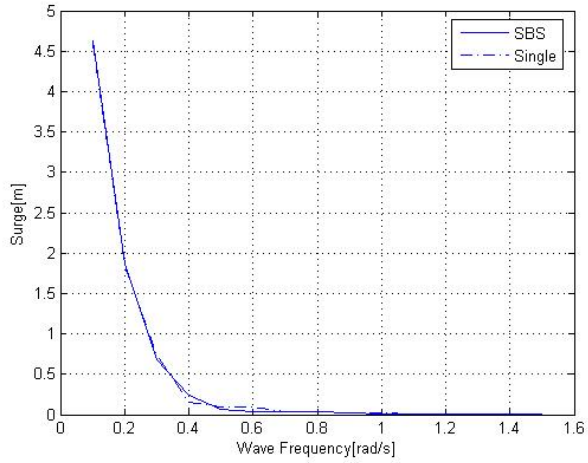

(a)

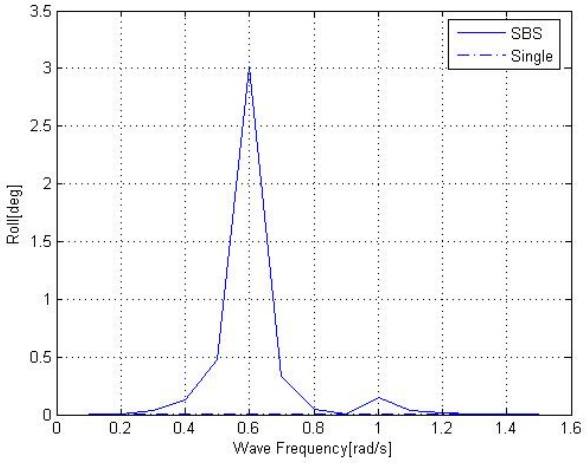

(d)

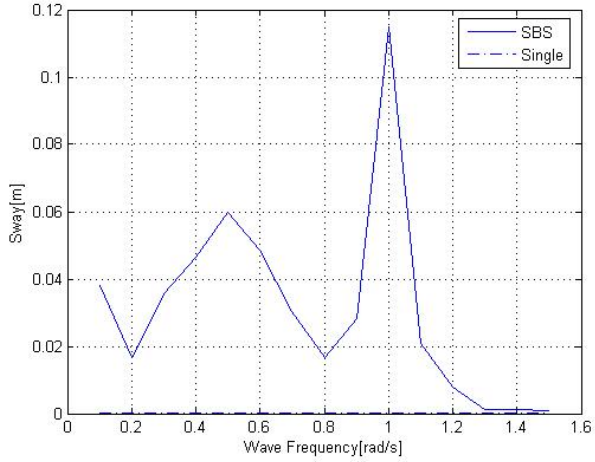

(b)

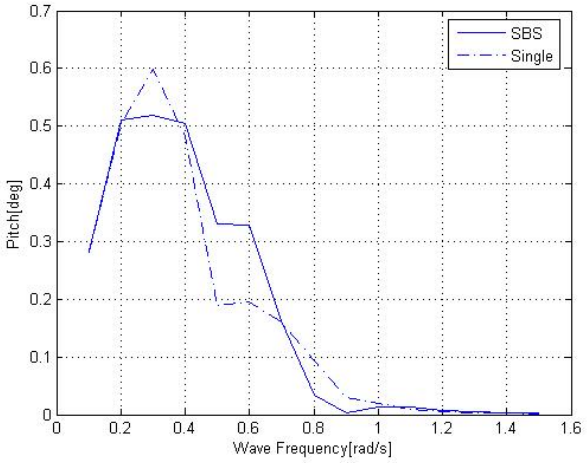

(e)

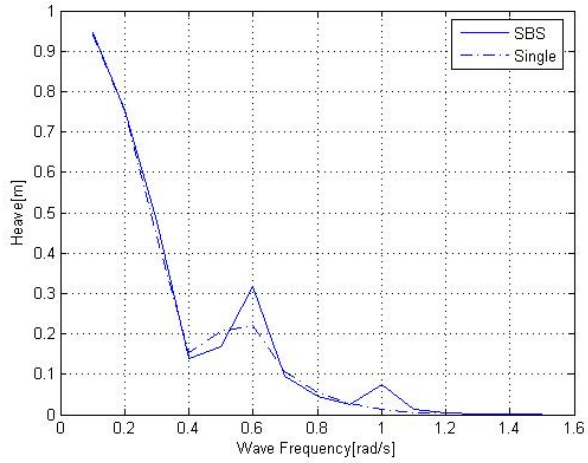

(c)

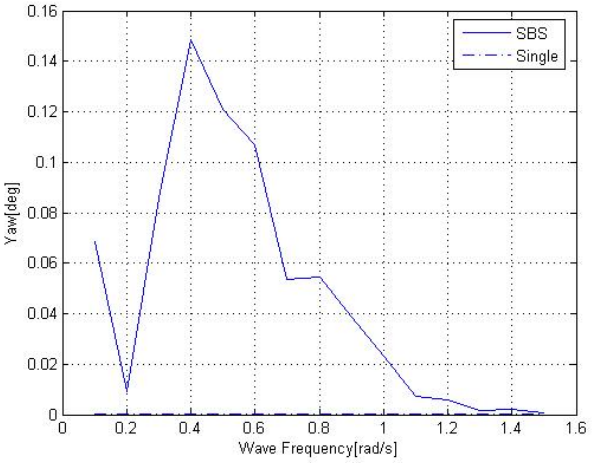

(f)

Figure 2-20. Motion response of LNG Carrier for 180 deg wave heading

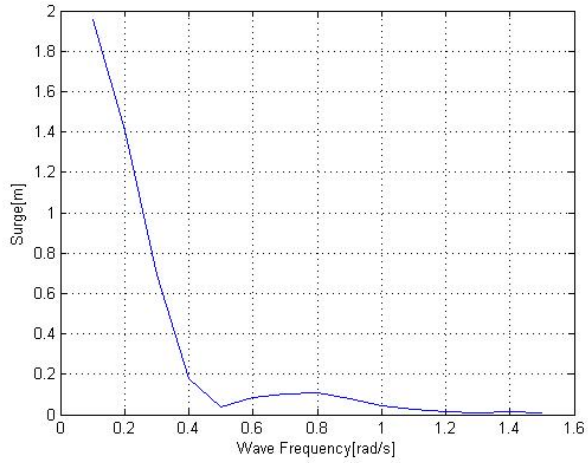

(a)

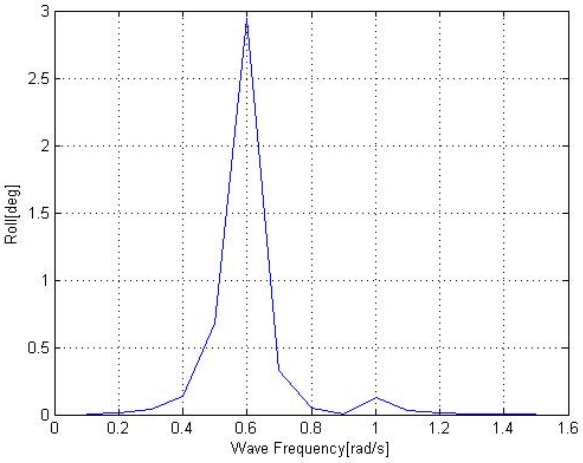

(d)

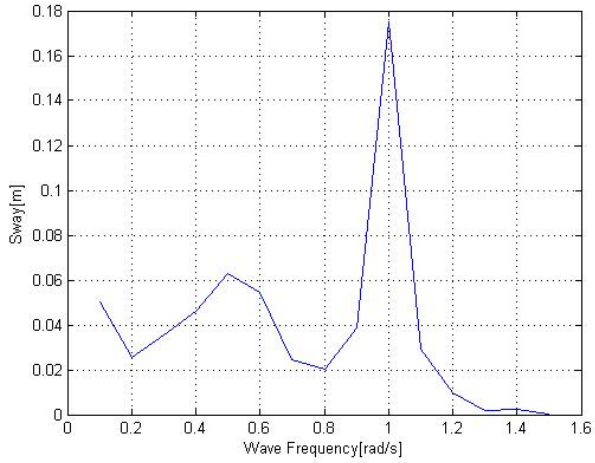

(b)

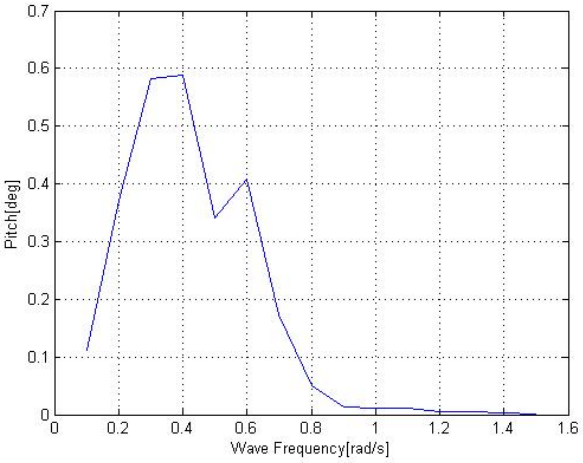

(e)

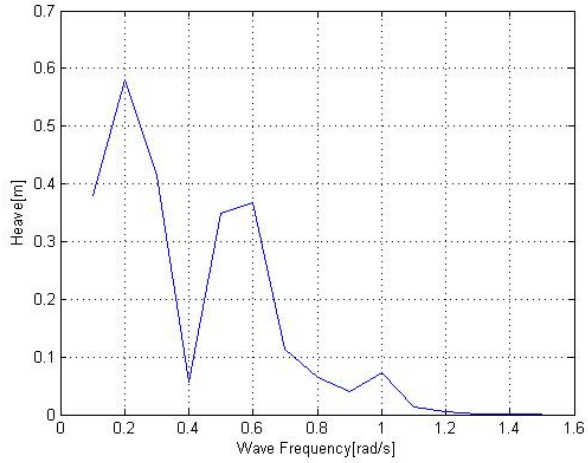

(c)

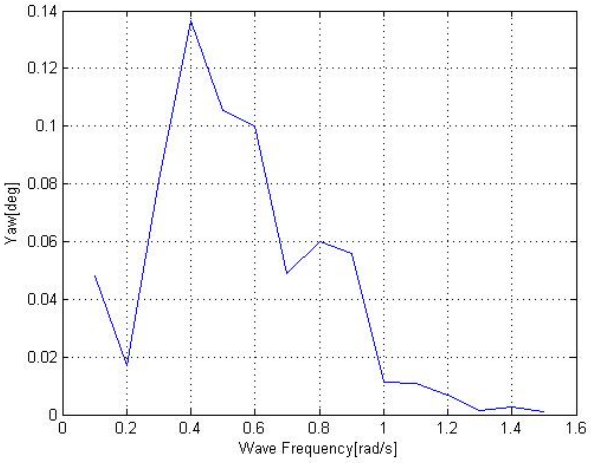

(f)

Figure 2-21. Relative motion response for 180 deg wave heading

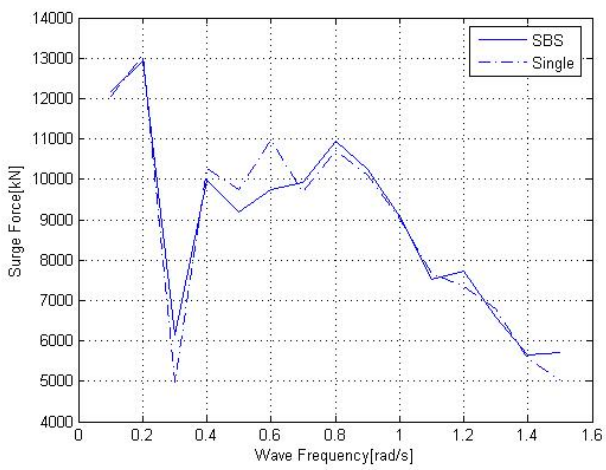

(a)

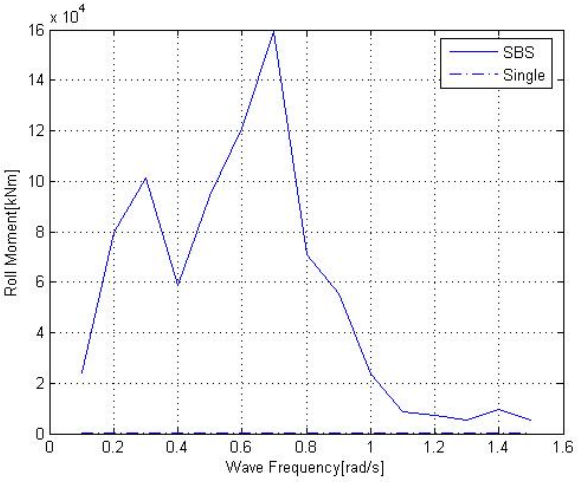

(d)

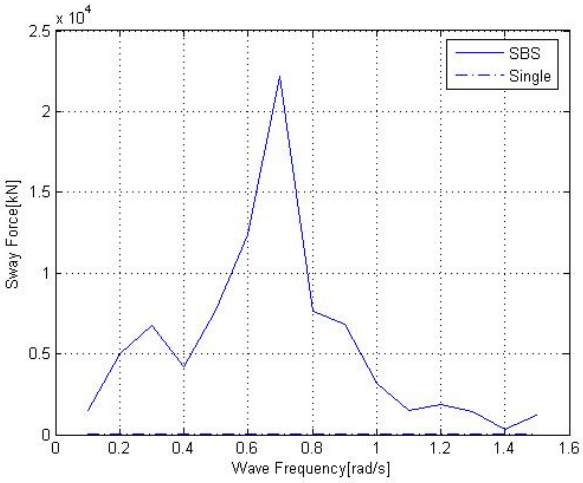

(b)

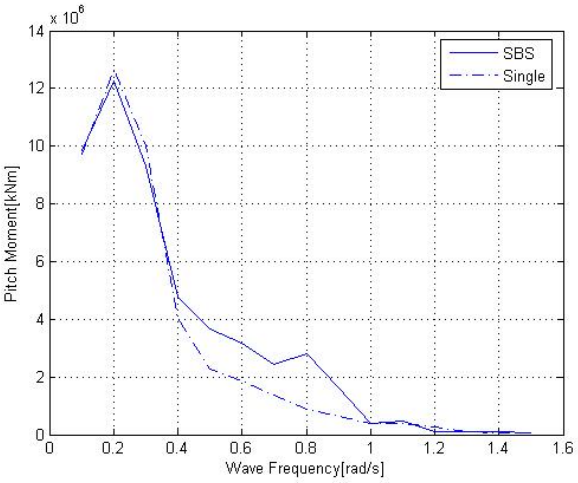

(e)

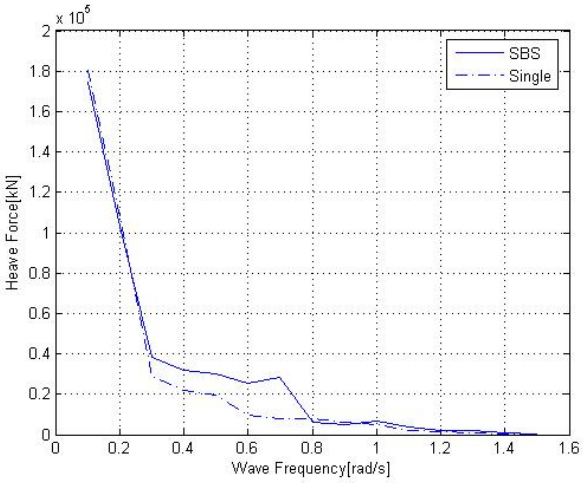

(c)

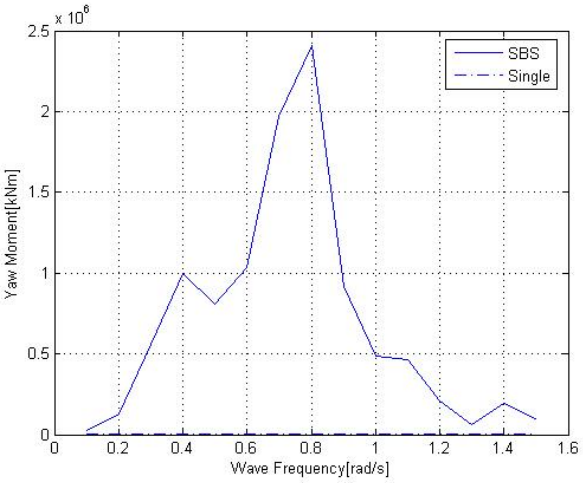

(f)

Figure 2-22. Wave exciting force on LNG Terminal for 180 deg wave heading

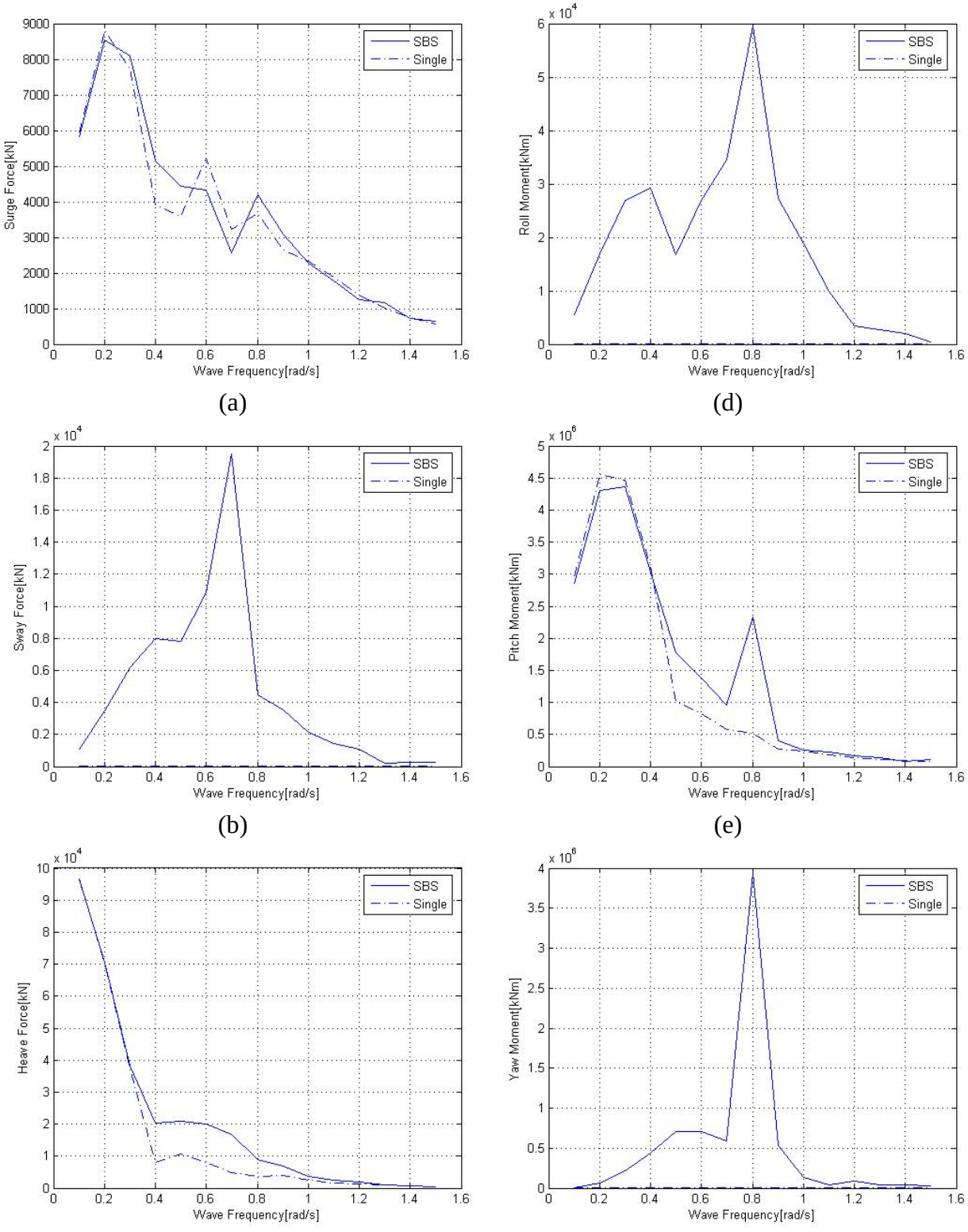

Figure 2-23. Wave exciting force on LNG Carrier for 180 deg wave heading

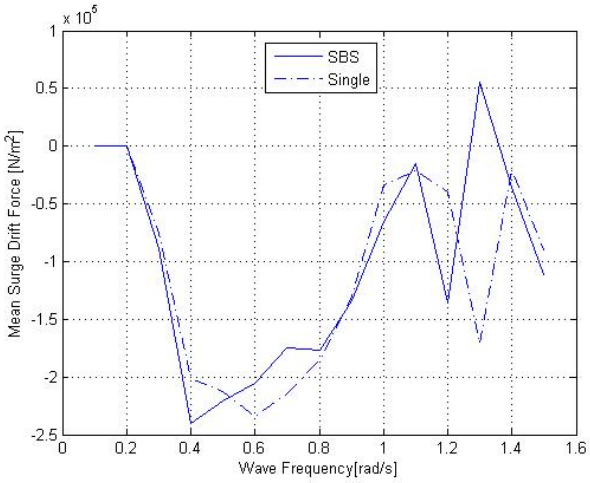

(a)

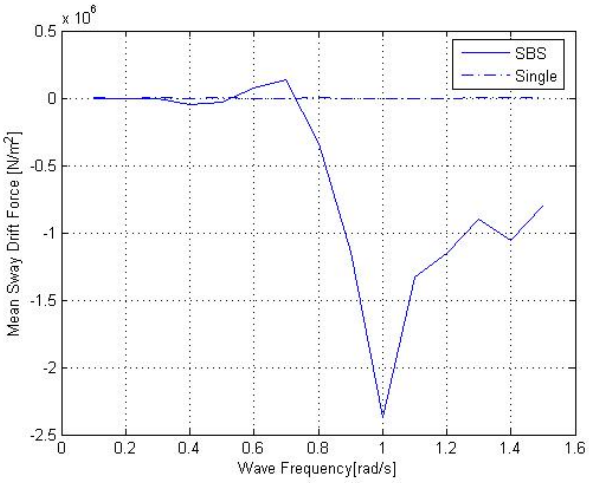

(b)

Figure 2-24. Mean drift force on LNG Terminal for 180 deg wave heading

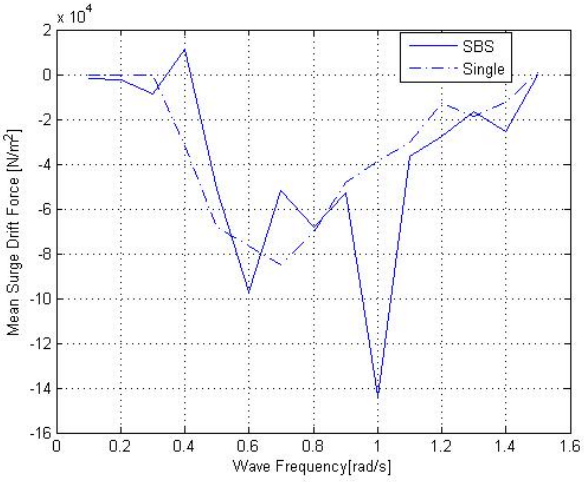

(a)

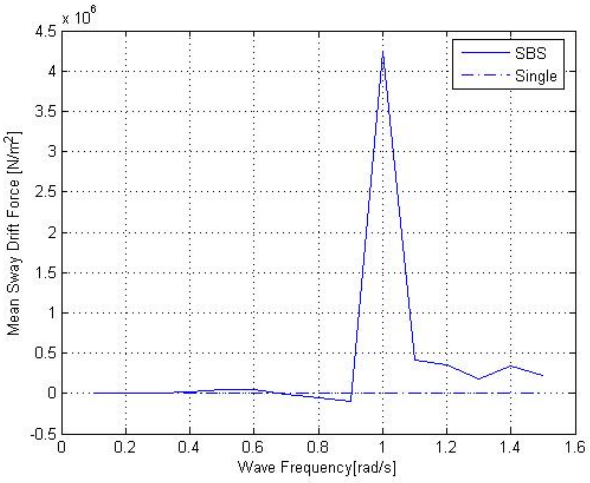

(b)

Figure 2-25. Mean drift force on LNG Carrier for 180 deg wave heading

2.2.6 Case 4. Wave Heading = 225 Degrees

Figure 2-26 shows the motion response of the LNG Terminal and Figure 2-27 shows the motion response of the LNG Carrier. The carrier roll motion has a peak response of 3 degrees at a wave frequency of 0.6 rad/s. Compared to the 135 deg case, the responses of the carrier are slightly lower in general due to the 'shielding' effect provided by the LNG Terminal. Figure 2-28 shows the relative motion between the terminal and the carrier for 225 deg wave heading. The relative roll response also has got a peak value of 3 degrees at 0.6 rad/s. Figure 2-29 shows the wave exciting forces and moments on the terminal and Figure 2-30 shows the wave exciting forces and moments on the carrier.

Figure 2-29(c) shows the heave wave exciting force on the LNG Terminal. The force is slightly higher than that in the single body case because of the existence of the reflected waves from the LNG Carrier in the region between the two bodies. Figure 2-30(b) shows the sway wave exciting force on the LNG Carrier. Except for 0.7 rad/s the force is less than that in the single body case. At 0.7 rad/s the force is higher because of the helmholtz resonance occurring in the region between the two bodies.

Figure 2-31(a) shows the mean surge wave drift force on the LNG Terminal and Figure 2-32(b) shows the mean surge wave drift force on the LNG Carrier. At 1 rad/s there is a sharp increase in the force on the carrier in the aftward direction whereas the force on the terminal is positive. Hence the forces are trying to push the bodies in the opposite directions at 1 rad/s. Similar situation is observed at 1.3 rad/s. Figure 2-31(b) shows the mean sway wave drift force on the terminal and Figure 2-32(b)shows the mean sway wave drift force on the carrier.

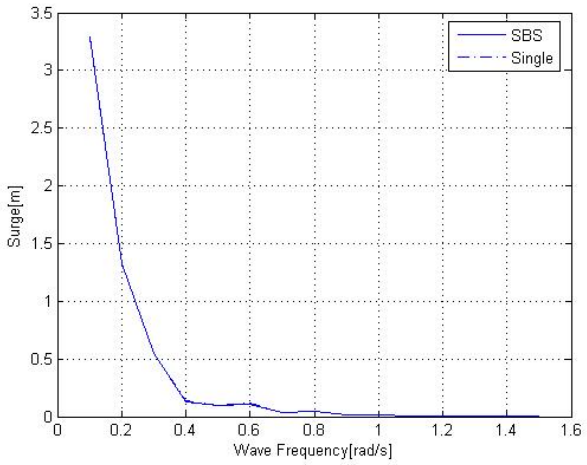

(a)

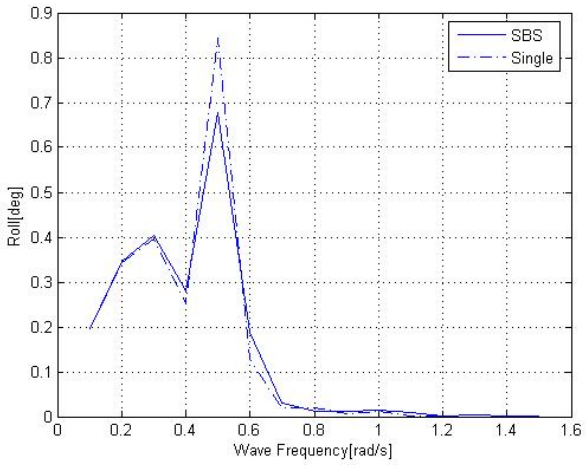

(d)

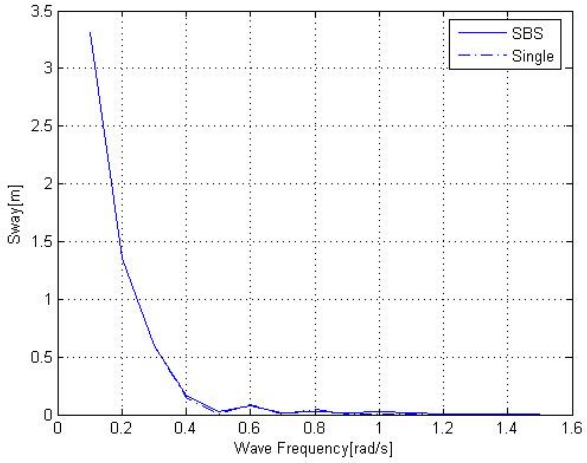

(b)

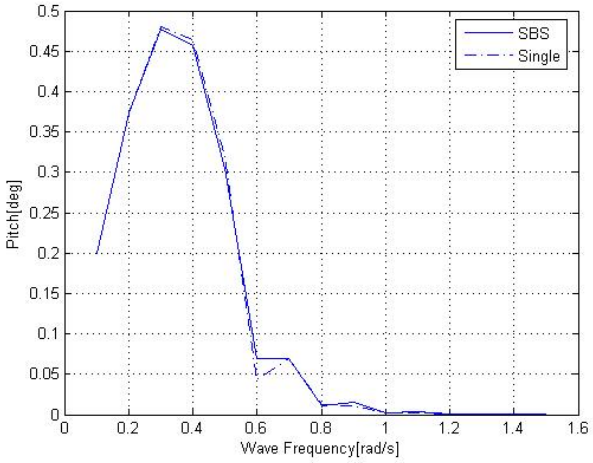

(e)

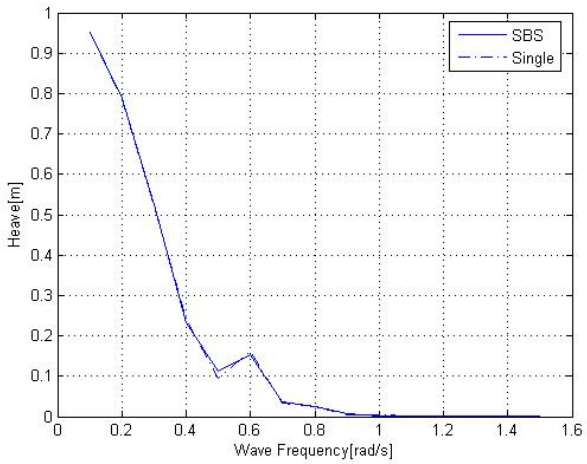

(c)

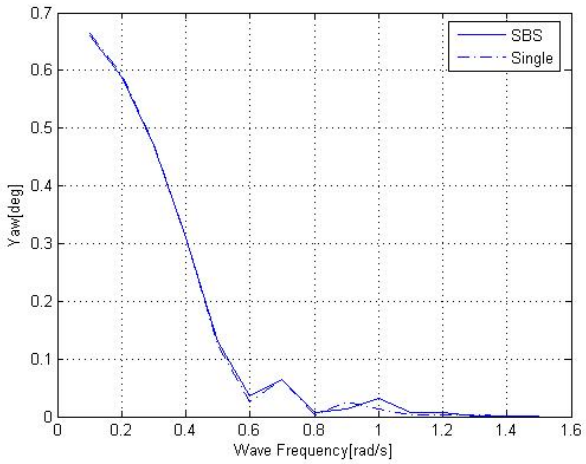

(f)

Figure 2-26. Motion response of LNG Terminal for 225 deg wave heading

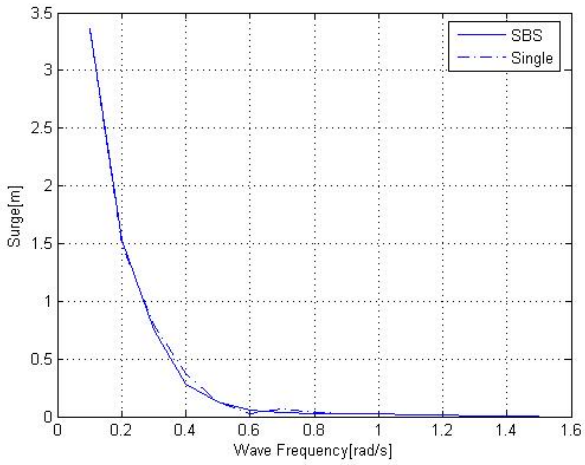

(a)

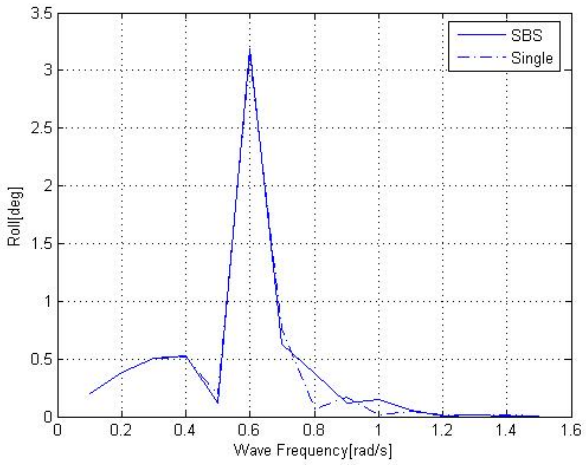

(d)

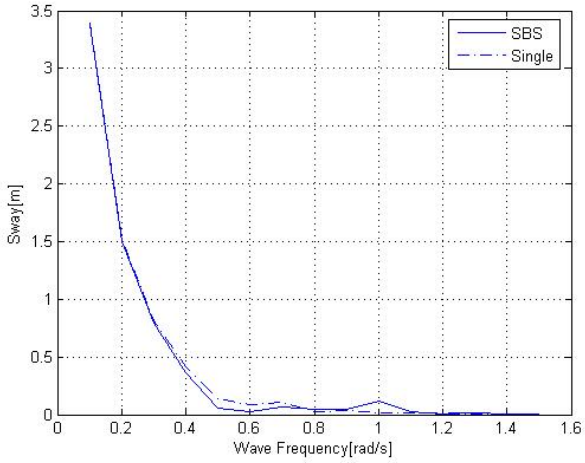

(b)

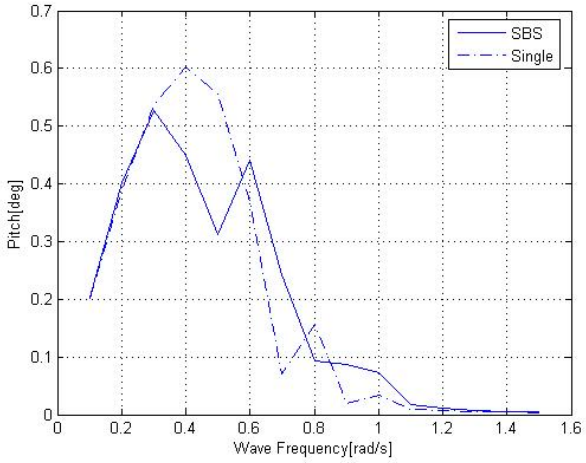

(e)

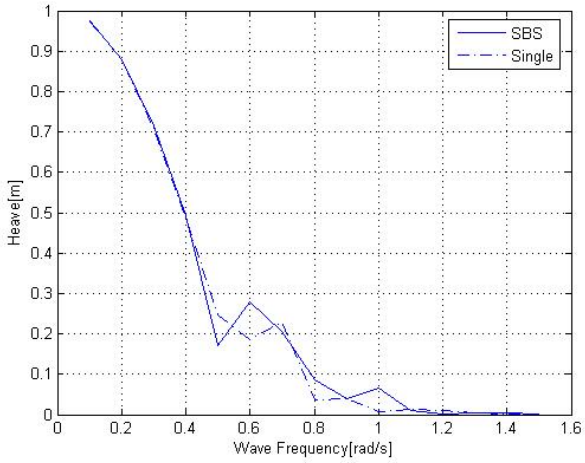

(c)

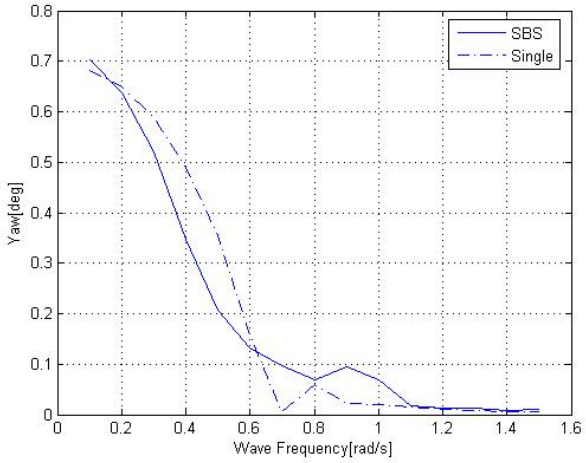

(f)

Figure 2-27. Motion response of LNG Carrier for 225 deg wave heading

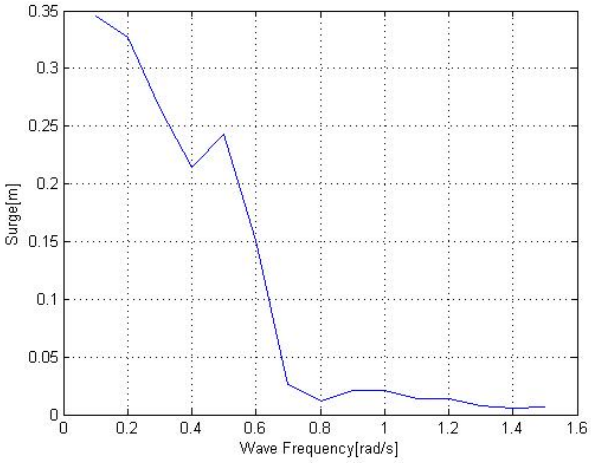

(a)

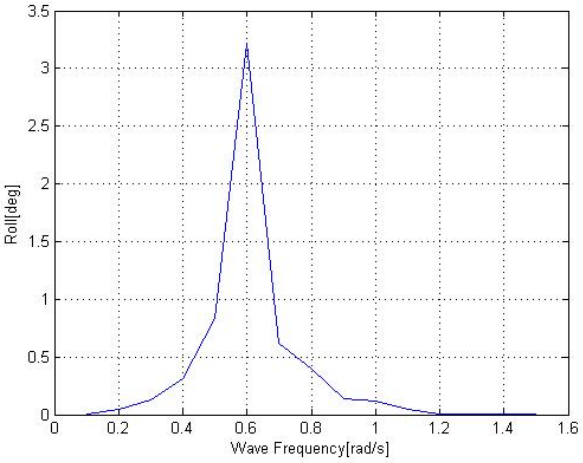

(d)

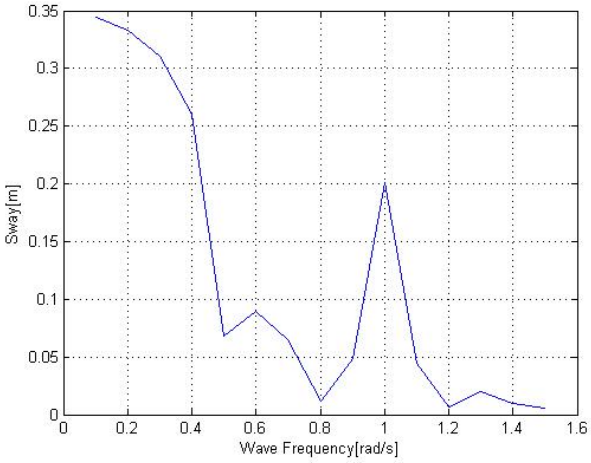

(b)

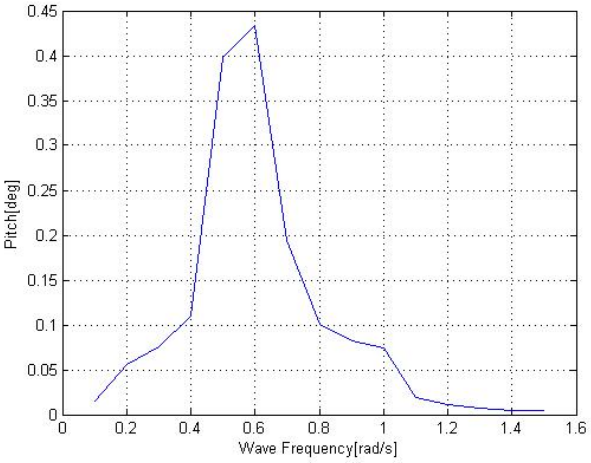

(e)

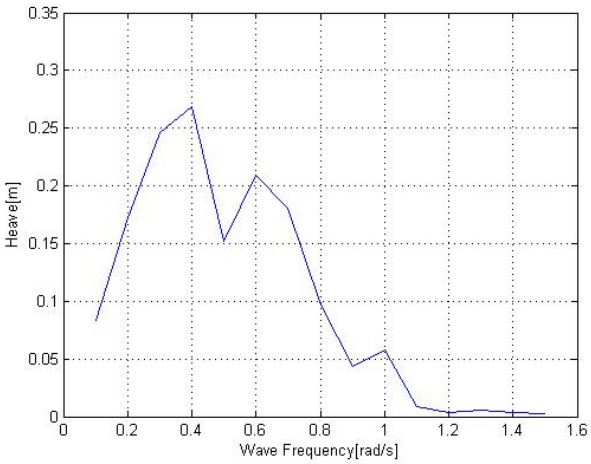

(c)

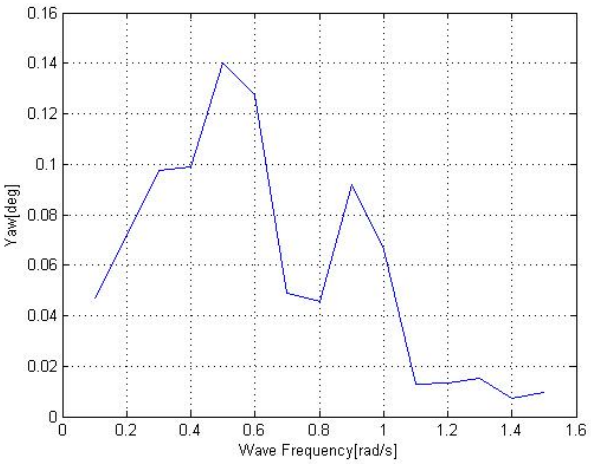

(f)

Figure 2-28. Relative motion response for 225 deg wave heading

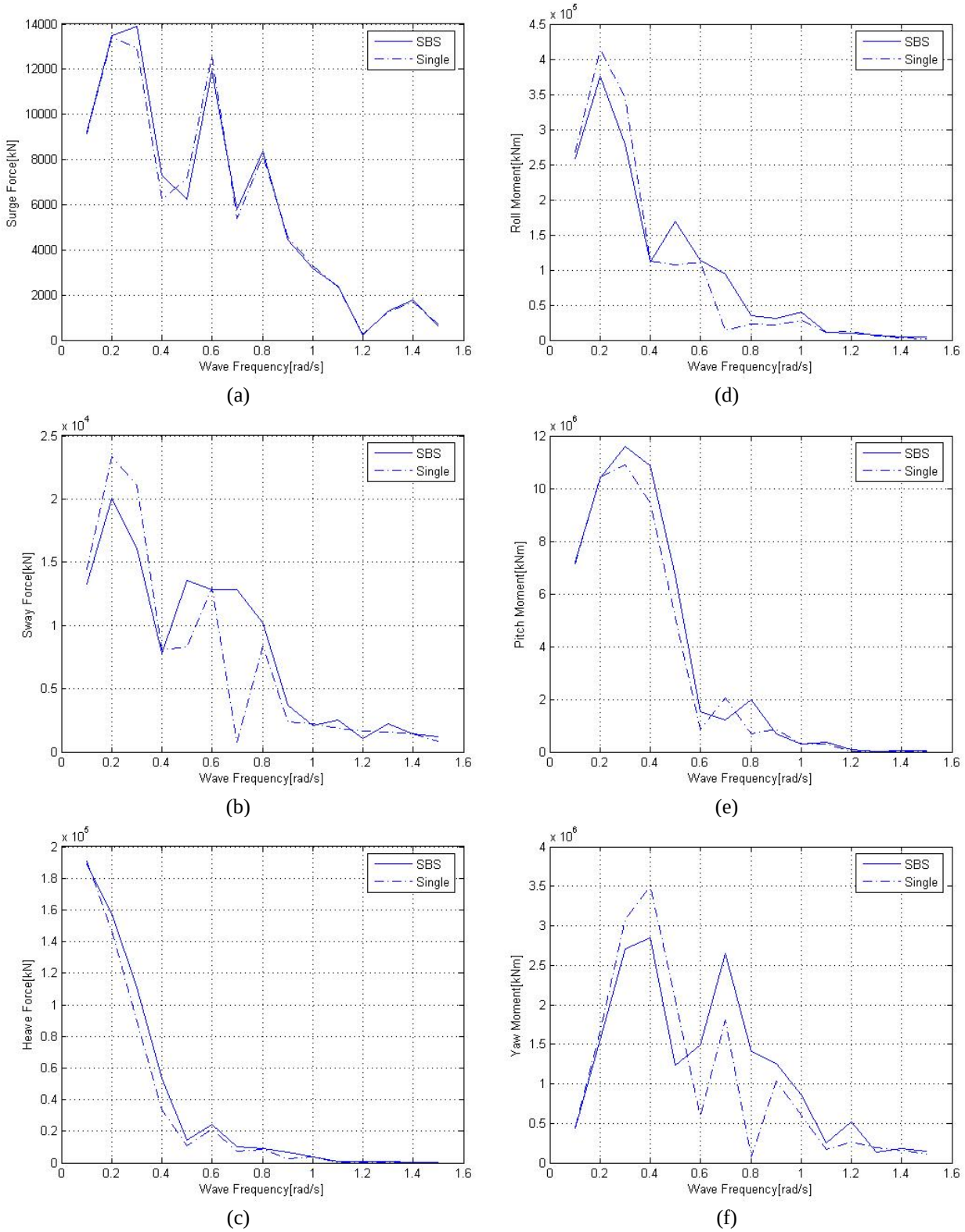

Figure 2-29. Wave exciting force on LNG Terminal for 225 deg wave heading

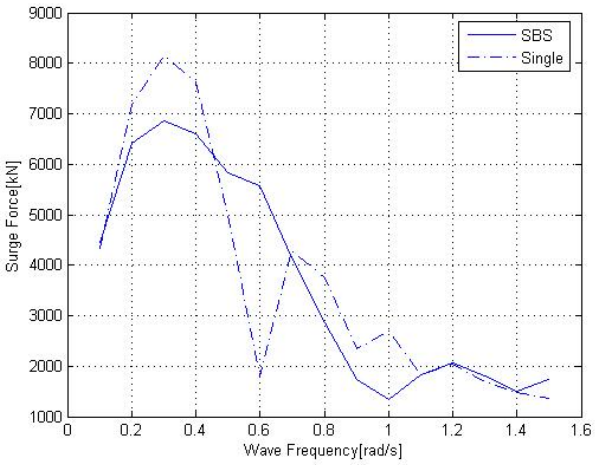

(a)

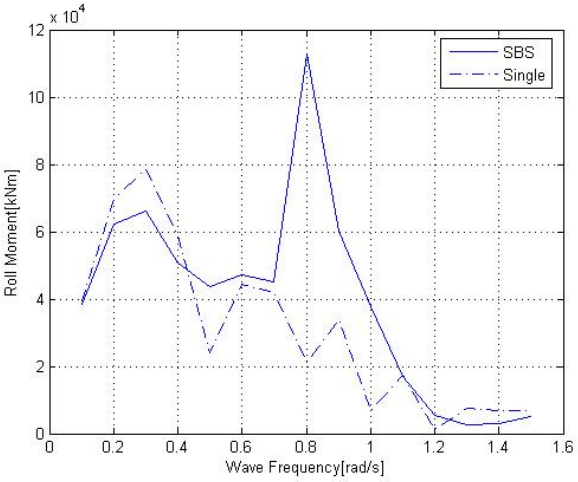

(d)

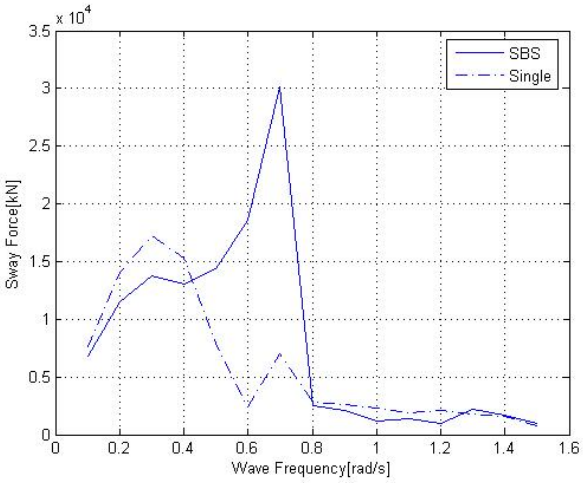

(b)

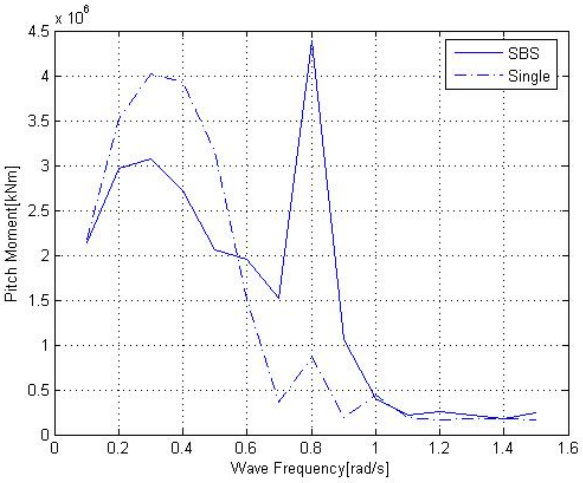

(e)

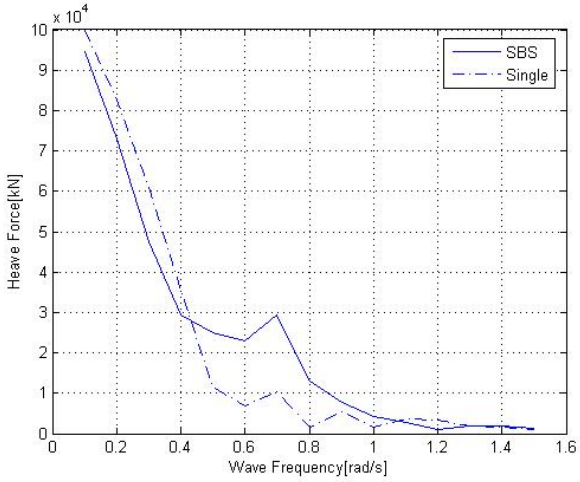

(c)

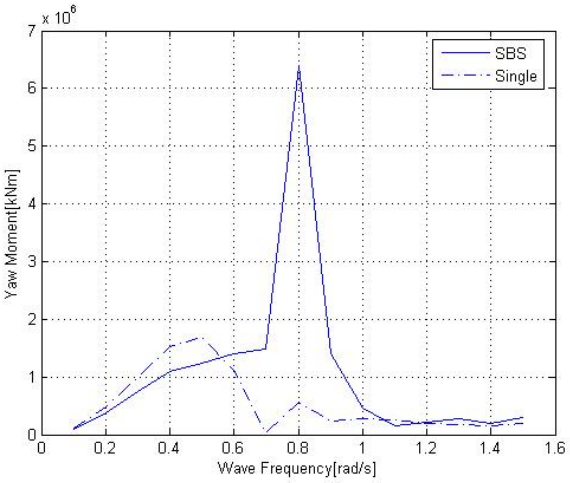

(f)

Figure 2-30. Wave exciting force on LNG Carrier for 225 deg wave heading

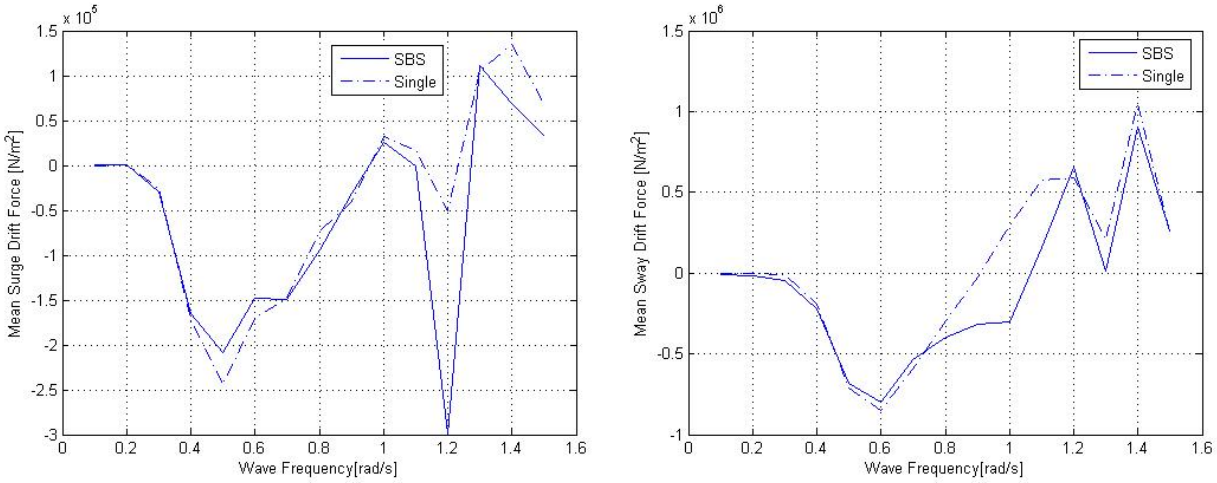

(a) (b)

Figure 2-31. Mean drift force on LNG Terminal for 225 deg wave heading

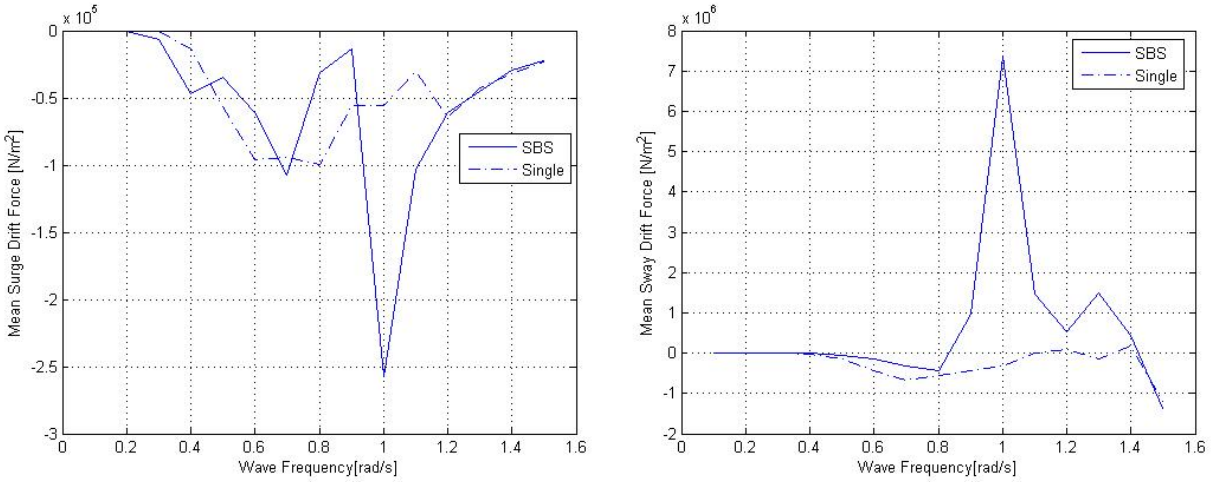

(a) (b)

Figure 2-32. Mean drift force on LNG carrier for 225 deg wave heading

2.2.7 Case 5. Wave Heading = 270 Degrees

This is the beam sea condition with the LNG Terminal on the weather side. The shielding effect due to the terminal is tremendous in this situation. Figure 2-33 shows the motion responses of the terminal. Figure 2-34(b) shows the sway response of the carrier. The peak at 0.7 rad/s in the single body case is suppressed in the multi-body case because of the shielding effect due to the terminal. The suppression of the heave response of the carrier in the multi-body case is even more significant as shown in Figure 2-34(c). Figure 2-35(d) shows the relative roll response. As in the case of relative heave response, the relative roll response too is significantly less than the 90 deg wave heading case due to the shielding provided by the terminal.

Figure 2-36 shows the wave exciting forces and moments on the terminal. Figure 2-37(a) shows the surge wave exciting force on the carrier. There is surge force in the single body case due to the asymmetry of the carrier w.r.t the X-Y plane. The positioning of the carrier behind the terminal adds even more asymmetry. Hence the force in the two-body case is higher than that in the single body case. However, at higher frequencies, the force in the two body case converges to that in the single body case due to decreasing diffraction. Figure 2-37(b) shows the sway wave exciting force on the carrier. Unlike in the 90 deg wave heading case, the force in the multi-body case never exceeds that in the single body due to the shielding provided by the terminal. Figure 2-37(c) shows the heave wave exciting force on the carrier. The heave response for the terminal in the multi-body case is higher than that in the single body case due to the fact that in addition to the incident waves, it is also subjected to the reflected waves from the carrier. However, at higher frequencies, most of the incident waves are fully reflected back at the terminal itself. Hence there is not much difference in the response for the single and multi-body cases at higher frequencies. Because of the shielding effect, the response of the carrier is much less than that in the single body case. However, there exists a peak in the heave response of the carrier in the multi-body case at 0.7 rad/s due the helmholtz resonance in the region between the two bodies.

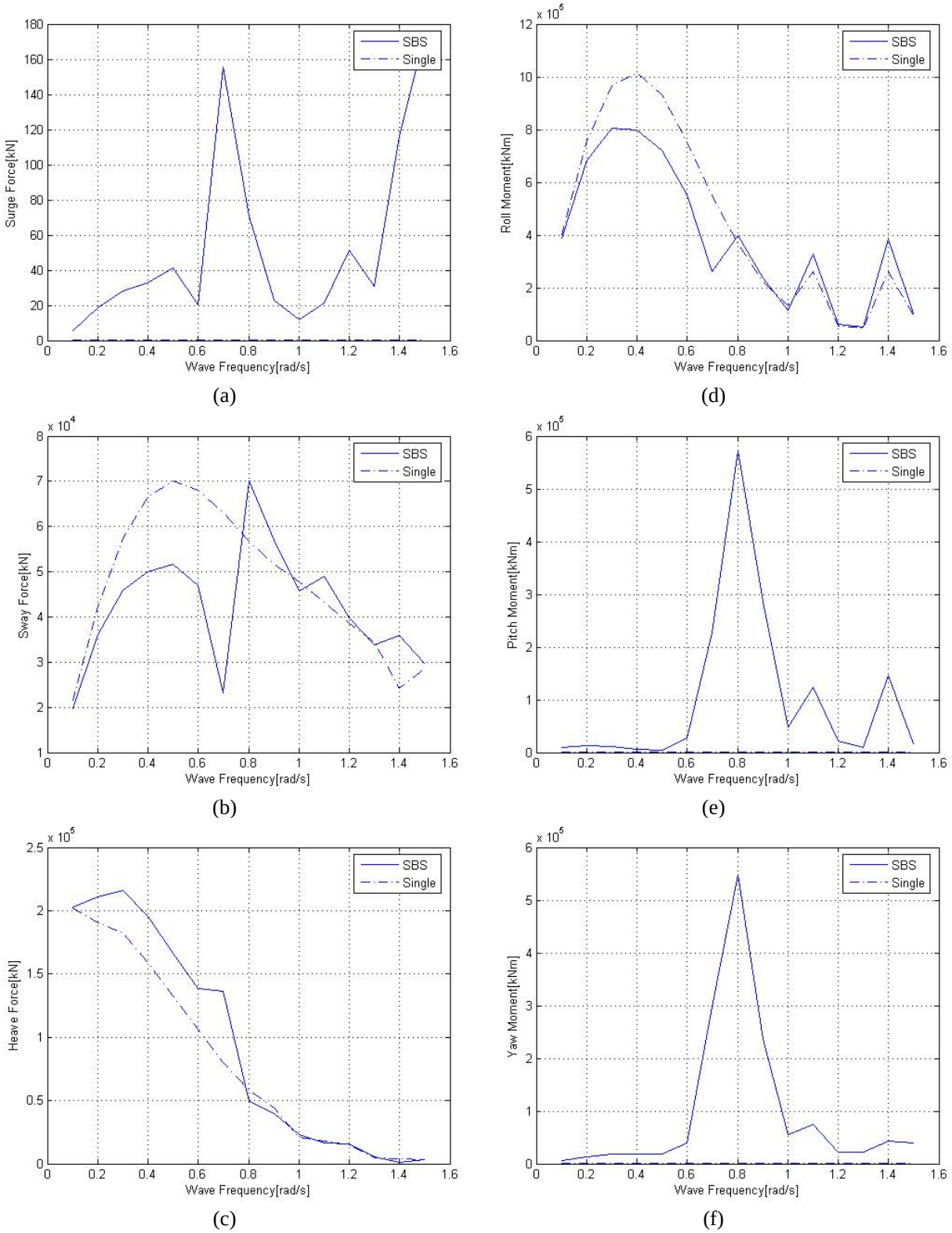

Figure 2-33. Motion response of LNG terminal for 270 deg wave heading

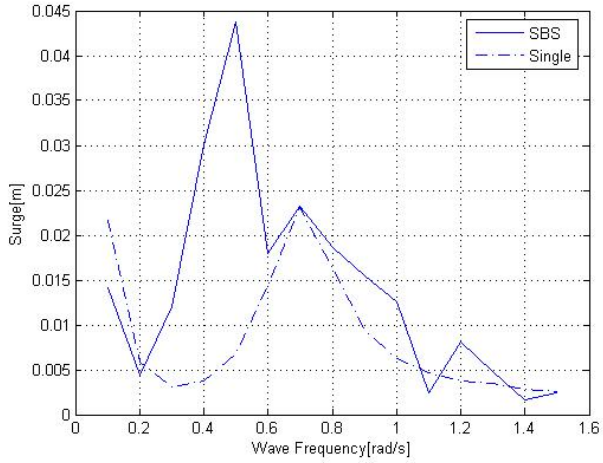

(a)

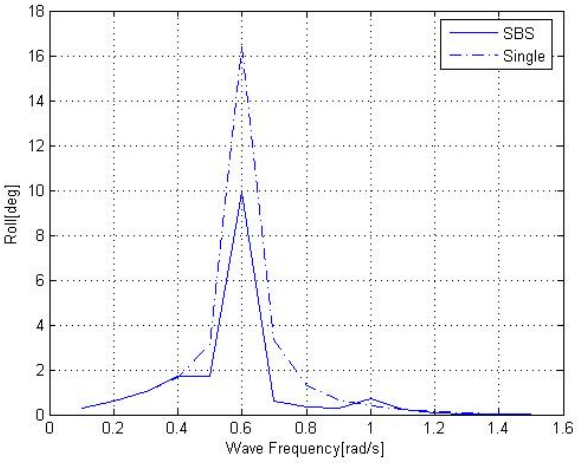

(d)

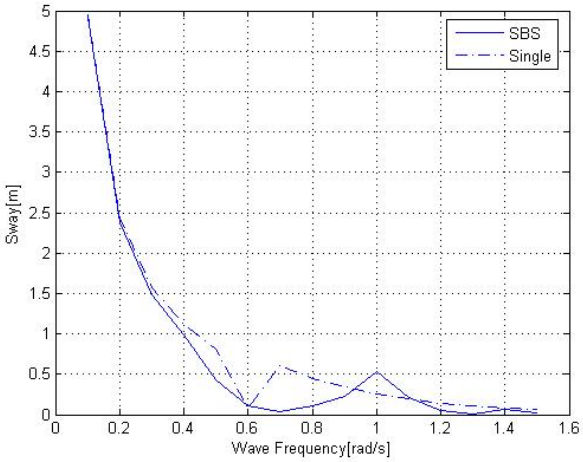

(b)

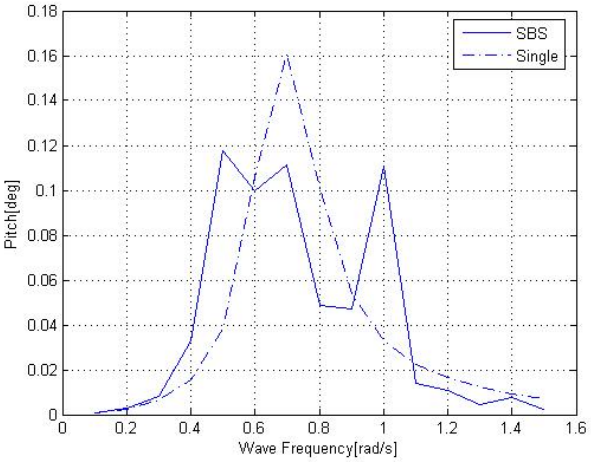

(e)

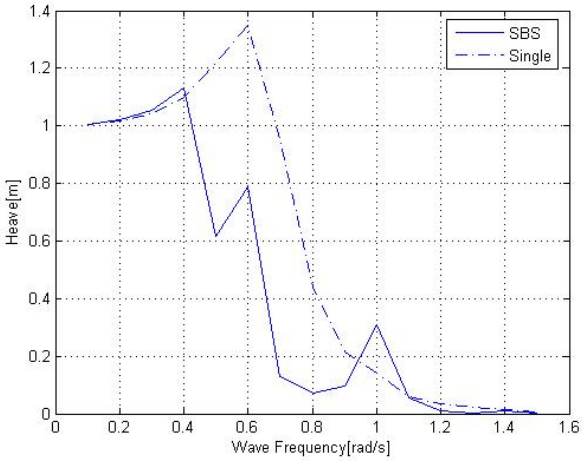

(c)

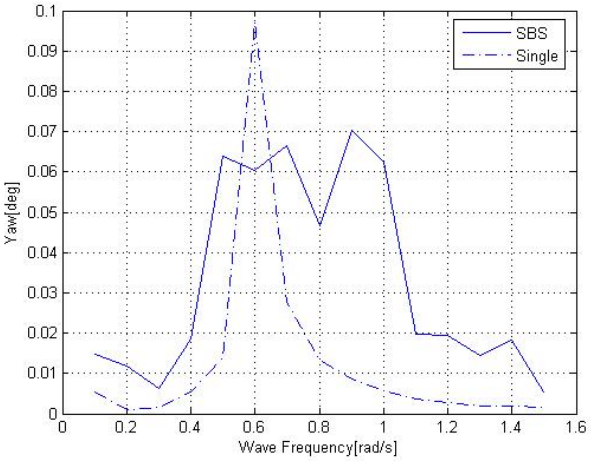

(f)

Figure 2-34. Motion response of LNG Carrier for 270 deg wave heading

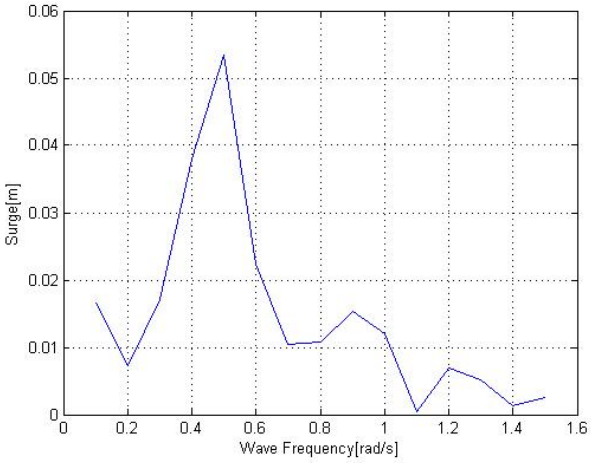

(a)

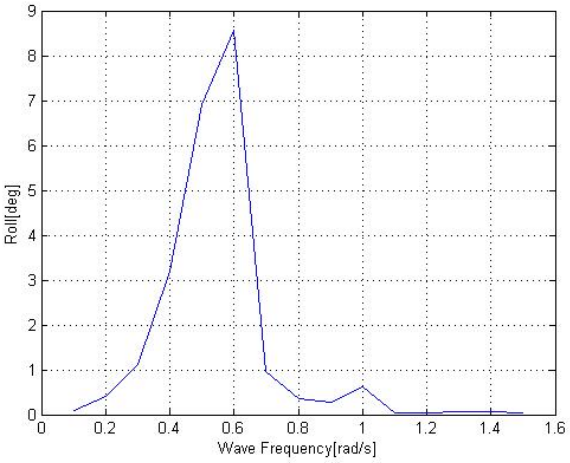

(d)

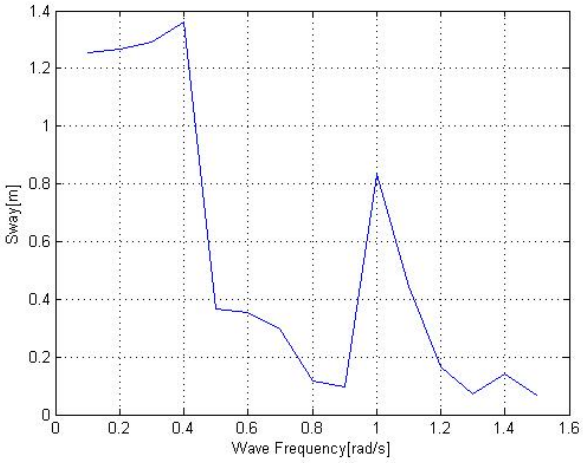

(b)

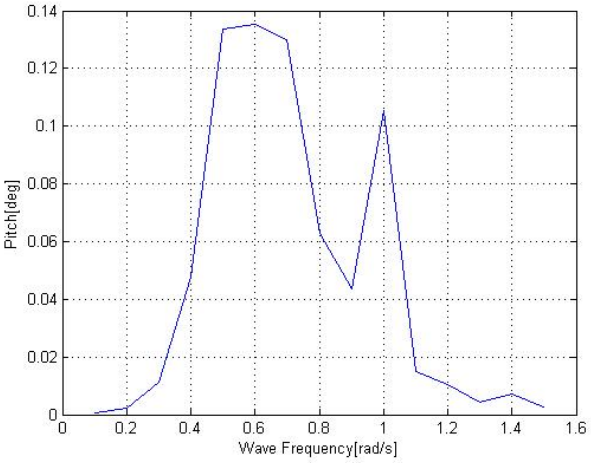

(e)

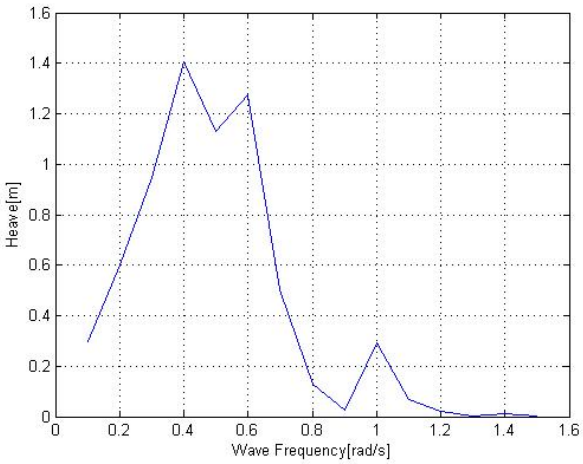

(c)

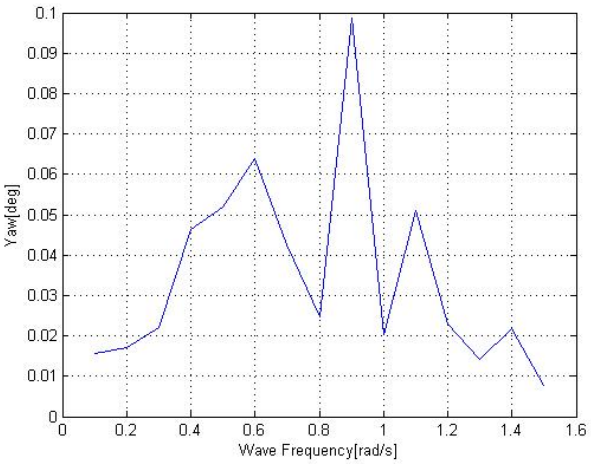

(f)

Figure 2-35. Relative response for 270 deg wave heading

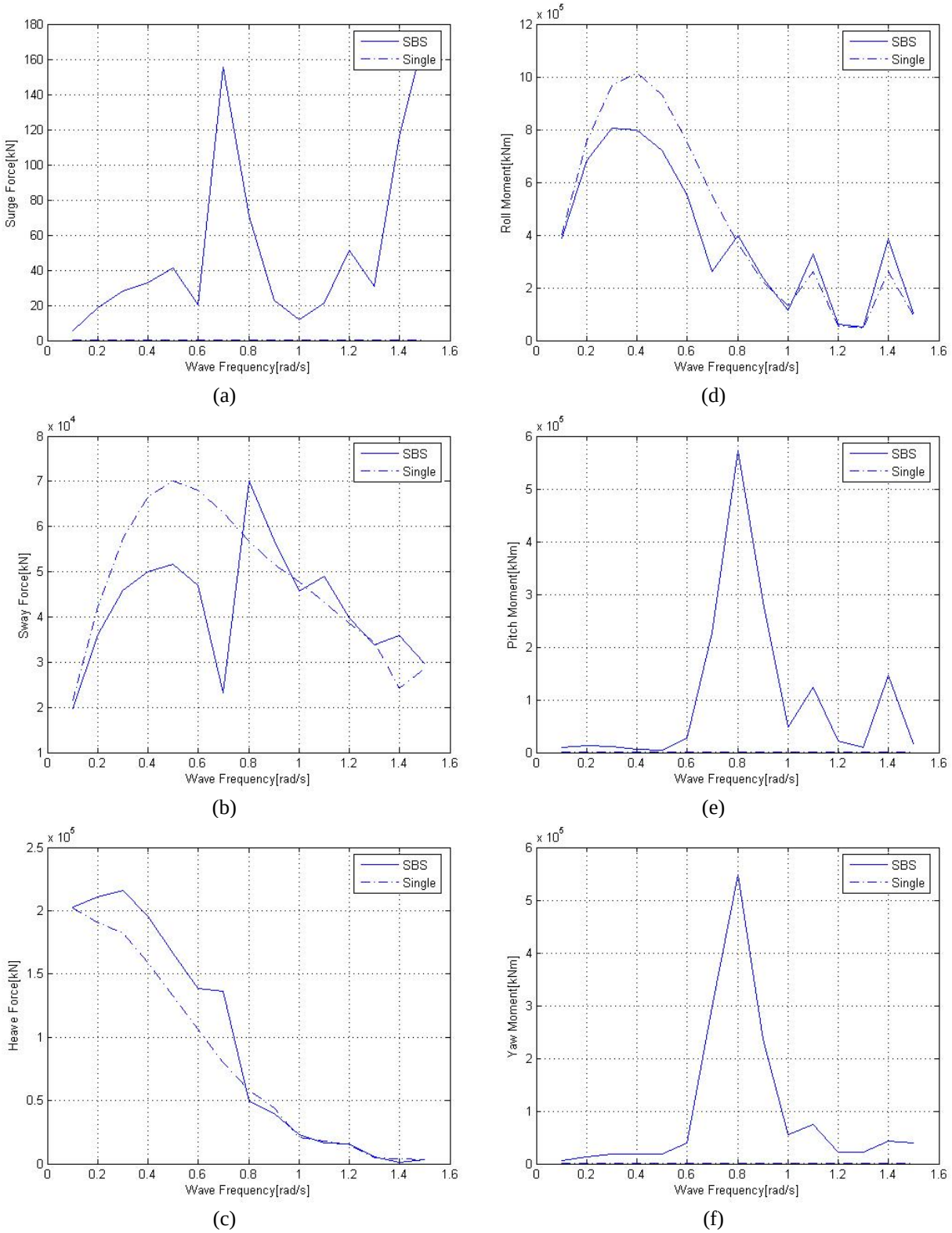

Figure 2-36. Wave exciting force on LNG Terminal for 270 deg wave heading

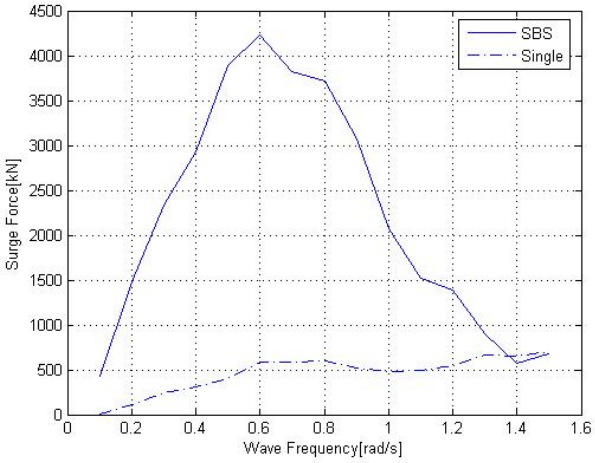

(a)

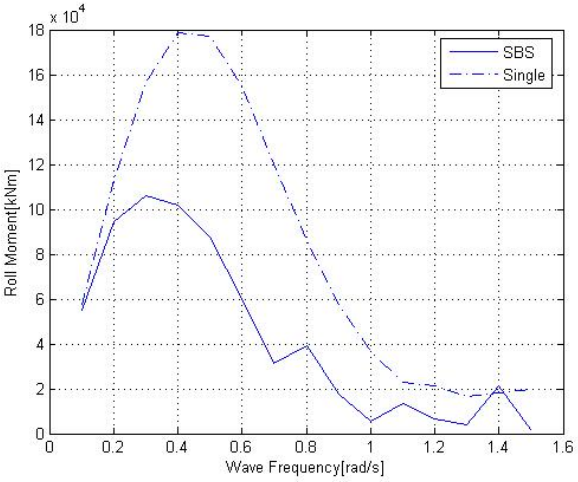

(d)

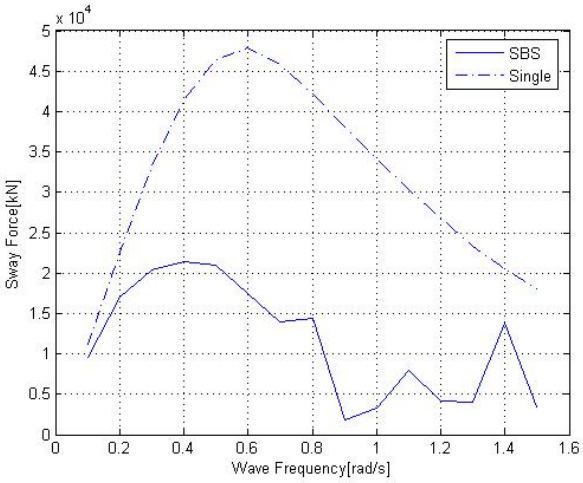

(b)

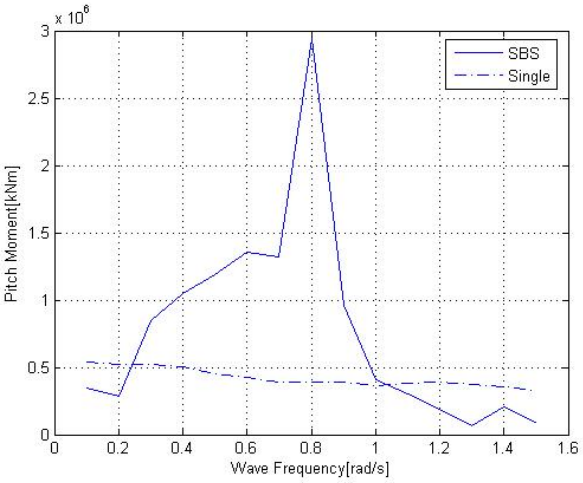

(e)

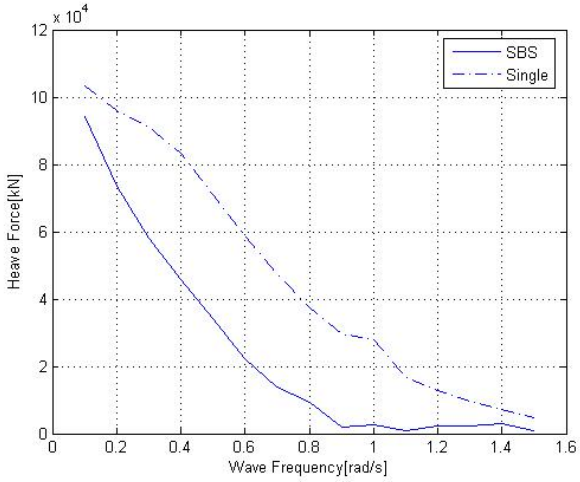

(c)

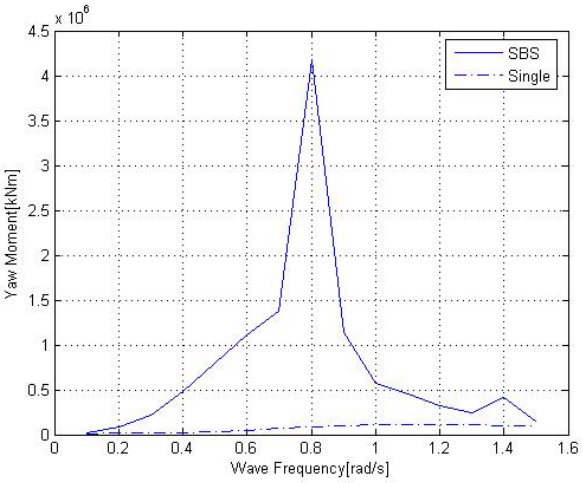

(f)

Figure 2-37. Wave exciting force on LNG Carrier for 270 deg wave heading

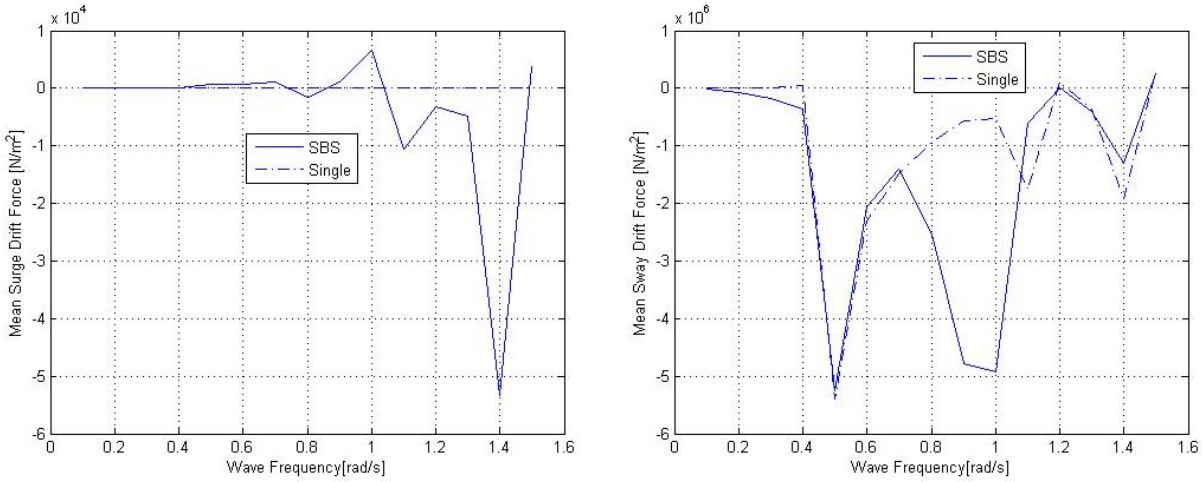

(a) (b)

Figure 2-38. Mean drift force on LNG Terminal for 270 deg wave heading

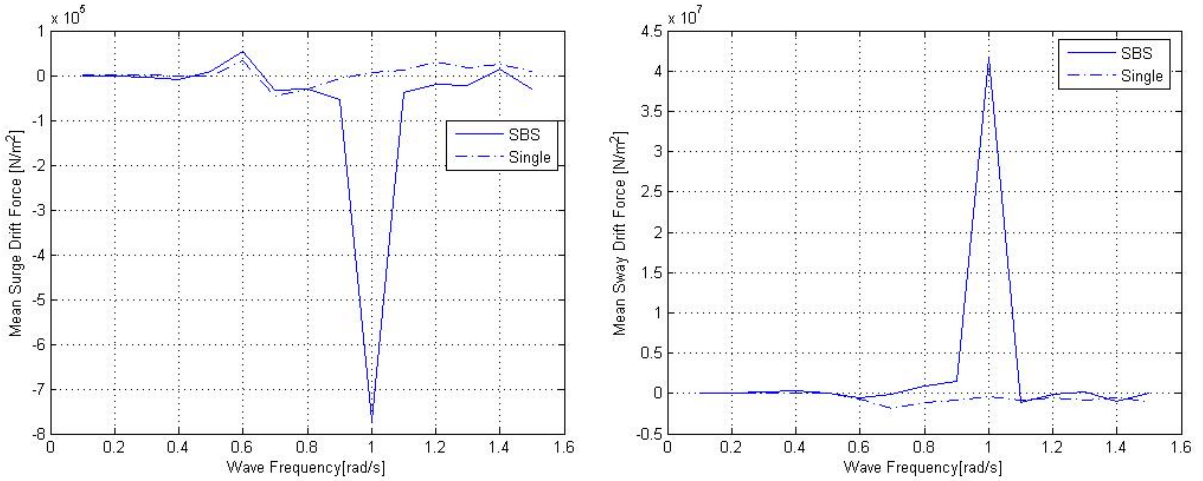

(a) (b)

Figure 2-39. Mean drift force on LNG Carrier for 270 deg wave heading

Figure 2-38(a) shows the mean drift surge force on the terminal. There a peak surge force in the aftward direction at 1.4 rad/s due to the asymmetric reflected waves from the carrier. As in the 90 deg wave heading case, for the single body, there is no surge drift force due to symmetry of the terminal about the Y-Z plane. Figure 2-38(b) shows the mean sway wave drift force on the terminal. Due to the interaction with the carrier there is a second peak in the sway drift force at 0.9 rad/s which is significantly higher than that in the single body case and is acting in the wave direction. Figure 2-39(b) shows the mean sway wave drift force on the carrier. There is a peak force at 0.7 rad/s which is significantly higher than that in the single body case and is in the direction opposite to the wave direction. Thus, as in the previous cases, at 0.7 rad/s, there exist large drift forces trying to bring the two bodies close together.

Coupled analysis in frequency domain also can be done using WAMIT. For this the external stiffness due to mooring lines, hawsers, etc need to be accurately estimated. Stiffness due to mooring lines can be derived based on catenary equations (R. K. Jain, 1980) or by conducting static offset tests numerically using programs like WINPOST which is explained later. The method of estimating the stiffness of hawsers or connecters between two floating bodies has been explained by Inoue et al. (1999).

2.3 Coupled Analysis in Time Domain

The time domain methods are generally used at the detailed design stages and also as a check for the frequency domain solutions. The coupled analysis in time domain is done using WINPOST. The hydrodynamic coefficients and forces are taken from the WAMIT output and are converted into the inputs for WINPOST using the program WAMPOST. In this analysis, the mooring lines, hawsers, fenders etc. are modeled and connected to the floating bodies properly and thereby we get a more realistic behavior of the system.The mooring lines and hawsers are modeled using rod elements, the theory of which has been already explained in section 2.1. The fender has been modeled as an external spring of constant stiffness. The fender modeling is critical since large compressive mean drift forces are acting on it as shown earlier.

2.3.1 Static Offset Test

Static offset test was done in WINPOST by applying variable static forces and estimating the corresponding displacements. By plotting the displacement against the applied force we obtain the stiffness curves. A typical stiffness curve for sway is shown in Figure 2-40. It can be seen that the stiffness curve is not exactly linear. In previous studies also, it has been shown that a nonlinear 'hardening' takes place with large offset and hence the behaviour.

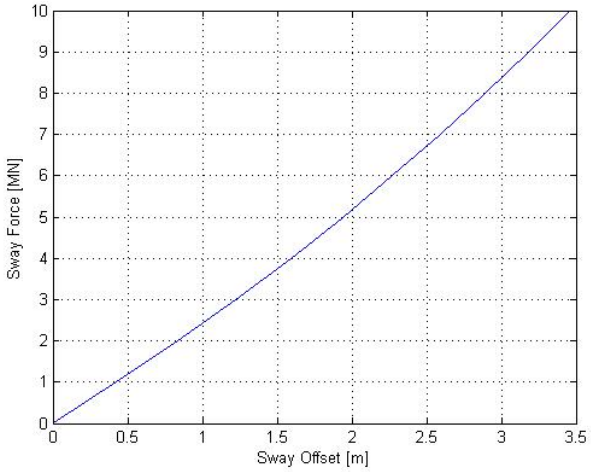

Figure 2-40. Sway static offset test

The mooring stiffness values for surge, sway and yaw obtained using the static offset test are given in Table 2-2.

Table 2-2. Mooring Stiffness Obtained Using Static Offset Test

Surge	5.0415E06 N/m
Sway	4.2032E06 N/m
Yaw	1.988E11 Nm/rad

The results from the time domain analysis are discussed below.

2.3.2 Case 1. Wave Heading = 270 Degrees

WINPOST analysis was done only for one wave heading. The results are discussed below.

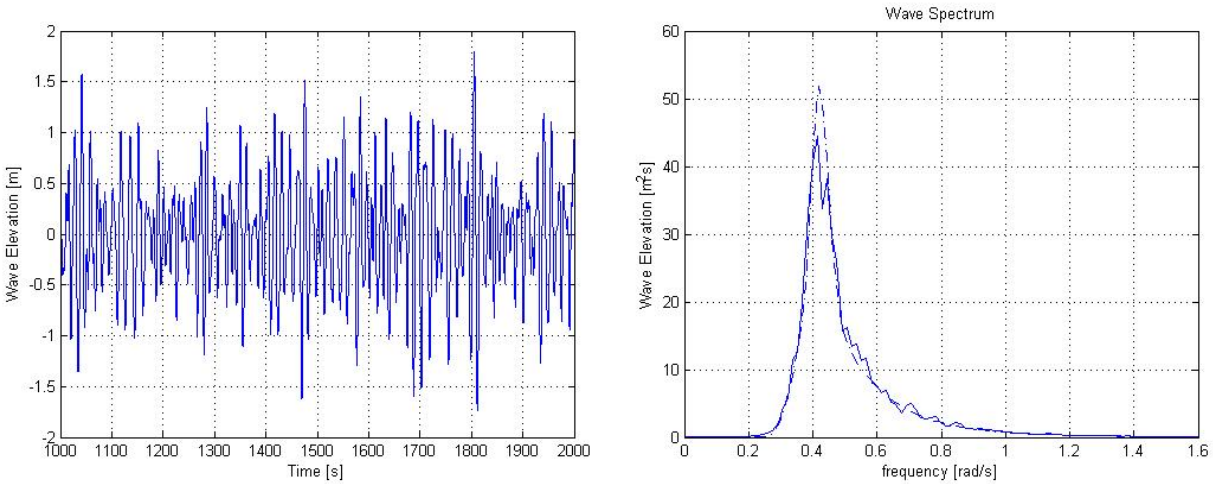

(a) (b)

Figure 2-41. Wave elevation time series and spectrum

The analysis is done for 1-year storm conditions, the data of which is given in Table 1-2. JONSWAP spectrum with the peakedness parameter γ = 3 is used to simulate the random sea state. Figure 2-41 shows the wave elevation time series and the wave spectrum. The dashed line represents the theoretical JONSWAP spectrum. The results were obtained by running the simulation for a simulation time of about 3 hours.

The motion responses of the LNG Terminal are discussed below:

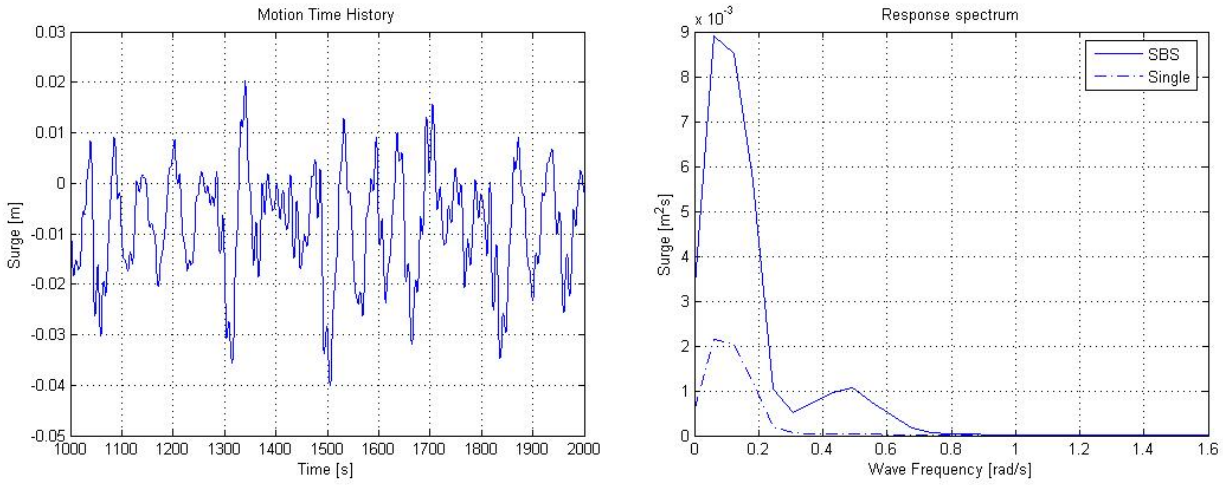

(a) (b)

Figure 2-42. LNG Terminal surge motion for 270 deg wave heading

Figure 2-42 shows the LNG Terminal surge motion time series and spectrum. The figure also shows a comparison with the single body case. The motion is much higher because of the existence of the reflected waves from the LNG Carrier. The surge motion is amplified since the reflected waves are not symmetric w.r.t the Y-Z plane as the LNG Carrier is not symmetric.

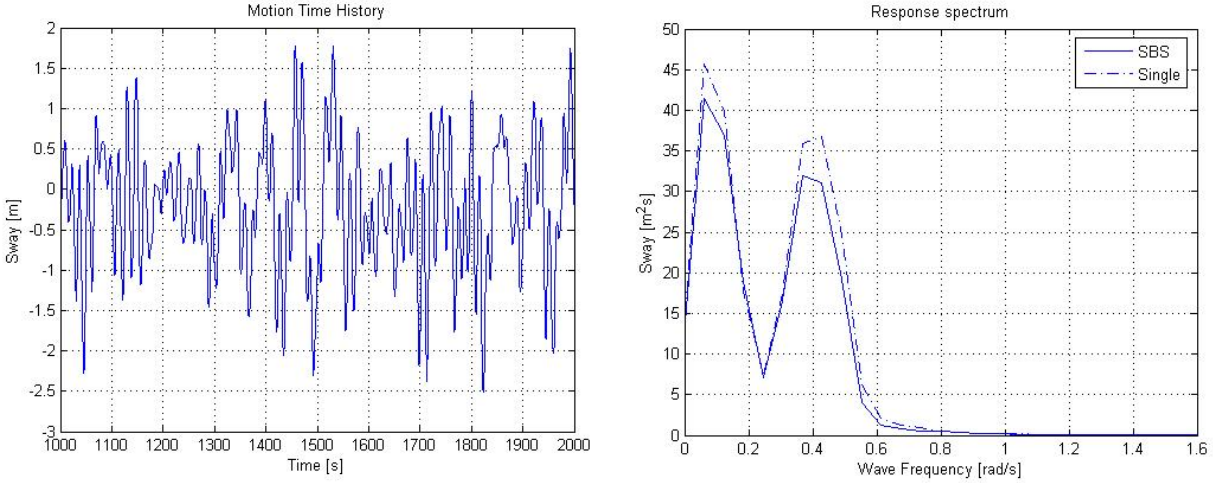

(a) (b)

Figure 2-43. LNG Terminal sway motion for 270 deg wave heading

Figure 2-43 shows the LNG Terminal sway motion time series and the spectrum. It can be seen that the sway response is a little less than that in the single body case because the connection to the LNG Carrier imposes a great additional mass and stiffness in the sway motion which dampens the sway response.

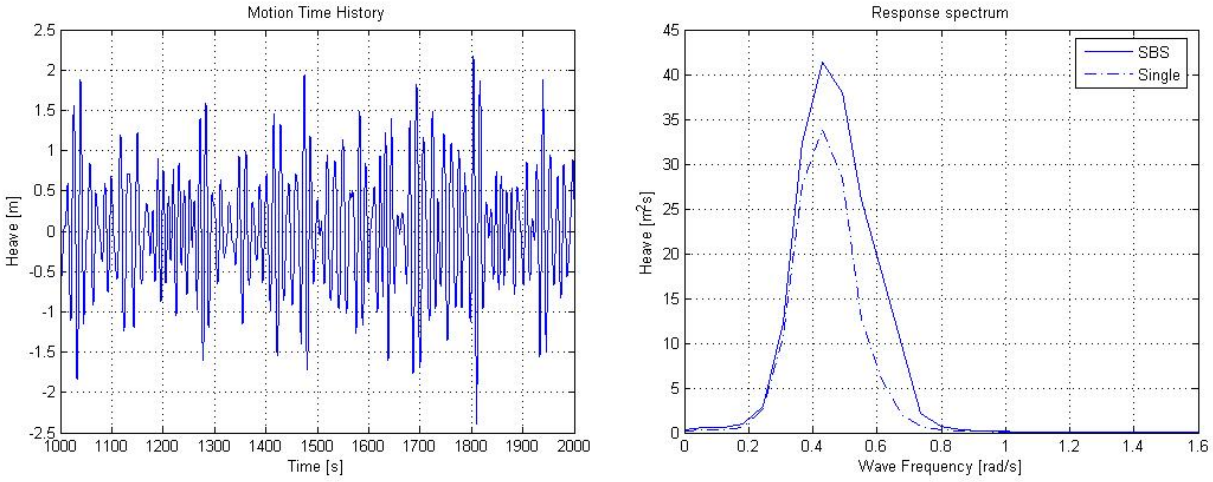

(a) (b)

Figure 2-44. LNG Terminal heave motion for 270 deg wave heading

Figure 2-44 shows the LNG Terminal heave motion time series and the spectrum. The heave response is higher than that in the single body case because of the incident wave and the reflected waves from the LNG Carrier forming a standing wave like pattern in the region between the two bodies.

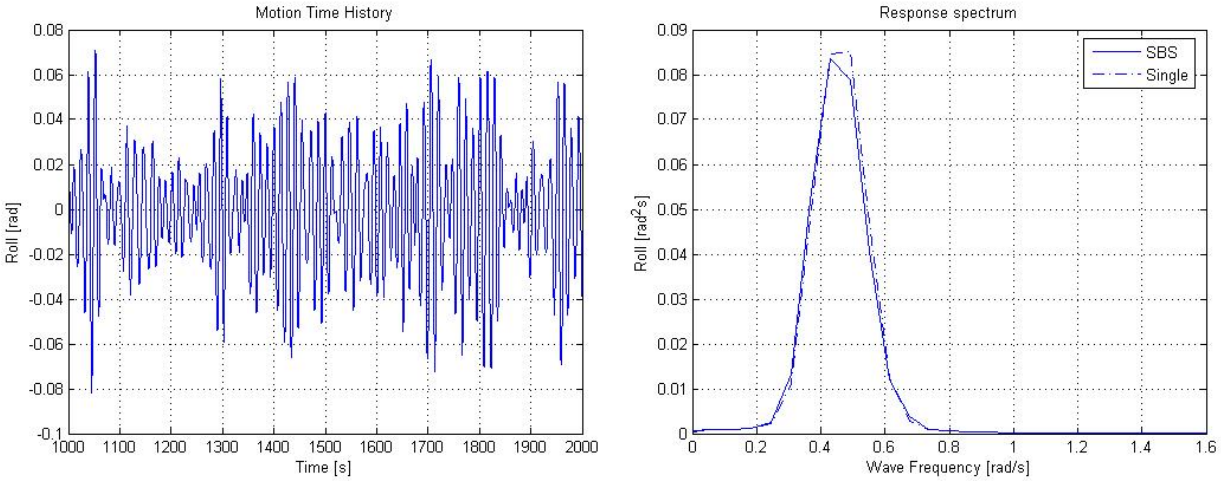

(a) (b)

Figure 2-45. LNG Terminal roll motion for 270 deg wave heading

Figure 2-45 shows the LNG Terminal roll motion time series and the spectrum. It can be seen than for the two-body case the response is slightly less than that in the single body case due to the additional stiffness provided by the hawsers and fenders.

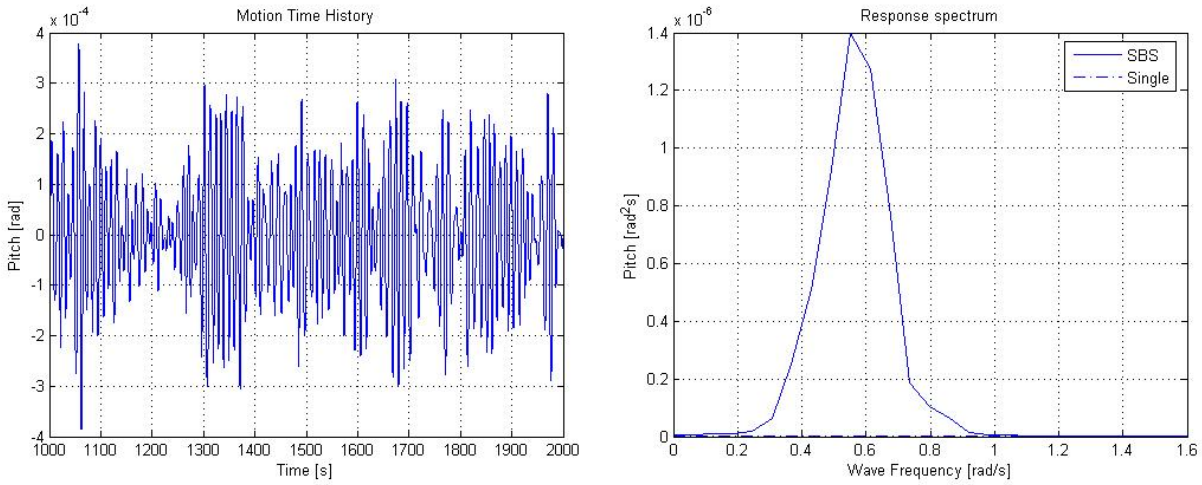

(a) (b)

Figure 2-46. LNG Terminal pitch motion for 270 deg wave heading

Figure 2-46 shows the LNG Terminal pitch motion time series and the spectrum. It can be seen that the pitch motion is much higher in the two-body case because of the asymmetric reflected waves from the LNG Carrier.

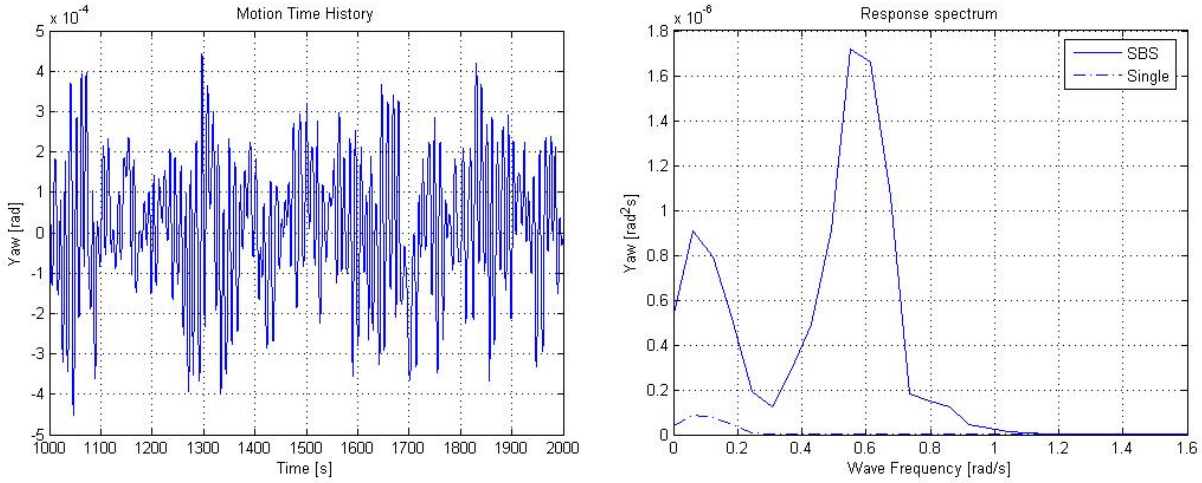

(a) (b)

Figure 2-47. LNG Terminal yaw motion for 270 deg wave heading

Figure 2-47 shows the LNG Terminal yaw motion time series and the spectrum. It can be seen that the presence of the LNG Carrier has a significant effect on the terminal

yaw motions. There low frequency response is amplified and there is also a greater second peak at 0.6 rad/s due to the interaction between the two bodies.

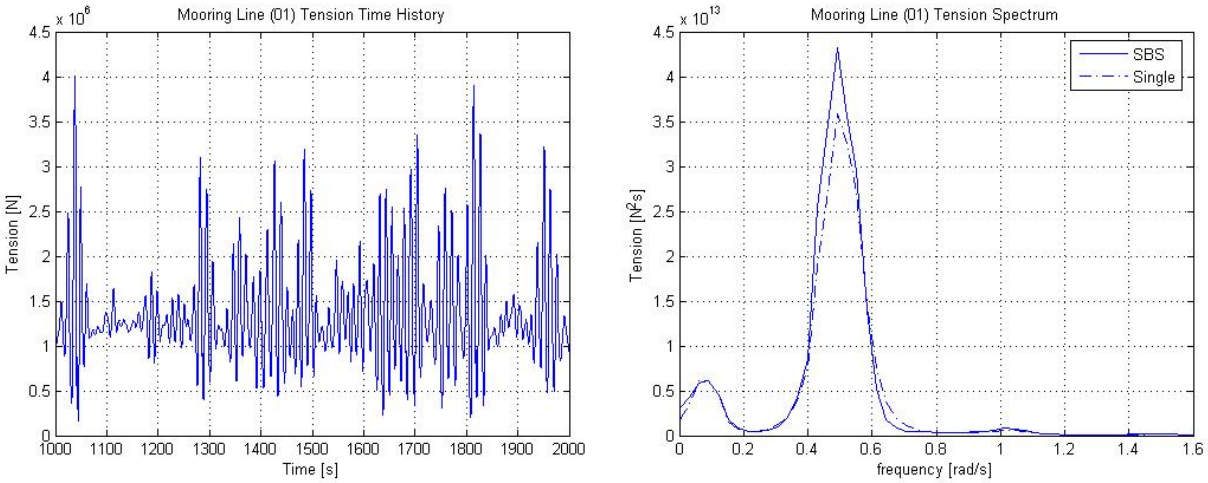

(a) (b)

Figure 2-48. Mooring line (01) tension

Figure 2-48 shows the mooring line tension time history and power spectrum. The statistical summary of the simulation (1 year storm) for the terminal motion is given in Table 2-3.

Table 2-3. Statistical Summary of the Simulation for Heading = 270 deg

		Side-by-side (Coupled)	Single
Surge [m]	Max	0.0885	-0.0234
	Mean	-0.0074	-0.0067
	Std. Dev.	0.0215	0.0043
Sway [m]	Max	-3.9292	-3.9848
	Mean	-0.2720	-0.2430
	Std. Dev.	0.8463	0.8395
Heave [m]	Max	-1.8917	-1.8397
	Mean	0.0057	0.0062
	Std. Dev.	0.5562	0.5852
Roll [rad]	Max	-0.1093	-0.1051
	Mean	-0.0012	-0.0011
	Std. Dev.	0.0310	0.0284
Pitch [rad]	Max	0.0008	0.0000
	Mean	0.0000	0.0000
	Std. Dev.	0.0003	0.0000
Yaw [rad]	Max	-0.0012	0.0002
	Mean	0.0000	0.0000
	Std. Dev.	0.0004	0.0000
Tension in line 01 [MN]	Max	5.6598	5.8179
	Mean	1.3543	1.3415
	Std. Dev.	0.5719	0.5429

The motion responses of the LNG carrier are discussed below.

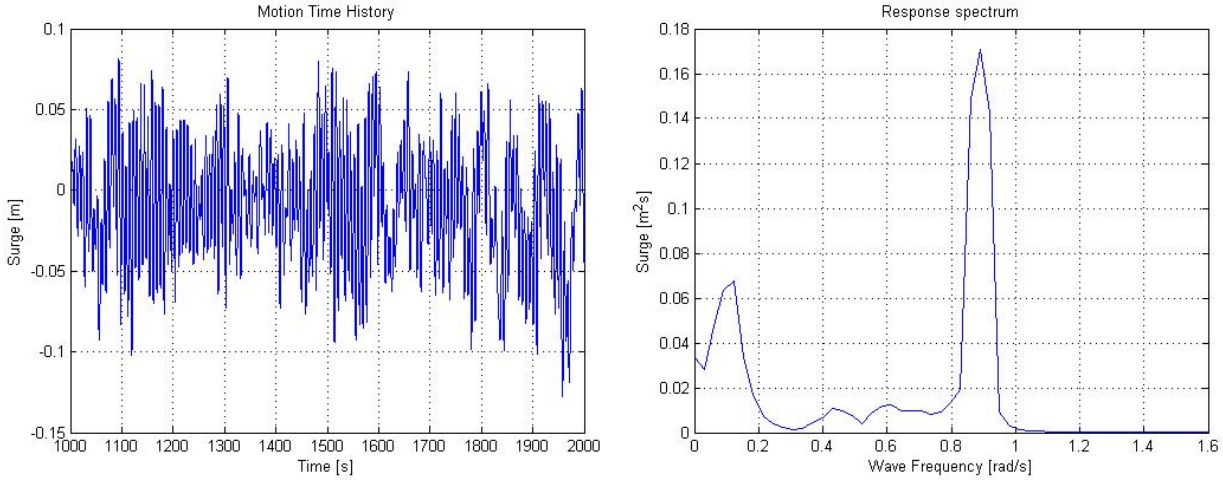

(a) (b)

Figure 2-49. LNG Carrier surge motion for 270 deg wave heading

Figure 2-49 shows the LNG Carrier surge motion time series and the spectrum. It can be seen that there are two peaks, one corresponding to the surge motion at the frequency of the terminal and another one at a higher frequency due to the high stiffness of the taut hawser lines.

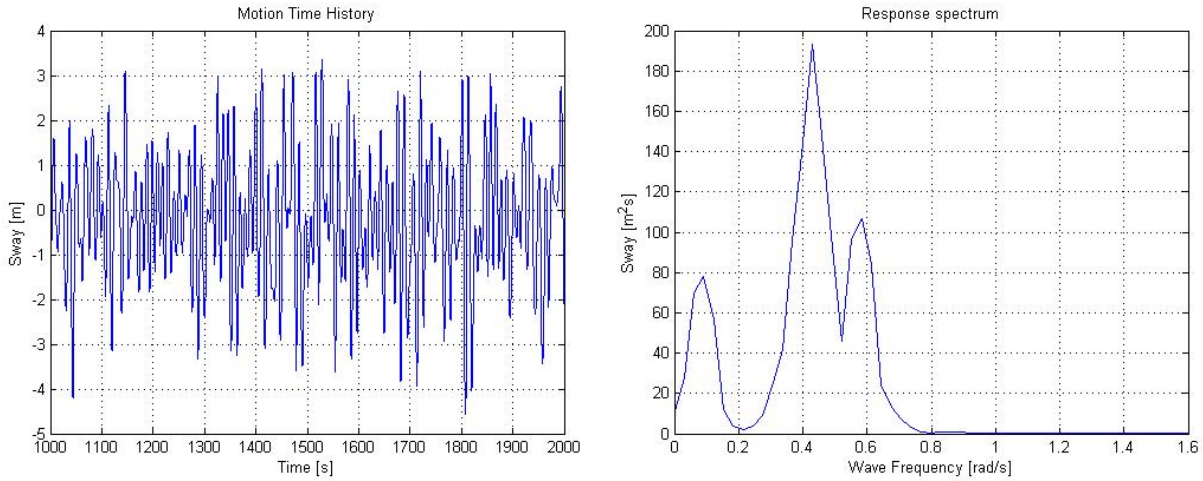

(a) (b)

Figure 2-50. LNG Carrier sway motion for 270 deg wave heading

Figure 2-50 shows the LNG Carrier sway motion time series and the spectrum. Here again it can be seen that there is a low frequency component which follows the motion of the terminal and another one at a higher frequency due to the taut hawser lines.

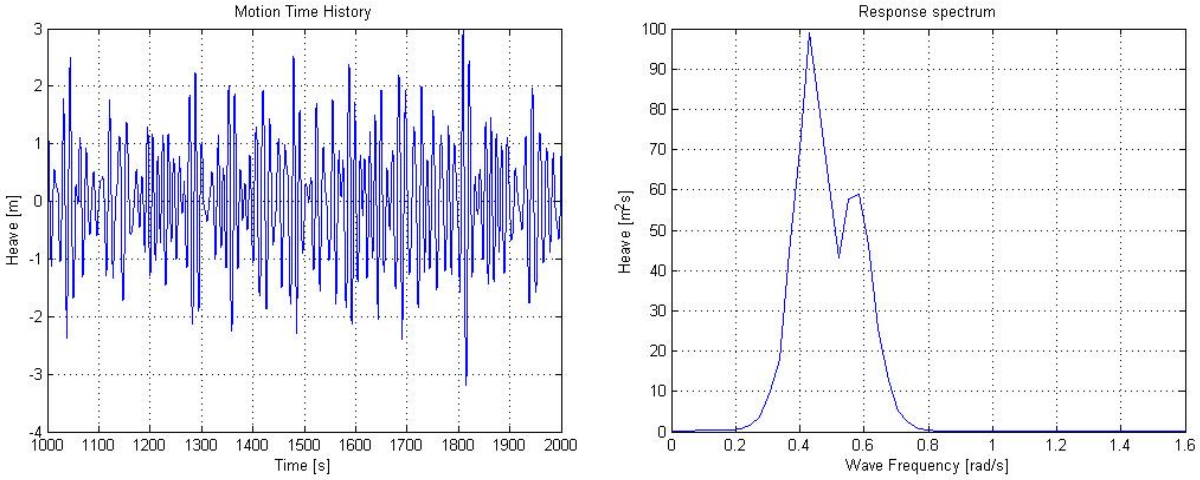

(a) (b)

Figure 2-51. LNG Carrier heave motion for 270 deg wave heading

Figure 2-51 shows the LNG Carrier heave motion time series and the spectrum. It can be seen that the heave motion occurs mainly at the wave frequency.

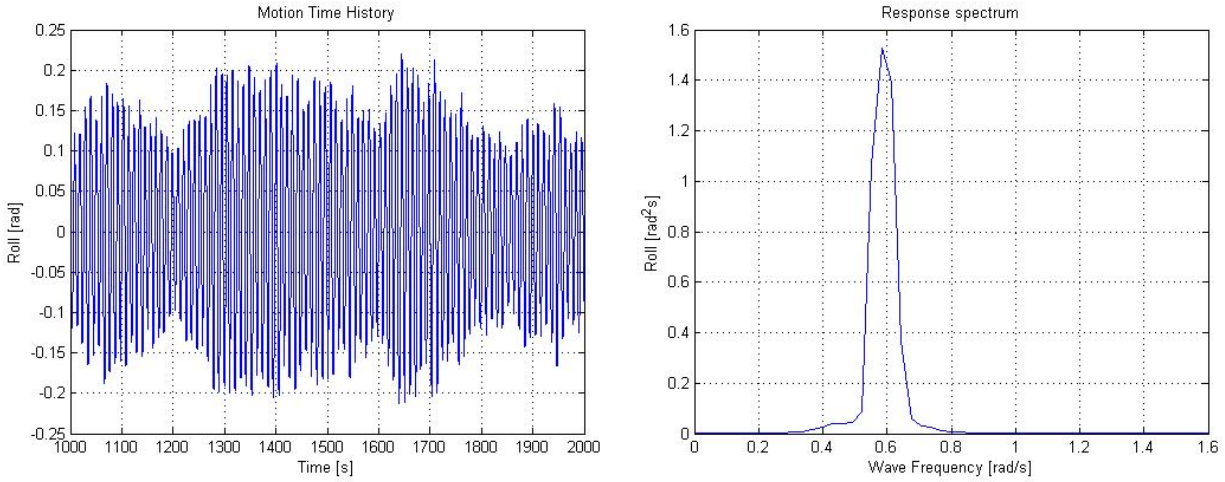

(a) (b)

Figure 2-52. LNG Carrier roll motion for 270 deg wave heading

Figure 2-52 shows the LNG Carrier roll motion time series and the spectrum. The roll motion occurs at a frequency little higher than the wave frequency at 0.6 rad/s

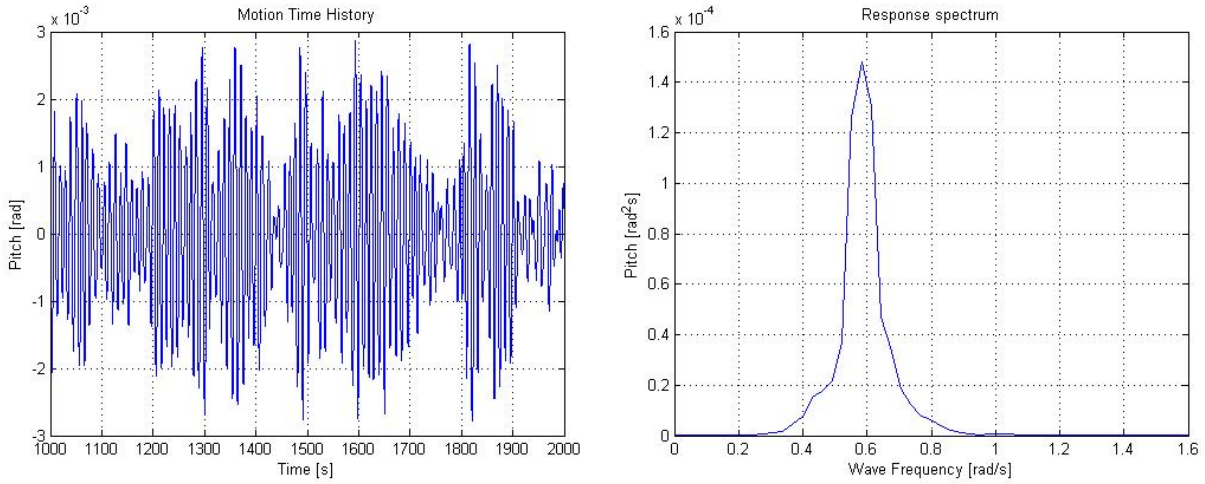

(a) (b)

Figure 2-53. LNG Carrier pitch motion for 270 deg wave heading

Figure 2-53 shows the LNG Carrier pitch motion time series and the spectrum. The pitch motion too takes place at a higher frequency than the wave frequency at 0.6 rad/s.

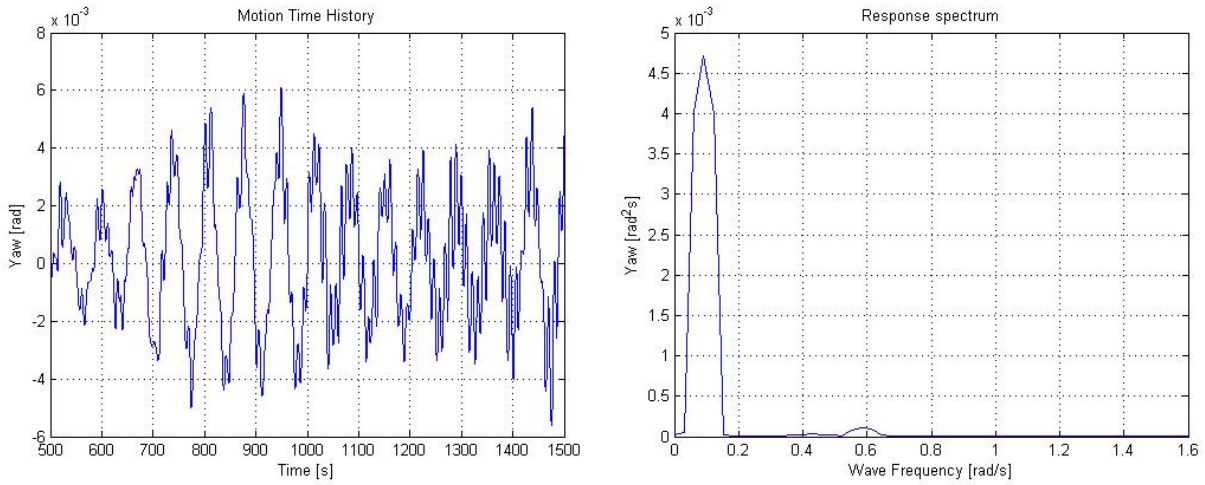

(a) (b)

Figure 2-54. LNG Carrier yaw response for 270 deg wave heading

Figure 2-54 shows the LNG Carrier yaw motion time series and the corresponding spectrum. It can be seen that the yaw motion occurs at a low frequency of 0.05 rad/s. The relative motion characteristics between the terminal and the carrier are discussed below.

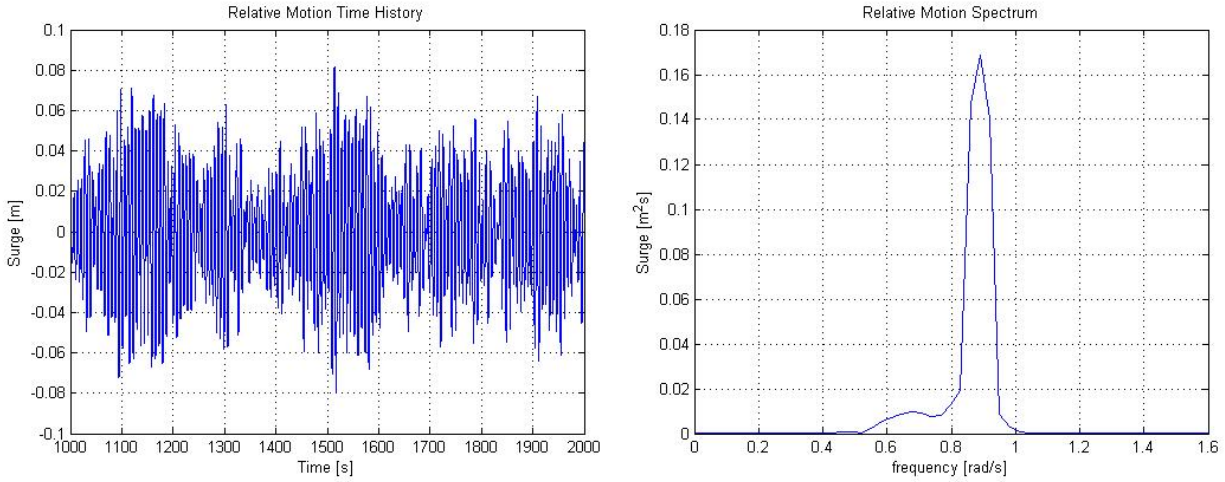

(a) (b)

Figure 2-55. Relative surge response for 270 deg wave heading

Figure 2-55 shows the relative surge motion time history and spectrum. It can be seen that the surge motion is insignificant, mainly because the waves are in the sway

direction. The little surge motion present is due to the interaction between the two bodies.

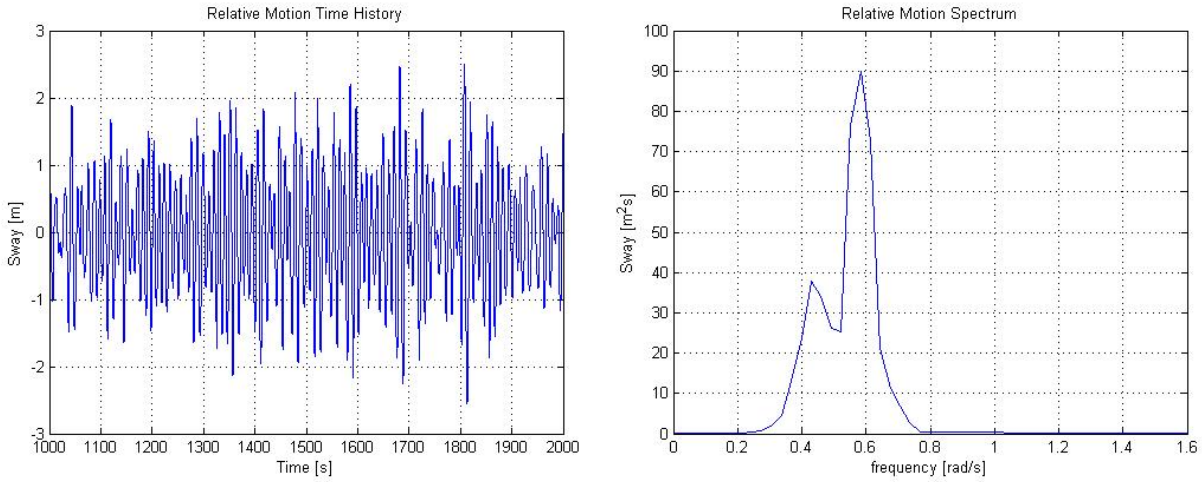

(a) (b)

Figure 2-56. Relative sway response for 270 deg wave heading

Figure 2-56 shows the relative sway response time history and power spectrum. The relative sway is relatively large, the maximum being 2.55 m.

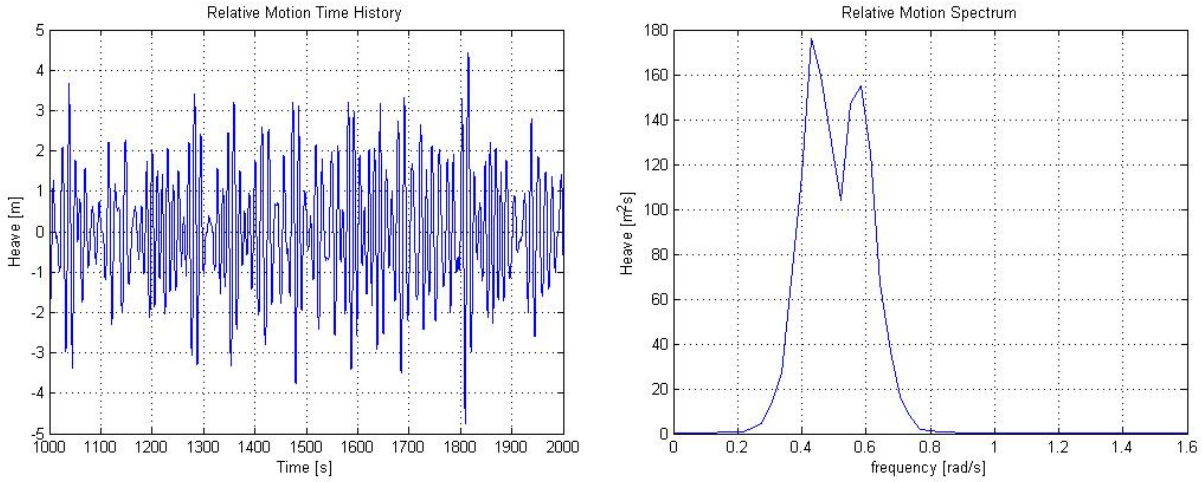

(a) (b)

Figure 2-57. Relative heave response for 270 deg wave heading

Figure 2-57 shows the relative heave response time history and power spectrum. The maximum relative heave is 4.74 m. The statistical summary of the relative motions is given in Table 2-4.

Table 2-4. Statistical Summary of Relative Motions for Heading = 270 deg

	Max	Mean	Std. Dev.
Relative Surge [m]	0.0817	0.0000	0.0276
Relative Sway [m]	-2.5477	0.0011	0.7584
Relative Heave [m]	-4.7395	0.0011	1.3535
Relative Roll [rad]	-0.2466	-0.0015	0.0811
Relative Pitch [rad]	0.0033	0.0000	0.0011
Relative Yaw [rad]	-0.0161	-0.0003	0.0048

3. CONCLUSIONS

Single body analysis does not take into consideration the interaction effects in cases where there are multiple bodies in close proximity to each other and the results obtained using single body analysis are quite different from the ones obtained using multi-body analysis. It has been shown that there can be significant hydrodynamic interactions resulting in forces and responses which can be even double as that in the single body case. Interaction effects are significant in head sea and beam sea conditions compared to oblique wave conditions. There is a shielding effect on the responses of the body on the leeward side. Hence it is preferable to keep the LNG Carrier on the leeward side as the LNG Terminal is less responsive compared to the carrier. It was found that large mean drift forces to the order of 10^6 N act on the bodies in the sway direction pushing them against each other in all the wave directions analysed. Analysis in time domain was done for the 270 deg case and it was found that the relative motions exceed the limits for 1 year storm condition.

REFERENCES

Buchner, B., Dijk, A., Wilde, J., 2001. Numerical multiple-body simulations of side-by-side mooring to an FPSO. In Proceedings of the Eleventh International Offshore and Polar Engineering Conference, Stavanger, Norway, 343-353.

Buchner, B., Gerrit B., Jaap W., 2004. The interaction effects of mooring in close proximity of other structures, In Proceedings of 14th ISOPE Conference, Toulon, France, 297-306.

Choi, Y.R., Hong, S.Y., 2002. An analysis of hydrodynamic interaction of floating multi-body using higher-order boundary element eethod. In Proceedings of the Twelfth International Offshore and Polar Engineering Conference, Kitakyushu, Japan, 303-308.

Hong, D.C., 1987. On improved Green integral equation applied to the water-wave radiation-diffraction problem. Journal of Society of Naval Architects in Korea 24 (1), 1-8.

Hong, S.Y., Kim, J.H., Cho, S.K., Choi, Y.R., Kim, Y.S., 2005. Numerical and experimental study on hydrodynamic interaction of side-by-side moored multiple vessels. Ocean Engineering 32, 783-801.

Huijsmans, R.H.M., Pinkster, J.A., Wilde, J.J., 2001. Diffraction and radiation of waves around side-by-side moored vessels. In Proceedings of the Eleventh International Offshore and Polar Engineering Conference, Stavanger, Norway, 406-412.

Inoue, Y., Islam, M.R., 1999. Comparative study of numerical simulation and experimental results for a parallely connected FPSO and LNG in waves. In Proceedings of the Ninth International Offshore and Polar Engineering Conference, Brest, France, 360-367.

Jain, R.K., 1980. A simple method of calculating the equivalent stiffnesses in mooring cables. Applied Ocean Research 2, No.3, 139-142.

Kim, M.H., 1997. WINTCOL/WINPOST User's Manual. Ocean Engineering Program, Civil Engineering Department, Texas A&M University, College Station, TX.

Kodan, N., 1984. The motions of adjacent floating structures in oblique waves. In Proceedings of the Third International Conference on Offshore Mechanics & Arctic Engineering, New Orleans, 1, 206-213.

Lee, C.H., 1995. WAMIT Theory Manual. Department of Ocean Engineering, Massachusetts Institute of Technology, Cambridge, MA.

Lee, D.H., Choi, H.S., 1998. The motion behavior of shuttle tanker connected to a turret-moored FPSO. In Proceedings of Third International Conference on Hydrodynamics, Seoul, South Korea, 173-178.

Lee, D.H., Kim, M.H., 2004. Two-body Resonant Interactions by Fully Coupled and Partially Coupled Method. Presented at the ASCE Civil Engineering Conference & Exposition, Civil Engineering in the Oceans VI, Baltimore.

Miller, R., Wattinger, R., Valkenburg, A.V., Foreman, F., et. al., 2004. Design of a Floating Storage and Regasification Unit (FSRU) for Offshore West Africa. Senior design project. Texas A&M University. Presented at the International Student Offshore Design Competition.

Ran, Z., 2000. Coupled Dynamic Analysis of Floating Structures in Waves And Currents, Ph.D. Dissertation. Texas A&M University.

Sannasiraj, S.A., Sundaravadivelu, R., Sundar, V., 2000. Diffraction-radiation of multiple floating structures in directional waves. Ocean Engineering, 28, 201-234.

Wehausen, J.Y., Laitone, E.V., 1960. Surface Waves, Encyclopedia of Physics, Springer-Verlag, New York.

VITA

Vinu P. Kuriakose
Sea Engineering Inc., 1400 Broadfield Blvd. Suite 200
Houston, TX 77084
Ph: (281) 579-9700 Email: vkuriakose@sea-engr.com

EDUCATION

- Master of Science August 2005
  Major: Ocean Engineering
  Texas A&M University
  GPA: 3.9
- Bachelor of Technology June 1998
  Major: Naval Architecture and Ship Building
  Cochin University of Science and Technology

EXPERIENCE

- Texas A&M University, College Station, Texas (Sep. 2004 - May 2005)
  Teaching Assistant, Civil Engineering Department
- Indian Register of Shipping, Mumbai (Jan 2002 – Aug 2003)
  Ship Surveyor, Hull Plan Approval Department
- Parametric Technology Corporation, Pune (Aug 2000 – Dec 2001)
  Software Engineer, Marine Software Division
- Mazagon Dock Ltd., Mumbai (Nov 1998 – Aug 2000)
  Naval Architect, Structural Design Office